

NATIONAL SCIENCE FOUNDATION GRANT NO. ENG74-21131

FINAL REPORT

PART 2

Report SM 77-1

SHEAR TRANSFER UNDER CYCLICALLY
REVERSING LOADING, ACROSS AN
INTERFACE BETWEEN CONCRETES
CAST AT DIFFERENT TIMES

by

Alan H. Mattock

Department of Civil Engineering
University of Washington
June 1977

1. Report No. SM77-1	2. Government Accession No.	3. Recipient's Catalog No. <i>PB 275258</i>
4. Title and Subtitle SHEAR TRANSFER UNDER CYCLICALLY REVERSING LOADING ACROSS AN INTERFACE BETWEEN CONCRETES CAST AT DIFFERENT TIMES	5. Report Date June 1977	6. Performing Organization Code
	7. Author(s) Alan H. Mattock	8. Performing Organization Report No. SM77-1
9. Performing Organization Name and Address University of Washington Department of Civil Engineering Seattle, Washington 98195	10. Work Unit No.	11. Contract or Grant No. Eng 74-21131
	12. Sponsoring Agency Name and Address National Science Foundation Washington, D.C. 20550	13. Type of Report and Period Covered Final Report, Part 2 15 Oct. 1974-Sept. 30, 1977
14. Sponsoring Agency Code		
15. Supplementary Notes		
<p>16. Abstract The total study is concerned with the shear transfer strength of reinforced concrete subject to both single direction and cyclically reversing loading, the latter simulating earthquake conditions. The primary topics studied were the influence of the existence in the shear plane of an interface between concretes cast at different times, and the influence of reinforcing bar diameter on shear transfer across a crack in monolithic concrete.</p> <p>This Part 2 of the Final Report is concerned with shear transfer across interfaces between concretes cast at different times, when subject to cyclically reversing shear. Cyclically reversing and monotonic shear transfer tests of companion initially cracked specimens are reported. Both composite and monolithic specimens of normal weight concrete were tested. The interfaces of all composite specimens were roughened. In some cases bond at the interface was deliberately broken.</p> <p>It was found that for a roughened interface with good bond, the shear transfer behavior was similar to that of comparable initially cracked, monolithic concrete. If the bond at the interface is broken, the shear transfer behavior under cyclic loading deteriorates rapidly and the shear strength is only about 0.6 of that under monotonic loading.</p>		
17. Key Words composite construction, construction joint, connections, precast concrete, reinforced concrete, seismic loading, shear transfer	18. Distribution Statement <i>Approved for NTIS by Dr. Babendri, NSF, Edg. Per telecom 1-5-78</i>	
19. Security Classif. (of this report) None	20. Security Classif. (of this page) None	22. Price PC AOS-A01

REPRODUCED BY
**NATIONAL TECHNICAL
 INFORMATION SERVICE**
 U. S. DEPARTMENT OF COMMERCE
 SPRINGFIELD, VA. 22161

PREFACE

This study was carried out in the Structural Research Laboratory of the University of Washington. It was made possible by the support of the National Science Foundation, through Grant No. ENG74-21131.

Contributions were made to the execution of this project by graduate student Research Assistants, C.L. Chou and A.B. Schroeder.

TABLE OF CONTENTS

	Page
I INTRODUCTION	1
1.1 The Total Study	1
1.2 Scope of the Entire Study	1
1.3 Sub-Division of the Final Report	2
1.4 Background to This Part of the Study	2
II EXPERIMENTAL STUDY	4
2.1 Scope	4
2.2 The Test Specimen	4
2.3 Materials and Fabrication	5
2.4 Testing Arrangements and Instrumentation	7
2.5 Testing Procedures	9
III TEST RESULTS	11
3.1 Loading History and Ultimate Strength	11
3.2 Specimen Behavior	11
IV DISCUSSION OF TEST RESULTS	16
4.1 General Behavior	16
4.2 Ultimate Shear Transfer Strength	22
V PRINCIPAL CONCLUSIONS	24
REFERENCES	26
APPENDIX A - NOTATION	
APPENDIX B - TYPICAL SHEAR-SLIP AND SLIP-SEPARATION DATA FOR CYCLIC LOADING TESTS	

LIST OF FIGURES

<u>Figure</u>	<u>Title</u>
2.1	Cyclic loading specimen.
2.2	Cyclic loading test frame.
2.3	General view of arrangements for test.
2.4	Initial cracking of specimen.
3.1	Typical shear-slip curves in monotonic loading tests.
3.2	Typical slip-separation curves in monotonic loading tests.
3.3	Typical shear-slip curves in cyclic loading tests.
3.4	Typical slip-separation curves in cyclic loading tests.
4.1	Variation of slip at maximum shear with number of cycles of load.
4.2	Comparison of shear-slip relations in cyclic and monotonic loading, for cracked, monolithic concrete specimens.
4.3	Comparison of shear-slip relations in cyclic and monotonic loading, for cracked, bonded, composite specimens.
4.4	Comparison of shear-slip relations in cyclic and monotonic loading, for composite specimens with bond broken.
4.5	Comparison of shear-slip relations in cyclic and monotonic loading for composite specimens with bond broken and also cracked before testing.
4.6	Comparison of shear-slip relations in cyclic and monotonic loading, for cracked, bonded, composite specimens made from concretes of different strength.
4.7	Shear transfer strength in monotonic loading tests of initially cracked, monolithic concrete and initially cracked, composite specimens with bond.

I - INTRODUCTION

1.1 The Total Study

The total study carried out with the support of the National Science Foundation under grant No. ENG74-21131, has been directed toward obtaining further information on shear transfer in reinforced concrete subject to both single direction and cyclically reversing loading. "Shear Transfer" is defined as the transfer of shear across a specific plane, with shear failure involving slippage along the plane.

The primary topics studied were the influence of the existence in the shear plane of an interface between concretes cast at different times, and the influence of reinforcing bar diameter on shear transfer across a crack in monolithic reinforced concrete.

The overall objectives of this study have been to improve our understanding of the mechanics of shear transfer in reinforced concrete, and to develop design recommendations for shear transfer in reinforced concrete subject to static or seismic loading conditions.

1.2 Scope of the Entire Study

Tests have been made of "push-off" type specimens and such modified versions of the simple push-off type of specimen as will permit the desired loading condition to be imposed on the specimen.

The following variables have been included in the test program:--

The use of composite or monolithic specimens.

The strengths of the concretes cast against one another.

The condition of the face of the precast concrete against which which other concrete is cast, i.e., smooth, deliberately roughened, bond deliberately broken or not.

The existence of a crack in the shear plane.

The shear transfer reinforcement parameters ρf_y .

The size of rebars used as shear transfer reinforcement.

The type of loading; i.e., single direction and cyclic reversal of loading.

1.3 Sub-Division of the Final Report

Part 1 of the final project report described ⁽¹⁾ that part of the study concerned with shear transfer across interfaces between concretes cast at different times, when subject to monotonically increasing shear.

Part 2 of the final report describes that part of the study concerned with shear transfer across interfaces between concretes cast at different times, when subject to cyclically reversing shear.

Part 3 of the final report will be concerned with the effect of reinforcing bar diameter on shear transfer across a crack, under both monotonic and cyclically reversing shear.

1.4 Background to this Part of the Study

Shear must be transferred across interfaces between concretes cast at different times, both in composite construction involving precast concrete members, and at construction joints in monolithic concrete construction. In the case of structures subject to earthquakes, the shear will alternate in sign.

Shear transfer type failures of construction joints in shear walls have occurred in earthquakes, and engineers have asked whether the "shear friction" provisions of the ACI Building Code, ACI 318-71, ⁽²⁾ may properly be used to design construction joints against this type of failure.

Prior studies ^(3, 4, 1) of shear transfer across interfaces between concretes cast at different times, have been limited to the case of monotonically increasing shear. The "shear friction" provisions of ACI 318-71 are also based on the results of monotonic shear transfer tests. In view of the

practical need for guidance concerning shear transfer design to resist alternating shear loads such as occur in earthquakes, it appeared desirable to make this study of shear transfer across interfaces subject to reversing shear.

II - EXPERIMENTAL STUDY

2.1 Scope

This experimental study is concerned with the transfer of shear across an interface between concretes cast at different times, when that interface is subject to cyclically reversing shear. This type of loading is likely to occur in earthquakes, across interfaces in composite construction and across construction joints in monolithic concrete construction.

The variables included in this study have been:

1. Loading history, - (a) monotonically increasing load.
(b) cyclically reversing load.
2. The existence of bond between the precast and cast-in-place concrete.
3. The strengths of the concretes, i.e., whether the precast and cast-in-place concretes have the same or different compressive strengths.
4. The existence of a crack at the interface.
5. The shear transfer reinforcement parameter ρf_y .

In Part 1 of the total study it was found that roughening of the interface as prescribed by Sec. 11.15 of ACI 318-71, is essential if high shear stresses are to be transferred across an interface between concretes cast at different times. For a given value of the shear transfer reinforcement parameter ρf_y , the shear which could be transferred across a smooth interface was less than half that which could be transferred across a roughened interface. The interfaces of all composite specimens tested in this part of the study were therefore roughened as prescribed by Sec. 11.15 of ACI 318-71.

2.2 The Test Specimen

The test specimen was developed from the standard push-off specimen. Details of a typical specimen are shown in Fig. 2.1. It is designed to be

gripped by friction on faces "A", as described in Sec. 2.4 of this report. Imposed displacements on sides "B" and "C", parallel to the shear plane and in opposite directions, produce shear without moment in the 50 in.² shear plane. The slots in the top and bottom of the specimen are designed to make shear conditions in the shear plane more critical than in the concrete adjacent to the shear plane.

As described later, the composite specimens were cast in two stages, the interface between the two concretes lying in the shear plane.

The shear transfer reinforcement was in the form of closed stirrups which wrapped around the longitudinal reinforcement, in order to ensure positive anchorage on both sides of the shear plane. Additional longitudinal reinforcement and reinforcement adjacent to the gripping faces "A" was provided, to prevent premature failures occurring in this region.

Five series of test specimens were tested, as indicated in Table 2.1. The variables between the test series are also detailed in Table 2.1. Each series consisted of two pairs of specimens. One pair of specimens was reinforced with two #3 bar closed stirrups and the other pair with three #3 bar closed stirrups. One specimen of each pair was tested monotonically and the other was subjected to progressively increasing, cyclically reversing shear.

In the numbering of the specimens, the first letter refers to the test series, the number is in the number of #3 bar stirrups, and the last letter indicates the type of loading to which the specimen was subject, (M - monotonic, C - cyclic).

The properties of the test specimens are detailed in Table 2.3.

2.3 Materials and Fabrication

The specimens were made from Type III Portland Cement, sand and 3/4 in. maximum size gravel, in the proportions shown in Table 2.2. In all cases,

water was added sufficient to produce a 3 inch slump. The gravel was a glacial outwash gravel obtained from a local pit. The concrete was mixed in a 5 cu. ft. capacity "Eirich Counter-Current Rapid Mixer" and was compacted in the forms using an immersion vibrator. The concrete strengths actually attained are shown in Table 2.3.

The deformed bar reinforcement used conformed to ASTM Specification A615. The bars used for the shear transfer reinforcement had a yield point of approximately 53 ksi. The actual yield point was determined for the reinforcement used in each specimen, and the values are listed in Table 2.3. The #6 bar longitudinal reinforcement had a yield point of 60 ksi.

The stirrups were welded closed on one of the shorter sides. Transverse anchor bars were welded to the ends of the longitudinal bars and the bars of the secondary reinforcement cages were welded together. The shear transfer stirrup reinforcement and the secondary reinforcement was then assembled and tied together with iron wire to form the complete reinforcement cage.

The composite specimens were cast in two stages. The first half of the specimen was cast with the shear plane of the completed specimen in the plane of the top of the metal form, (i.e. horizontal). The reinforcement projected from this face at this stage. The concrete was "struck off" even with the edges of the form and the surface was roughened to a full amplitude of 1/4 in. to conform with Section 11.15.7 of ACI 318-71. (By following this procedure, the undulations formed in the interface were uniformly distributed on either side of the shear plane in the completed specimen).

The half specimen was cured under polythene sheets for 3 days. It was then removed from the form, the projecting reinforcement and the concrete interface were cleaned, and it was then placed in a form for the complete specimen. The remaining concrete was cast and the specimen was cured under

polythene sheets a further 4 days before being removed from the form and tested.

In Series M and Q, in which it was desired to obtain bond between the concretes of the two halves of the specimen, the interface was thoroughly wetted before the second half of the specimen was cast. In series N and P, in which it was desired that there be no bond between the concretes of the two halves of the specimen, the interface was given a thin coating of bond breaker before casting the second half of the specimen. The bond breaker was a mixture of soft soap and talc, as used to prevent bond between "match cast" parts in a local precast concrete plant. (By volume, 5 parts Flaxoap: 1 part Talc.)

The specimens of Series L were cast in one piece and were cured in the forms under polythene sheets for seven days before testing.

2.4 Testing Arrangements and Instrumentation

The specimens were tested in a two part frame designed for the purpose. A section through the frame is shown in Fig. 2.2 and an over-all view of the arrangements for test is shown in Fig. 2.3. The opposite sides of the specimen are attached to the two parts of the frame by gripping plates. These plates are bolted to the frame and grip the specimen by friction. The clamping force is provided by high strength steel rods passing through the plates and through oversize holes in the specimen. The rods are tensioned before the anchor nuts are tightened, using a hydraulic center hole ram mounted on a stool and equipped with an extension rod and coupler, (see lower center in Fig. 2.3). For specimens containing two stirrups, five rods are used, each tensioned to 30 kips. For the specimens with three stirrups, four rods are used, each tensioned to 33 kips. Two soft rubber O-rings are used to center each rod in the oversize holes in the test specimen, so as to avoid the possibility of the rods bearing directly against the concrete.

The shearing forces are provided by two opposed pairs of 60 kips capacity hydraulic center hole rams. These rams are arranged so that they can alternately push the two parts of the frame apart vertically or pull the two parts together vertically. The loads are applied to the opposite parts of the frame through tension-compression load cells, so that the shear applied to the specimen can be monitored continuously. Each linear assembly of rams, pull-rods and load cell is attached to both parts of the frame, by a gimbal arrangement at one end and a spherical bearing arrangement at the other. This allows the two parts of the frame to articulate as the specimen deforms under load, and prevents the frame from restraining the deformation of the specimen. The rams are coupled to a Riehle "Pendomatic" pumping and pressure measuring unit through a four way valve. This permits pressure to be supplied as needed to make rams A advance and rams B retract, or vice versa.

Four small screwjacks positioned between the two parts of the frame are used together with a jig-plate, to align the two parts of the frame accurately before the concrete specimen is put in place. During test the screw jacks are retracted so as not to restrain movement of the two parts of the frame.

Both the slip (or relative motion parallel to the shear plane of the two halves of the specimen), and the separation (or relative motion normal to the shear plane of the two halves of the specimen), were measured continuously using linear differential transformers as the sensing elements of slip and separation gages attached to reference points embedded in the face of the specimen. The separation gage was located at the middle length of the shear plane and the slip gage 2 inches below it, as can be seen in Fig. 2.3. The embedded reference points were located 1 1/2 inches either side of the shear plane. Both the slip and separation gages, and the load cells were monitored continuously during the test by a Sanborn strip chart recorder. The slip and separation gages were calibrated directly before test, using a micrometer

head to impose pre-determined displacements on the core of the linear differential transformer. The load cells were calibrated in a hydraulic testing machine, using specially fabricated equipment to enable the load cells to be subjected to tension and compression alternately without removal from the testing machine.

2.5 Testing Procedures

2.5.1 Initial Cracking - All the specimens except those of Series N were cracked in the shear plane before being subjected to shear loading. The crack was produced by applying line loads to the back and front faces of the specimen along the line of the shear plane. To do this, the specimen was placed in a horizontal position and the line loads were applied through a pair of round edged steel wedges by the Baldwin testing machine, as shown in Fig. 2.4. The dilation of the specimen normal to the shear plane was measured during the cracking operation, using dial gages attached to a reference frame surrounding the specimen. Loading was continued until an average dilation of about 0.013 inches was obtained. When the line loads were removed a residual dilation of 0.010 inch remained.* This was the average initial width of the crack in the shear plane before shear was applied to the specimen.

2.5.2 Shear Loading - In the case of the monotonically loaded specimens, the shear was simply increased continuously until failure occurred. Failure was considered to have occurred when the shear along the shear plane could not be increased further and slip and separation both increased rapidly. Continuous measurements of applied shear, slip and separation were made during the test, and continuing for some time after failure.

*In all specimens except L2M and L3C for which the initial crack widths were 0.012 and 0.011 respectively.

In the case of the cyclically loaded specimens, the shear was first of all continuously increased to 50 percent of the calculated shear transfer strength, the shear was then reduced to zero. Immediately following this, a shear of opposite sign was applied to the specimen, again being continuously increased to 50 percent of the calculated shear transfer strength. The shear was then reduced to zero, so completing the first cycle of loading. This process was continued until 10 cycles of loading had been completed. The maximum positive and negative values of shear were then increased by 8 percent of the calculated shear transfer strength, i.e. to ± 58 percent of V_u (calc.) for the next 5 loading cycles. After each succeeding 5 cycles of load the maximum positive and negative shear was increased by the same increment of 8 percent of the calculated shear transfer strength. This process was continued until failure of the specimen occurred.

In all these tests, continuous records were obtained of applied shear, slip and separation.

The calculated ultimate shear transfer strength of the specimens was based on the mean equation proposed by Mattock ⁽⁵⁾:

$$v_u = 400 + 0.8\rho f_y \quad \dots\dots\dots (2.1)$$

$$\text{but } \neq 0.3f'_c$$

or
$$V_u = A_{cr} (400 + 0.8\rho f_y) \quad \dots\dots\dots (2.2)$$

$$\text{but } \neq 0.3f'_c A_{cr}$$

III - TEST RESULTS

3.1 Loading History and Ultimate Strength

The loading history and the ultimate shear transfer strength of each specimen tested is given in Table 3.1.

The ultimate shear is defined as the maximum shear carried by the specimen during the test. In a cyclic loading test this may be either the maximum shear to which the specimen has been cycled, or the maximum shear reached when the maximum shear was being increased at the end of a group of cycles of load to a constant maximum shear.

Specimen failure was characterized by both slip and separation increasing rapidly with the load carried by the specimen either held constant or decreasing.

3.2 Specimen Behavior

3.2.1 Monotonic Loading Tests - The behavior of the monotonically loaded specimens was in general similar to that of the monotonically loaded push-off specimens, reported in Part I (1). Both slip and separation occurred at all levels of applied shear, (as may be seen in Figs. 3.1 and 3.2,) the rate of slip and separation increasing as the shear increased.

Diagonal tension cracks occurred adjacent to the shear plane in all specimens, more cracks occurring in the more heavily reinforced specimens. In the monolithic specimens and in the bonded, composite specimens, the cracks were uniformly distributed along the shear plane. In the composite specimens in which bond at the interface was deliberately broken, the cracks tended to concentrate in the vicinity of the shear transfer reinforcement. In these specimens also, a few cracks perpendicular to the shear plane occurred near failure, at the locations of the shear transfer reinforcement.

Failure was assumed to have occurred when the applied shear could not be increased and both slip and separation were increasing rapidly. At failure a slight amount of spalling occurred adjacent to the shear plane in most specimens. The spalling was most pronounced in the specimens in which the bond at the interface was broken. In these specimens the spalling occurred primarily in the vicinity of the shear transfer reinforcement.

3.2.2 Cyclic Loading Tests - In these tests, the response of the specimens changed as the number of cycles of loading and the level of loading increased. This is illustrated in Figs. 3.3 and 3.4, which show typical shear-slip and slip-separation curves at different stages of loading for initially cracked specimens, (both monolithic and composite.)

In these figures, positive shear and positive slip are shear and slip measured in the direction in which shear was first applied to the specimen. The separation plotted in all figures in this report, is the change in separation due to application of shear to the specimen. (To obtain the total separation, the initial crack width and/or the width of any gap at the interface due to use of the bond breaking agent, must be added to the separation shown in the figures.)

Response to the first cycle of loading is characterized by a gradual reduction in shear stiffness as the applied shear is increased in both positive and negative directions, and by retention of almost all of the slip caused by the maximum shear until the shear reduces to about half its maximum value. This can be seen in Fig. 3.3(a).

Response to succeeding cycles of load is characterized by a low shear stiffness at low values of shear and a gradual increase in shear stiffness with increase in shear in both positive and negative directions. As the

number of load cycles increases, the shear stiffness at low shears decreases and the increase in shear stiffness with increase in shear becomes greater. This results in the shear-slip curve for a complete cycle of load assuming a progressively more pinched appearance as the number of load cycles increases. This trend in behavior was particularly marked in the case of Series P, in which the bond at the interface was deliberately broken and the specimens were also cracked before testing.

The slip at maximum shear increased slightly each cycle, for about the first five cycles. Thereafter, except for the specimens in which the bond at the interface was broken, the specimens responded in a stable manner. The slip at maximum shear and the shape of the shear-slip curve remained essentially the same for a given maximum shear, until the maximum shear reached about 90 percent of the load at which failure occurred. At and above this load, the slip at maximum shear increased with each cycle, and by progressively increasing amounts. The characteristic shape of the shear-slip curve also changed, in that after increasing as the shear increased, the shear stiffness then decreased again as the maximum shear was approached, see Fig. 3.3(c). Failure occurred when the shear stiffness under increasing load reduced to zero, after which the slip increased rapidly even though the shear was decreasing.

In the case of the specimens in which the bond at the interface was broken, the slip at maximum shear increased by varying amounts in all load cycles. The increase in slip at maximum shear, without increase in shear, was greatest in Series P, in which the specimens were also cracked before testing. In these specimens also, the shear stiffness at shears near zero was very small and the shear slip curves became very "pinched" and elongated.

The shear-slip curves were in general approximately symmetrical about

both the shear and the slip axes. However, in some cases more slip occurred at maximum load due to shear acting in one direction than in the other. This was presumably due to irregularities in the shape of the crack surfaces. The general shape of the shear-slip curve was unaltered, but the relative motion of the two halves of the specimen became centered on a relative position different from the starting position.

In all the initially cracked specimens, the separation at zero shear decreased during about the first five cycles of loading. The crack width at zero shear usually stabilized at from 3 to 5 thousandths of an inch less than the initial value. When this occurred, the slip-separation curve also stabilized, its form being similar to that shown in Fig. 3.4(b). The exact shape of the slip-separation curve would be a function of the profile of the crack faces in any particular case. As the maximum shear per cycle increased, both the slip and the separation at maximum shear increased, but the separation at zero shear remained approximately constant until shortly before failure. However, in the last few load cycles before failure, the separation at zero shear increased with each cycle of load, as shown in Fig. 3.4(c). This increase in separation at zero shear occurred in the same cycles in which the shear stiffness started to decrease when approaching maximum shear, and the slips at maximum load increased significantly with each cycle of load.

In the case of the Series N specimens in which bond at the interface was broken, but the specimens were not cracked before testing, the separation of zero shear did not decrease initially, but subsequent behavior was similar to that of the specimens in the other test series.

Samples of the shear-slip and slip-separation curves obtained for each type of specimen, are shown in Appendix B. These curves show examples of

initial behavior, stable behavior at intermediate loads, and behavior approaching failure.

Diagonal tension cracks occurred in all specimens subjected to cyclic loading. Two sets of cracks occurred, both inclined at 45 degrees to the shear plane, and at right angles to one another. The two sets of cracks opened and closed alternately, as the direction of the applied shear was reversed. Until near to failure, the cracks were almost invisible at zero load. As in the case of the monotonic tests, the cracks were fairly uniformly distributed along the shear plane in the case of the monolithic specimens and the composite specimens in which the bond at the interface was not broken. In the case of those specimens in which the bond at the interface was broken, the diagonal tension cracks tended to concentrate in the vicinity of the shear transfer reinforcement. In these specimens a few cracks also occurred perpendicular to the shear plane, in the vicinity of the shear transfer reinforcement.

At failure, one set of diagonal tension cracks widened and compression spalling of the concrete occurred adjacent to the shear plane. This spalling was more extensive than in the case of the specimens subject to monotonic loading.

In the case of the Series Q specimens, much more extensive cracking and spalling occurred in the 3000 psi concrete than in the 6000 psi concrete.

IV - DISCUSSION OF TEST RESULTS

4.1 General Behavior

To facilitate the subsequent discussion of specimen behavior, it is convenient to define here the ways in which shear resistance is developed, when shear acts along a crack which is crossed at right angles by reinforcement; they are as follows:

1. By friction between the faces of the crack; due to the tension force developed in the reinforcement, as a result of separation of the rough crack faces when slip occurs.
2. By direct bearing of small asperities projecting from the faces of the crack.
3. By dowel action of the reinforcement crossing the crack; i.e. direct resistance of the bars to shearing action at the crack.

The probable inter-relation of observed behavior and the mechanics of shear transfer in cracked monolithic concrete subject to cyclically reversing shear along the crack, have been discussed in detail previously ⁽⁶⁾. The results obtained in this current study support the hypotheses contained in that discussion. The similarity in behavior of the specimens of Series L and M indicate that the hypothesised mechanics of behavior are probably also applicable to the transfer of shear across an initially cracked, rough, bonded interface between concretes cast at different times.

A summary of the probable mechanics of behavior is as follows:

1. During the first load cycle; - At low loads on first applying shear, the shear stiffness is very high and little or no separation occurs. This indicates that, at this stage, most of the resistance to shear comes from the direct bearing of asperities on the faces of the crack. As increasing numbers

of asperities are crushed, the intensity of bearing pressure on the remaining asperities increases more rapidly than the applied shear. Deformations therefore increase more rapidly, i.e., the shear stiffness decreases.

When the shear is reduced to zero, the slip does not reduce until the applied shear is less than the net restoring force due to the combined effects of elastic deformation of the reinforcing bars and of the concrete against which they bear, and any friction between the crack surfaces. When the applied shear is zero, some slip remains, corresponding to whatever frictional force continues to act between the crack faces.

As the shear is increased in the reverse direction for the first time, the mechanisms by which shear resistance is developed are the same as on first loading. The behavior on unloading will also be similar to the behavior on first unloading in the opposite direction.

2. Subsequent loading cycles; - In order for the asperities to be brought into bearing, a slip must occur almost equal to the maximum slip which has previously occurred. While this slip is occurring, shear resistance is developed only by dowel action of the reinforcement and by any small friction between the crack faces. The shear stiffness is consequently much lower than in the first cycle of loading, (see Fig. 3.3.) When the asperities come into bearing, further slip requires deformation of the asperities. The resistance of the asperities to deformation results in a sharp increase in resistance to shear and an increasing tangent shear stiffness until the maximum shear is reached.

On removing the shear the response and underlying mechanism of behavior are as in the first cycle. When the shear is reversed in direction, the response and mechanism of behavior is as just described.

With each cycle of load, the surfaces in contact are abraded and become smoother. This further reduces the frictional resistance to shear at low shears and is reflected in a further reduction in shear stiffness at low shears.

As the maximum shear is increased, the maximum slips and separations become greater. This leads to the development of larger dowel forces and tensile strains in the reinforcing bars. At high values of maximum shear, an increasing fraction of the shear is resisted by friction between the crack surfaces and by dowel action.

3. Loading cycles approaching failure; - In these cycles the separation at zero shear starts to increase, the shear stiffness approaching maximum shear starts to decrease, and both slip and separation at maximum shear increase significantly in each cycle. This behavior is in large part due to local crushing of the crack faces. Some of the mortar particles produced by this become trapped between the faces of the crack, wedging it open and acting like "ball bearings" when the crack faces move relative to one another. Progressive yielding of the reinforcing bars, under the combination of direct tension and of bending and shear resulting from dowel action, will also contribute to the deterioration in behavior at this stage.

It can be seen in Figs. 3.1, 3.2, 4.1, 4.2 and 4.3, and Table 3.1, that the behavior and strength of the initially cracked composite specimens with good bond at the roughened interface, was very similar to that of the initially cracked, monolithic specimens in both the monotonic and cyclic loading tests. This was also found to be the case in the earlier ⁽¹⁾ monotonic loading tests.

In the case of composite specimens, in which bond at the interface was

deliberately prevented, the behaviour in monotonic loading tests ⁽¹⁾ was found to be similar to that of initially cracked, bonded composite specimens. However, in cyclic loading tests the behaviour of the unbonded composite specimens deteriorated much more rapidly than did that of the initially cracked, bonded specimens. (see Fig. 4.1, 4.3 and 4.4*). It can be seen that in the unbonded composite specimens, the slip at maximum shear never stabilized for a given range of shear, as was the case in cracked, bonded composite specimens and cracked, monolithic specimens.

The ultimate shear transfer strengths under monotonic loading obtainable with both cracked, bonded, and unbonded interfaces were found ⁽¹⁾ to be almost the same for low and medium values of $\rho_f y$. In the cyclic loading tests, however, the ultimate strengths obtained when bond was prevented at the interface were only about 60 percent of the strength of comparable initially cracked, bonded composite specimens. The difference in behavior of the specimens with these two types of interface is thought to be due to the difference in the minor roughness of the interfaces in the two cases. The major roughness, corresponding to the large amplitude deliberate roughening of the interface, would be similar in both cases.

Previous studies ⁽⁷⁾ have indicated that shear transfer behavior is significantly influenced by the minor or small amplitude roughness of the shear plane, which is super-imposed on the large amplitude roughness. In a cracked monolithic specimen the major roughness is due to the propagation of the crack around large aggregate particles, while the minor roughness is due to the propagation of the crack around the sand particles. In the case of the cracked, bonded composite specimens it is likely that the crack propagated along and close to the formed interface, but that sand particles

*In these figures, the slip plotted for cyclic loading tests is the numerical average of the slip occurring at the maximum positive and negative shears in each load cycle.

would be exposed so as to create minor roughness conditions over a major part of the shear plane, approaching that for a crack in monolithic concrete. This minor roughness in the cracked, bonded composite specimens was evidently able to resist the repeated abrasion of cyclic loading as effectively as was the minor roughness in the cracked monolithic concrete, since in both cases the reduction in shear transfer strength due to cyclic loading was about the same.

In the case of the composite specimens in which bond at the interface was deliberately broken, the reduction in shear transfer strength due to cyclic loading was very much greater than in the case of the cracked, bonded composite specimens. The bond breaker formed the equivalent of a fine crack at the interface, and the major roughness was probably the same as for the cracked, bonded composite specimen. However, the minor roughness would only be that formed incidentally in the mortar, when the interface was roughened at the time the first half of the specimen was cast. In this case, the interface would have a coating of cement paste and some of the minor roughness would simply be small indentations in the cement paste. The minor roughness of such an interface would be softer and less able to resist the repeated abrasion of cyclic loading, than would the minor roughness consisting of exposed sand grains in the cracked, bonded composite specimens and cracked monolithic specimens.

The shear-slip curves obtained for the unbonded composite specimens of Series N are similar to the shear-slip curves obtained ⁽⁶⁾ in cyclic loading tests of cracked, monolithic all-lightweight concrete. In that case also, minor roughness resulting from the crack propagating around sand grains was absent.

The test results reported here indicate the absolute necessity for good bond at an interface in composite construction, or at a construction joint in cast-in-place construction, if that interface or joint is likely to be subject to cyclic reversals of load such as occur in earthquakes. It is clearly vital that adequate inspection be provided to ensure that (1) the interface is properly roughened, and (2) that the interface is thoroughly cleaned to ensure good bond between the two concretes meeting at the interface.

The unbonded composite specimens of Series P were also cracked in addition before testing. Figs. 3.1, 4.1 and 4.5 show the deleterious effect that this combination of cracking and absence of bond at the interface, had on shear transfer behavior and strength. The behavior of these specimens was very similar to that observed ⁽⁶⁾ in cracked, monolithic specimens previously tested, in which the crack width was between 0.020 and 0.025 inches. The lower shear stiffness and strength, and the "flat top" shape of the shear-slip curve occurred in both cases. The similarity in behavior is reasonable, since the total width of the crack in the Series P specimens at the start of the test would be the sum of the width of the gap at the interface caused by use of the bond breaker, plus the 0.01 inch widening due to the cracking process. The total crack width would probably approach 0.02 inches.

The effect of an increase in crack width is to reduce the engagement of asperities on the faces of the crack. This results in higher local bearing stresses on the remaining asperities in contact, for a given shear. This in turn leads to greater deformation of the asperities and to larger slips. Also, for a greater initial crack width a larger slip is necessary to produce a given separation of the faces of the crack, in order to produce a given

reinforcement tension and consequent frictional resistance to shear.

The behavior under cyclic loading of the Series Q cracked, bonded composite specimens in which concrete strengths of 6000 and 3000 psi were used, was similar to that of the Series M cracked, bonded composite specimens in which both concretes had a strength of 6000 psi. As may be seen in Fig. 4.6., the slip at maximum shear did not increase significantly while the maximum shear was held constant. The deformations were somewhat greater and the strengths somewhat less in the Series Q specimens than in the Series M specimens, reflecting the fact that failure occurred primarily in the 3000 psi concrete in the Series Q specimens, as compared to the 6000 psi concrete of the Series M specimens. Large changes in the character of the response to cyclic loading appear to result from changes in the interface condition, i.e., roughness, effectiveness of bonding at the interface, and width of crack; rather than from changes in concrete strength.

4.2 Ultimate Shear Transfer Strength

In Table 4.1 a comparison is made of the ultimate strengths of companion pairs of specimens, one of which was subjected to cyclic loading and the other to monotonic loading.

With the exception of Series N, the reduction in strength due to cyclic loading was approximately the same as had been observed previously ⁽⁶⁾ in tests of initially cracked, monolithic concrete specimens. In those tests, the overall average value of the ratio of the strength under cyclic loading to the strength under monotonic loading was 0.83 for sand and gravel concrete and 0.79 for lightweight concrete. On the basis of those tests, it was recommended that for design purposes, the shear transfer strength under cyclically reversing loading should be taken as 0.8 of the calculated shear

transfer strength under monotonic loading. The results of this present study indicate that the recommendation is also applicable to the case of shear transfer across an interface between concretes cast at different times, providing the interface is roughened as required by Sec. 11.15.7 of ACI 318-71 (2) and precautions are taken to obtain good bond at the interface.

The strengths under cyclic loading of the specimens of Series N and P, in which bond at the interface was broken, was only about 60 percent of the strength of comparable specimens with bond intact, subject to monotonic loading. These test results indicate the importance of good bond at the interface between concretes cast at different times, if that interface is to be subject to cyclically reversing loads. Such a situation is a construction joint in a shear wall intended to resist earthquake forces.

It can be seen in Fig. 4.7, that the shear transfer strengths under monotonic loading, of both the initially cracked, monolithic specimens, and the initially cracked, composite specimens with good bond at the interface, are conservatively predicted by equation (2.1).

$$v_u = 0.8 \rho f_y + 400 \text{ psi} \quad (2.1)$$

$$\text{but } \leq 0.3 f'_c$$

This equation is quite conservative for the Series L and M specimens, for which $f'_c = 6000$ psi. This is consistent with the data presented in Part I of this Final Report (1). It was suggested there that the constant 400 psi might reasonably be replaced by a function of concrete compressive strength. $6.5\sqrt{f'_c}$ would be a possible value. Such a function of f'_c probably would reflect the contribution to shear transfer strength of the resistance to shearing off of asperities on the crack faces.

V - PRINCIPAL CONCLUSIONS

Based on the test data reported, the following conclusions may be drawn concerning shear transfer across an interface between concretes cast at different times, when subject to cyclically reversing shear.

1. If the interface is roughened as prescribed in Sec. 11.15.7 of ACI 318-71 and if good bond is obtained at the interface, then, after cracking, the shear transfer behavior will be essentially the same as in the case of shear transfer across a crack in monolithic concrete.

2. If the interface is as specified in 1, above, the shear transfer strength under cyclically reversing shear, may for design purposes be taken as 80 percent of the calculated shear transfer strength for monotonic loading.

3. If bond at the interface is destroyed, the shear transfer behavior under cyclic loading deteriorates rapidly and the shear transfer strength is only about 60 percent of the shear transfer strength under monotonic loading.

4. The concentration of cracking in the vicinity of the reinforcement in composite specimens in which bond at the interface was destroyed, indicates that with this interface condition a considerable proportion of the shear must be transferred across the interface by dowel action.

5. Because of the considerable influence on shear transfer behavior and strength, of interface roughness and of bond at the interface, every precaution should be taken to obtain adequate roughness and good bond at interfaces which are likely to be subject to cyclically reversing load, (e.g., construction joints in shear walls designed to resist earthquake forces.)

6. The change in the shape of the shear-slip hysteresis loop after the first cycle of loading, and in particular, the great reduction in shear stiff-

ness at low shear loads, indicates the major contribution to shear transfer resistance that is provided by resistance to shearing off of asperities on the faces of the crack, on first loading by shears of up to about half the ultimate shear.

REFERENCES

1. Mattock, A.H., "Shear Transfer Under Monotonic Loading, Across an Interface Between Concretes Cast at Different Times," University of Washington, Structures and Mechanics Report SM76-3, September, 1976.
2. "Building Code Requirements for Reinforced Concrete," (ACI 318-71), American Concrete Institute, 1971.
3. Hanson, N.W., "Precast Prestressed Concrete Bridges, 2 - Horizontal Shear Connections," Journal of PCA Research and Development Laboratories, V. 2, No. 2, May 1960, pp. 38 - 58.
4. Anderson, A.R., "Composite Designs in Precast and Cast-in-place Concrete," Progressive Architecture, V. 41, No. 9, September 1960, pp. 172-179.
5. Mattock, A.H., "Shear Transfer in Concrete Having Reinforcement at an Angle to the Shear Plane," American Concrete Institute Publication SP-42, "Shear in Reinforced Concrete," 1974, pp. 17 - 42.
6. Mattock, A.H., "The Shear Transfer Behavior of Cracked Monolithic Concrete Subject to Cyclically Reversing Shear," University of Washington, Structures and Mechanics Report SM74-4, November 1974.
7. Mattock, A.H., Li, W.K. and Wang, T.C., "Shear Transfer in Lightweight Reinforced Concrete," Journal of the Prestressed Concrete Institute, Vol. 21, No. 1, January/February 1976, pp. 20 - 39.

TABLE 2.1 - PROGRAM OF TESTS

Series	Type of Specimen	Planned f'_c at test (psi)	Bond Condition of Interface	Initial Condition
L	Monolithic	6000	--	Cracked
M	Composite	6000 & 6000	Bonded	Cracked
N	Composite	6000 & 6000	Bond Broken	Uncracked
P	Composite	6000 & 6000	Bond Broken	Cracked
Q	Composite	6000 & 3000	Bonded	Cracked

TABLE 2.2 - CONCRETE MIX PROPORTIONS (lb./cu. yd)

Concrete Strength f'_c (psi) and Age at Test (days)	3000 4	6000 7	6000 4
Type III Portland Cement	460	680	755
3/4 in. Gravel	1760	1715	1620
Sand	1415	1230	1230

Note: In all mixes, water was provided to produce a 3 inch slump.

TABLE 2.3(a) - PROPERTIES OF SPECIMENS

Specimen No.	Concrete Strength		Reinf. Yield Point, f_y (ksi)	Reinf. Parameter ρf_y (psi)	V_u (calc.) (kips)
	f'_c (1) (psi)	f_t (2) (psi)			
<u>Series L</u> (Monolithic)					
L2M	6120	398	53.6	472	38.9
L2C	6000	380	53.0	466	38.6
L3M	6000	468	53.6	708	48.3
L3C	6145	394	52.2	689	47.6
<u>Series M</u> (Composite)					
M2M	6200 5760	394 400	53.4	470	38.8
M2C	6115 5770	424 356	53.4	470	38.8
M3M	6100 6260	416 360	51.4	678	47.1
M3C	6030 5970	389 407	52.6	694	47.8
<u>Series N</u> (Composite)					
N2M	6120 6120	387 383	53.8	473	38.9
N2C	6160 6120	419 393	53.9	474	39.0
N3M	5750 6170	434 483	53.2	702	48.1
N3C	6220 5820	374 447	53.5	706	48.2

TABLE 2.3(b) - PROPERTIES OF SPECIMENS (continued)

Specimen No.	Concrete Strength		Reinf. Yield Point, f_y (ksi)	Reinf. Parameter ρ_f (psi)	V_u (calc.) (kips)
	f'_c (1) (psi)	f_t (2) (psi)			
<u>Series P</u> (Composite)					
P2M	6150	460	53.8	473	38.9
	5960	354			
P2C	6080	424	53.0	466	38.6
	5750	356			
P3M	6140	460	53.3	704	48.2
	5970	354			
P3C	6150	476	53.6	708	48.3
	5930	450			
<u>Series Q</u> (Composite)					
Q2M	6295	398	49.4	435	37.4
	2750	263			
Q2C	6070	475	51.1	450	38.0
	2790	224			
Q3M	5750	---	52.3	690	47.6
	2945	---			
Q3C	6030	380	53.6	708	48.3
	3010	260			

(1) f'_c = compressive strength measured on 6 x 12 inch cylinders.

(2) f_t = splitting tensile strength measured on 6 x 12 inch cylinders.

(3) Calculated ultimate shear strength, using Eq. (2.2).

TABLE 3.1(a) - TEST RESULTS

Specimen No.	Loading Cycles	History Range of Load + % of \bar{V}_u (calc.)	(1)	(1)	Ultimate Shear Strength (kips)
			Slip at Failure (in.)	Separation at Failure (in.)	
<u>Series L: Monolithic, Initially cracked.</u>					
L2M	(Monotonic)		0.028	0.032	52.7
L2C	1-10	50			
	11-15	58			
	16-20	66			
	21-25	74			
	26-30	82			
	31-35	90			
	36-40	98			
	41-44	106	0.032	0.054	41.7
L3M	(Monotonic)		0.026	0.034	66.1
L3C	1-10	50			
	11-15	58			
	16-20	66			
	21-25	74			
	26-30	82			
	31-35	90			
	36-40	98			
	41-45	106			
46-47	114	0.033	0.026	56.0	
<u>Series M: Composite, Bond intact, Initially cracked.</u>					
M2M	(Monotonic)		0.035	0.026	50.0
M2C	1-10	50			
	11-15	58			
	16-20	66			
	21-25	74			
	26-30	82			
	31-35	90			
	36-40	98			
	41-45	106			
46	114	0.030	0.007	44.2	

TABLE 3.1(b) - TEST RESULTS (continued)

Specimen No.	Loading	History	(1) Slip at Failure (in.)	(1) Separation at Failure (in.)	Ultimate Shear Strength (kips)
	Load Cycles	Range of Load + % of \bar{V}_U (calc.)			
M3M	(Monotonic)		0.017	0.010	59.2
M3C	1-10	50			
	11-15	58			
	16-20	66			
	21-25	74			
	26-30	82			
	31-35	90			
	36-40	98			
	41-45	106			
	46-47	114	0.022	0.038	54.5
<u>Series N:</u> Composite, Bond broken, Initially uncracked.					
N2M	(Monotonic)		0.025	0.014	42.6
N2C	1-10	50			
	11-15	58			
	16-20	66	0.066	0.028	25.7
N3M	(Monotonic)		0.021	0.022	60.9
N3C	1-10	50			
	11-15	58			
	16-20	66			
	21	74	0.030	0.030	35.7
<u>Series P:</u> Composite, Bond broken, Initially cracked.					
P2M	(Monotonic)		0.100	0.036	26.7
P2C	1-10	50			
	11-14	58	0.077	0.023	22.4
P3M	(Monotonic)		0.025	0.006	40.0
P3C	1-10	50			
	11-15	58			
	16-19	66	0.061	0.020	31.9

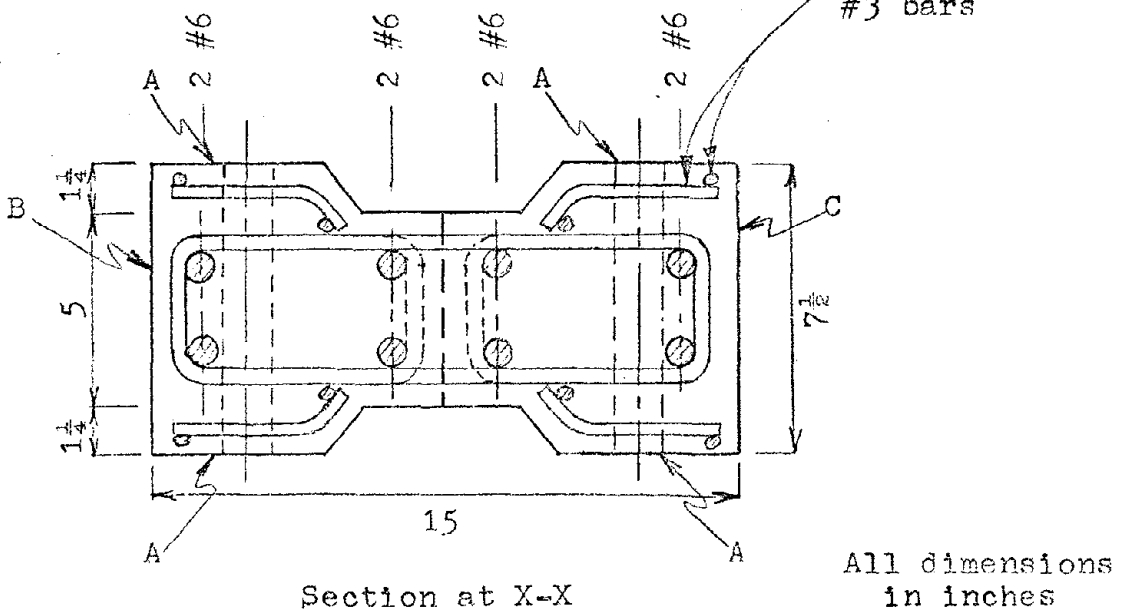
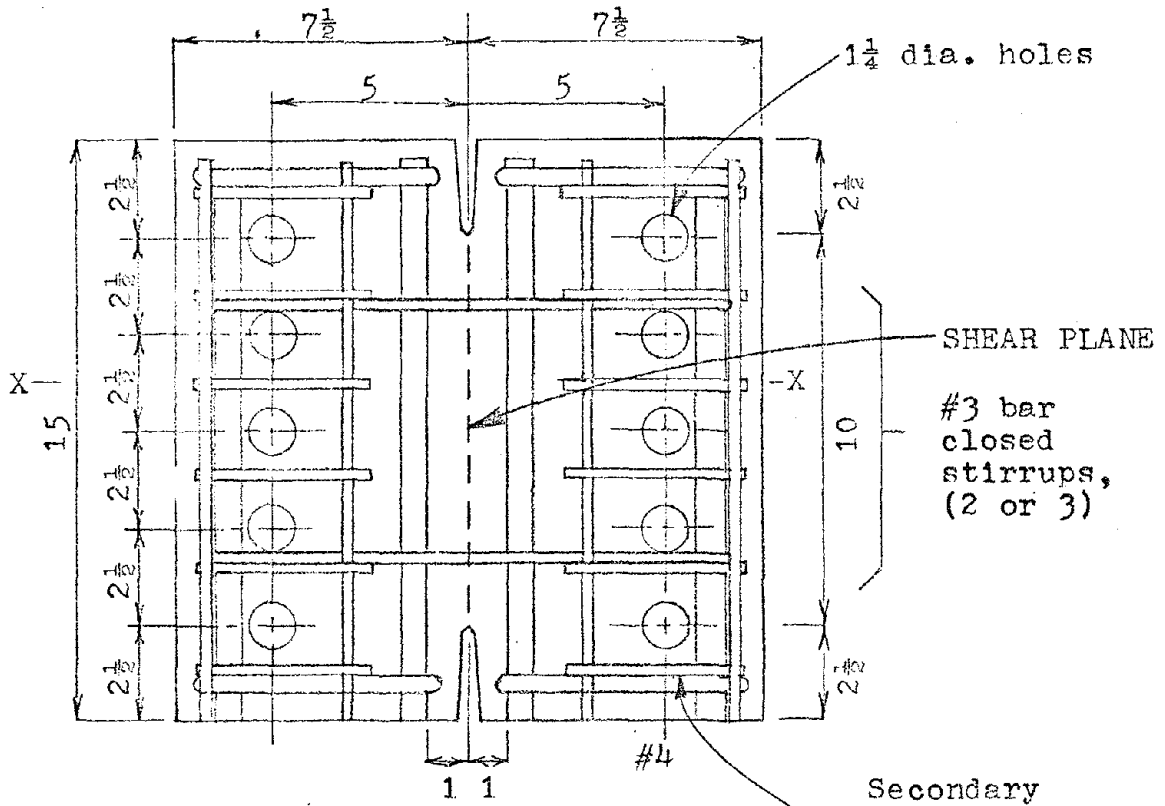
TABLE 3.1(c) - TEST RESULTS (continued)

Specimen No.	Loading	History	(1) Slip at Failure (in.)	(1) Separation at Failure (in.)	Ultimate Shear Strength (kips)
	Load Cycles	Range of Load + % of \bar{V}_u (calc.)			
<u>Series Q:</u> Composite (different concrete strengths), Bond intact, Initially cracked.					
Q2M	(Monotonic)		0.027	0.007	38.0
Q2C	1-10	50	0.038	0.035	38.8
	11-15	58			
	16-20	66			
	21-25	74			
	26-30	82			
	31-35	90			
	36-39	98			
Q3M	(Monotonic)		0.033	0.018	47.2
Q3C	1-10	50	0.032	0.030	43.4
	11-15	58			
	16-20	66			
	21-25	74			
	26-30	82			
	31-32	90			

(1) For cyclic loading, the values of slip and separation tabulated are the averages of the values measured at the maximum positive and negative shears in the last complete load cycle before failure.

TABLE 4.1 - COMPARISON OF ULTIMATE STRENGTH
FOR MONOTONIC AND CYCLIC LOADING

Cyclic Loading Specimen	Monotonic Loading Specimen	$\frac{V_u \text{ (cyclic)}}{V_u \text{ (Monotonic)}}$
<u>Series L:</u> Monolithic, Initially cracked		
L2C	L2M	0.79
L3C	L3M	0.85
<u>Series M:</u> Composite, Bond intact, Initially cracked		
M2C	M2M	0.88
M3C	M3M	0.92
<u>Series N:</u> Composite, Bond broken, Initially uncracked		
N2C	N2M	0.60
N3C	N3M	0.59
<u>Series P:</u> Composite, Bond broken, Initially cracked		
P2C	P2M	0.84
P3C	P3M	0.80
<u>Series Q:</u> Composite (different concrete strengths,) Bond intact, Initially cracked		
Q2C	Q2M	1.02
Q3C	Q3M	0.92



All dimensions in inches

Fig. 2.1 - Cyclic loading specimen

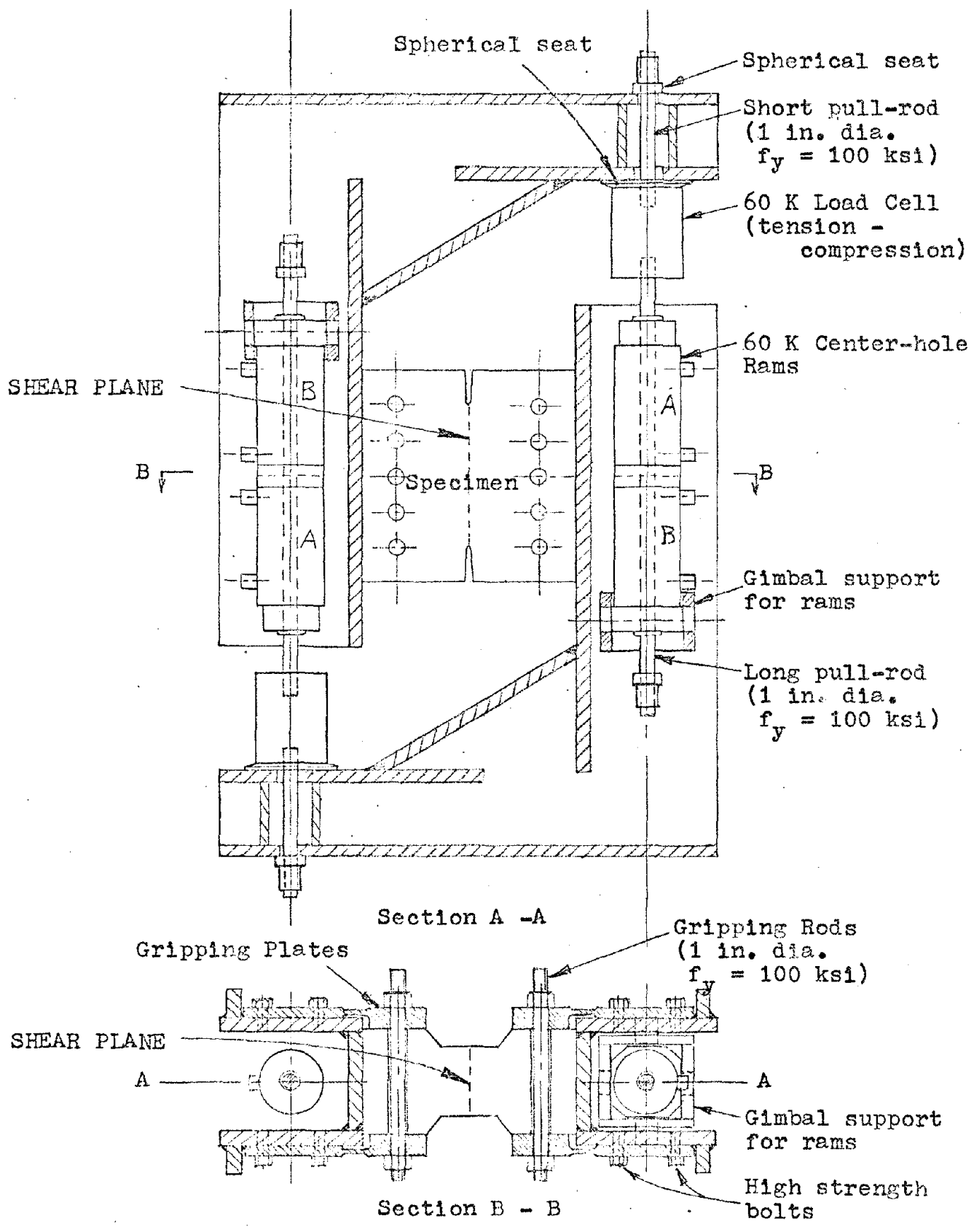


Fig. 2.2 - Cyclic loading test frame

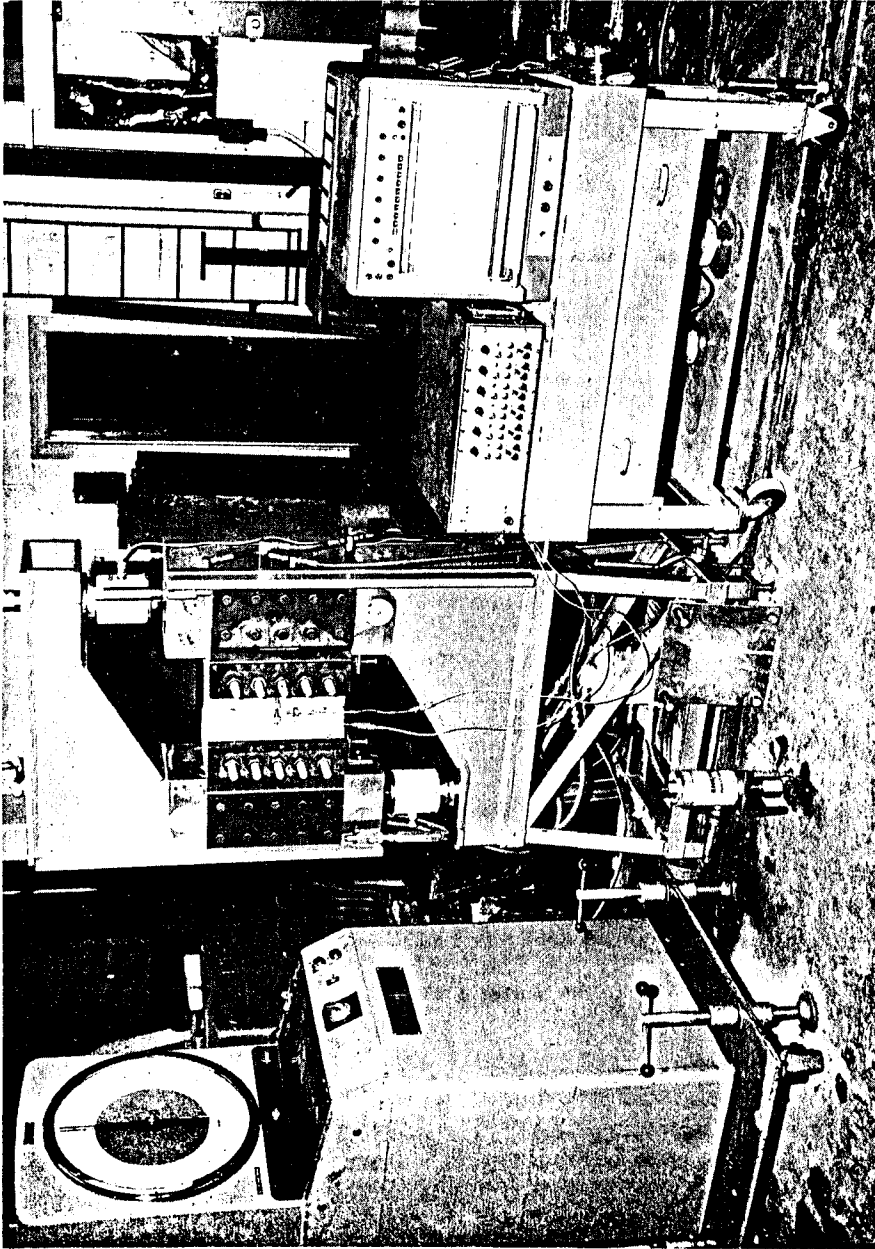



Fig. 2.3 - General view of arrangements for test.

Reproduced from
best available copy. 

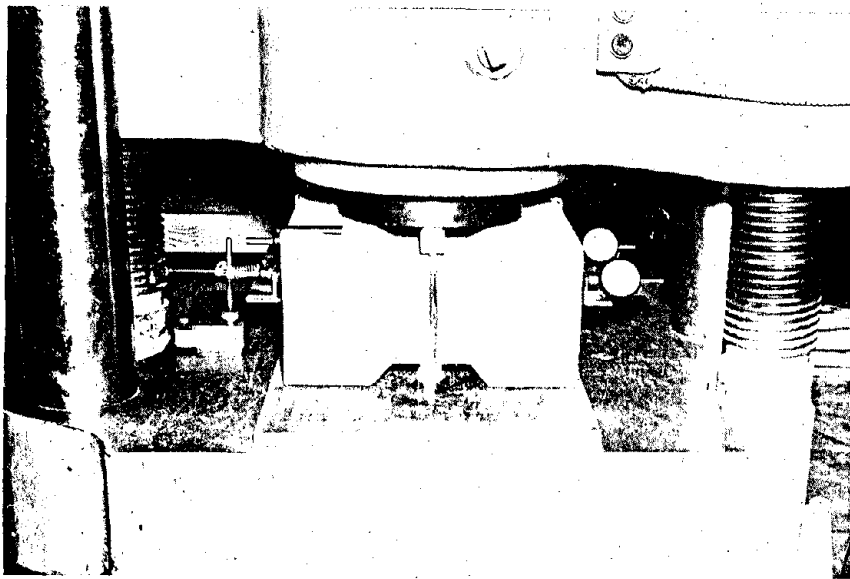
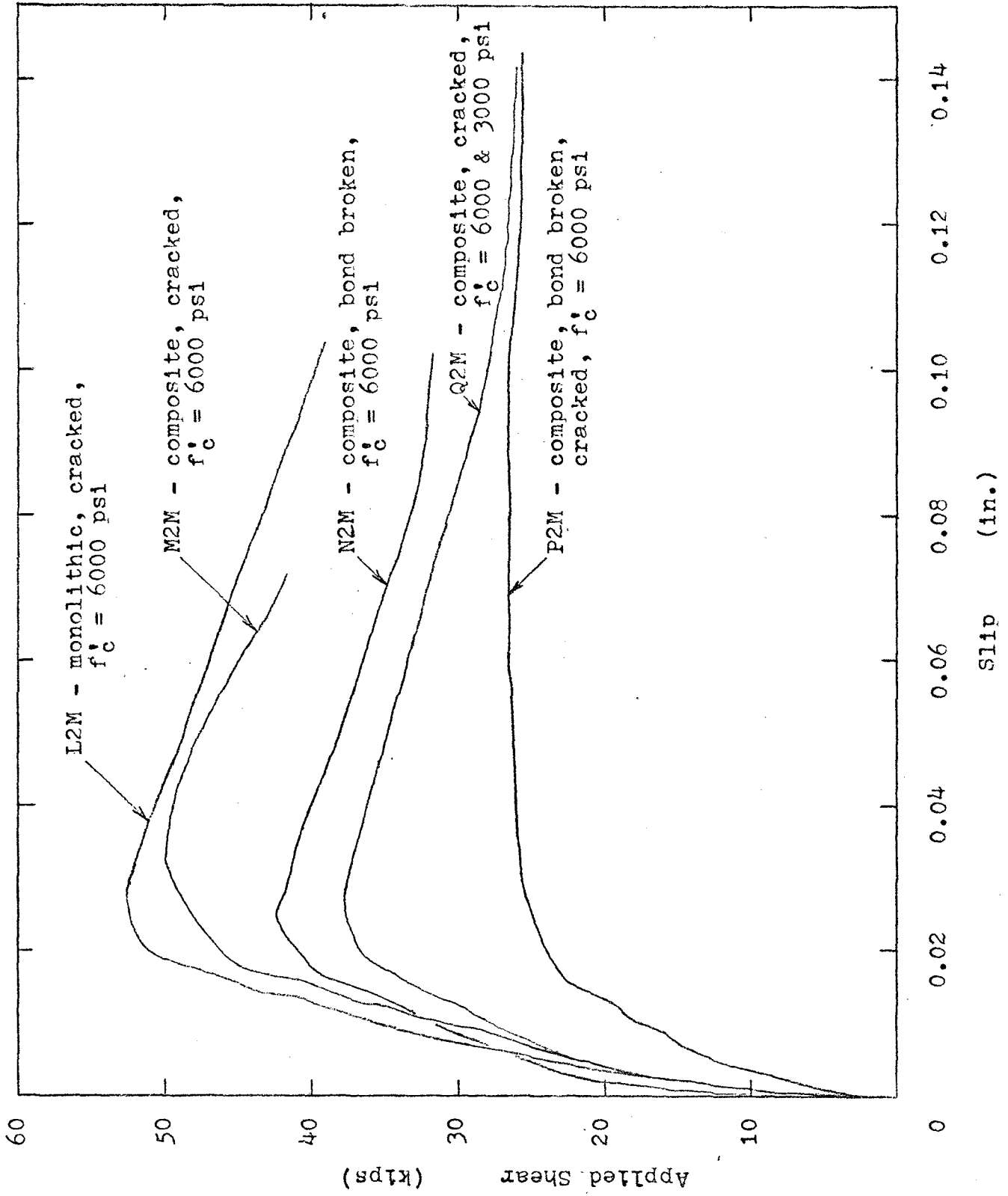


Fig. 2.4 - Initial cracking of specimen



38

Fig. 3.1 - Typical shear - slip curves in monotonic loading tests.

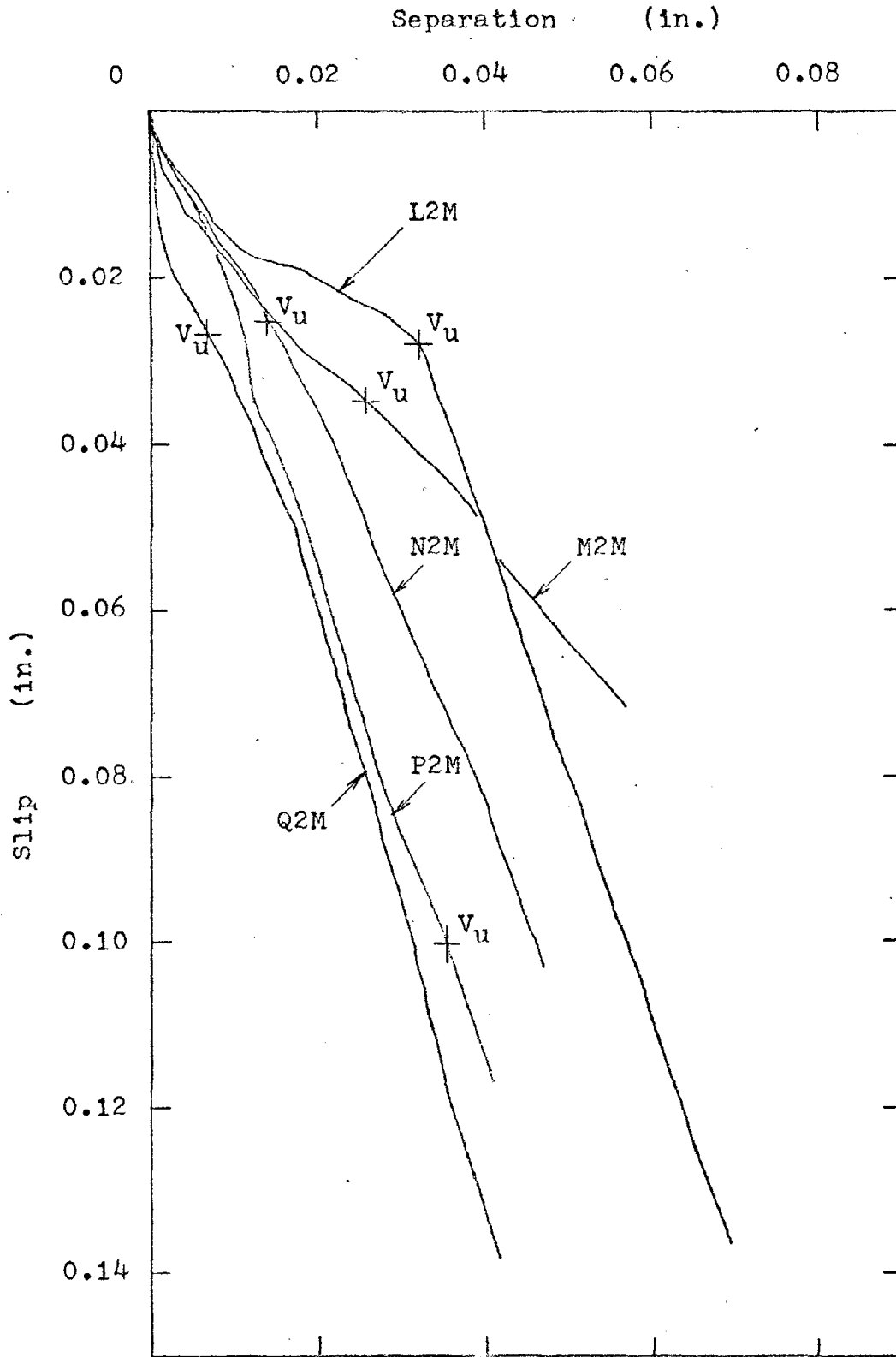


Fig. 3.2 - Typical slip - separation curves in monotonic loading tests.

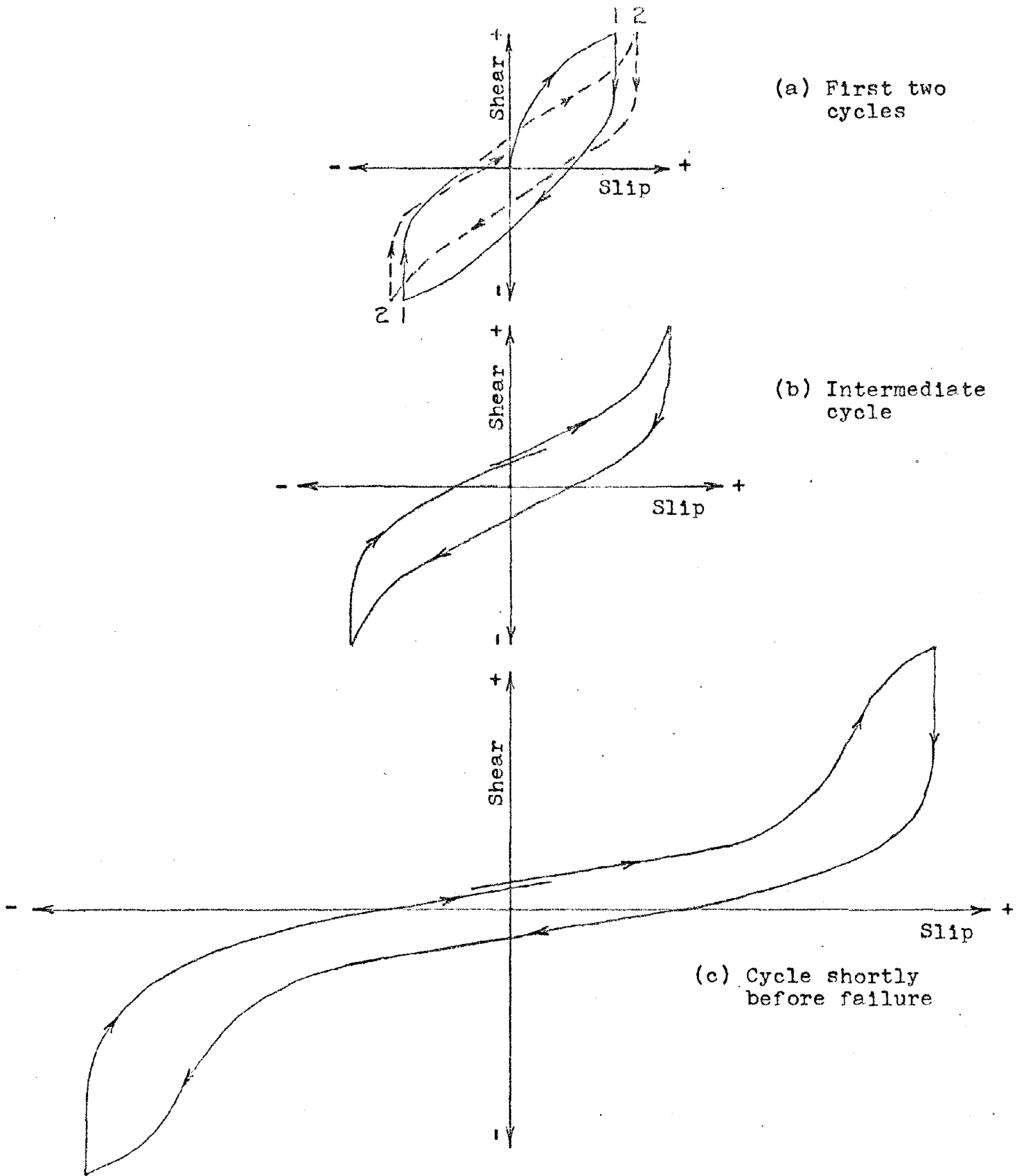


Fig. 3.3 - Typical shear - slip curves in cyclic loading tests.

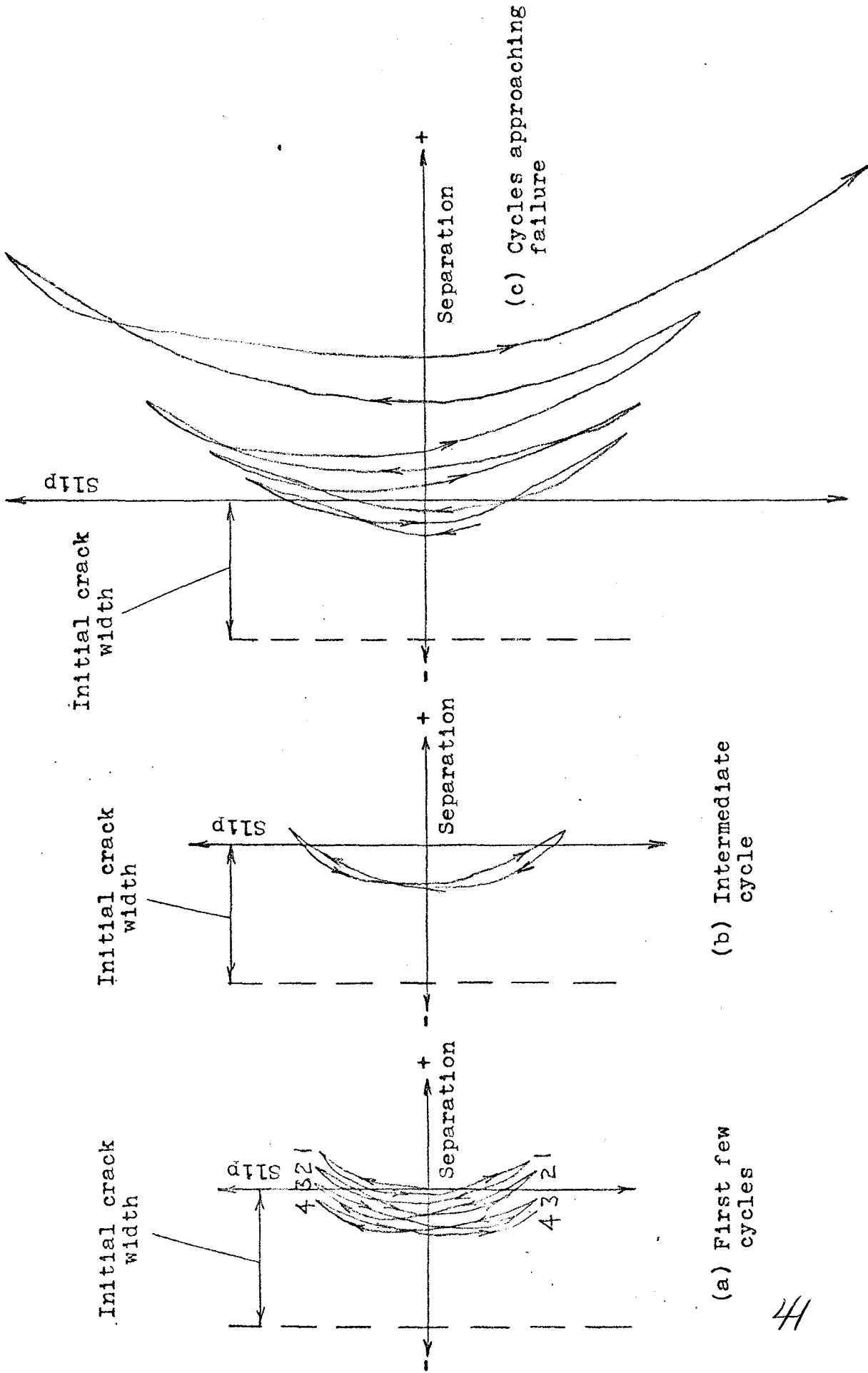


Fig. 3.4 - Typical slip - separation curves in cyclic loading tests.

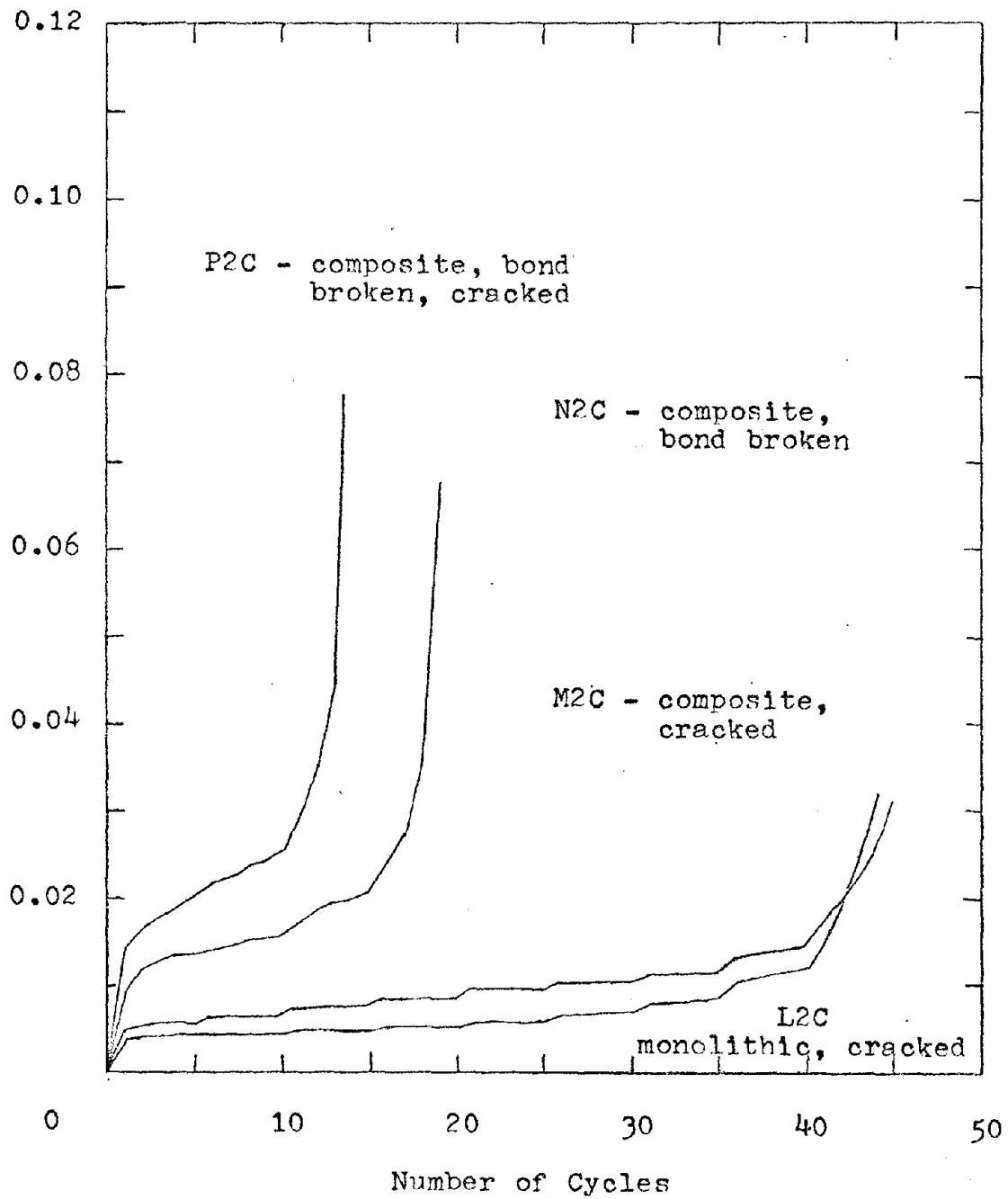


Fig. 4.1 - Variation of slip*at maximum shear with number of cycles of load.

*Numerical average of slip occurring at maximum positive and negative shear in each cycle.

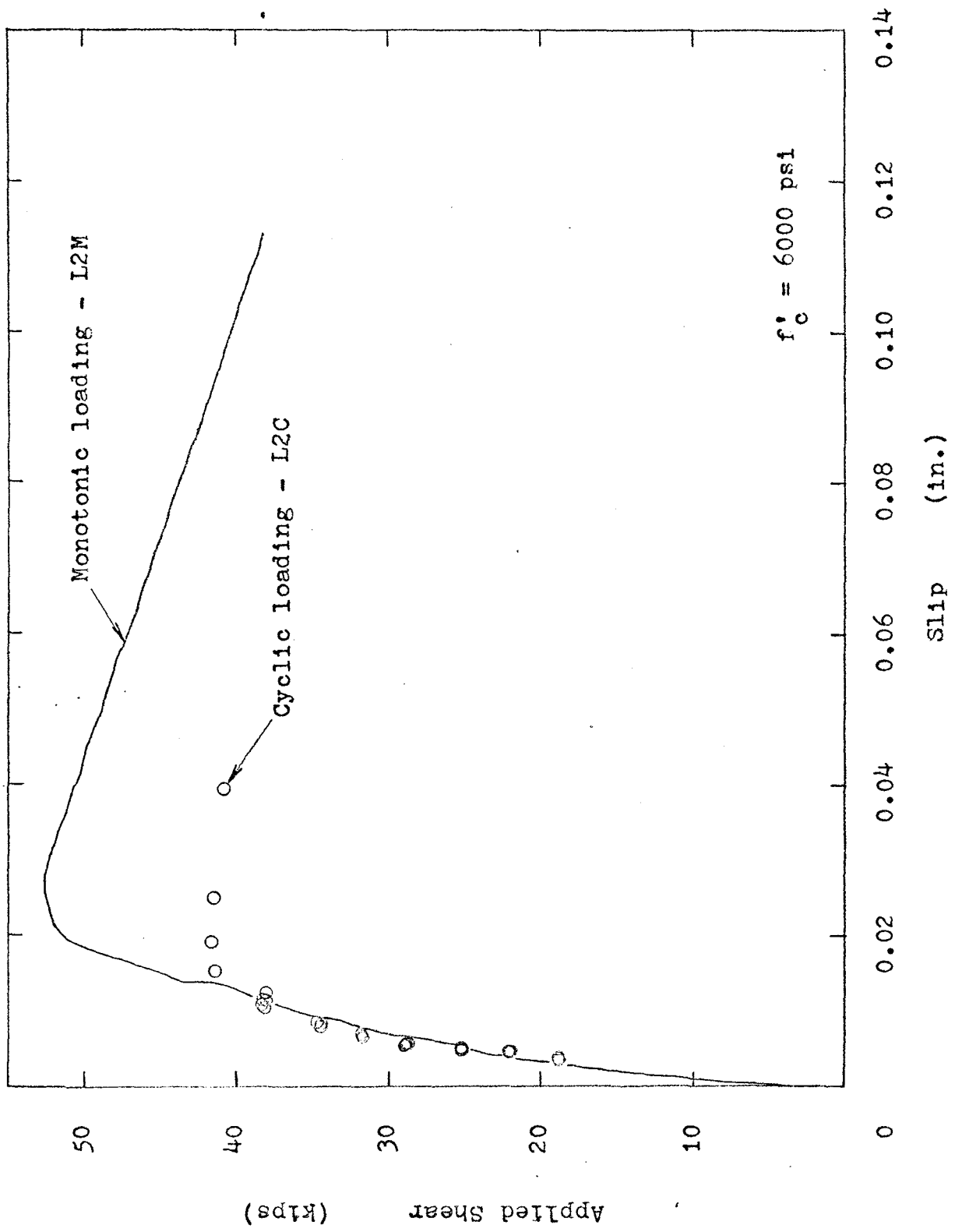


Fig. 4.2 - Comparison of shear - slip relations in cyclic and monotonic loading, for cracked, monolithic concrete specimens.

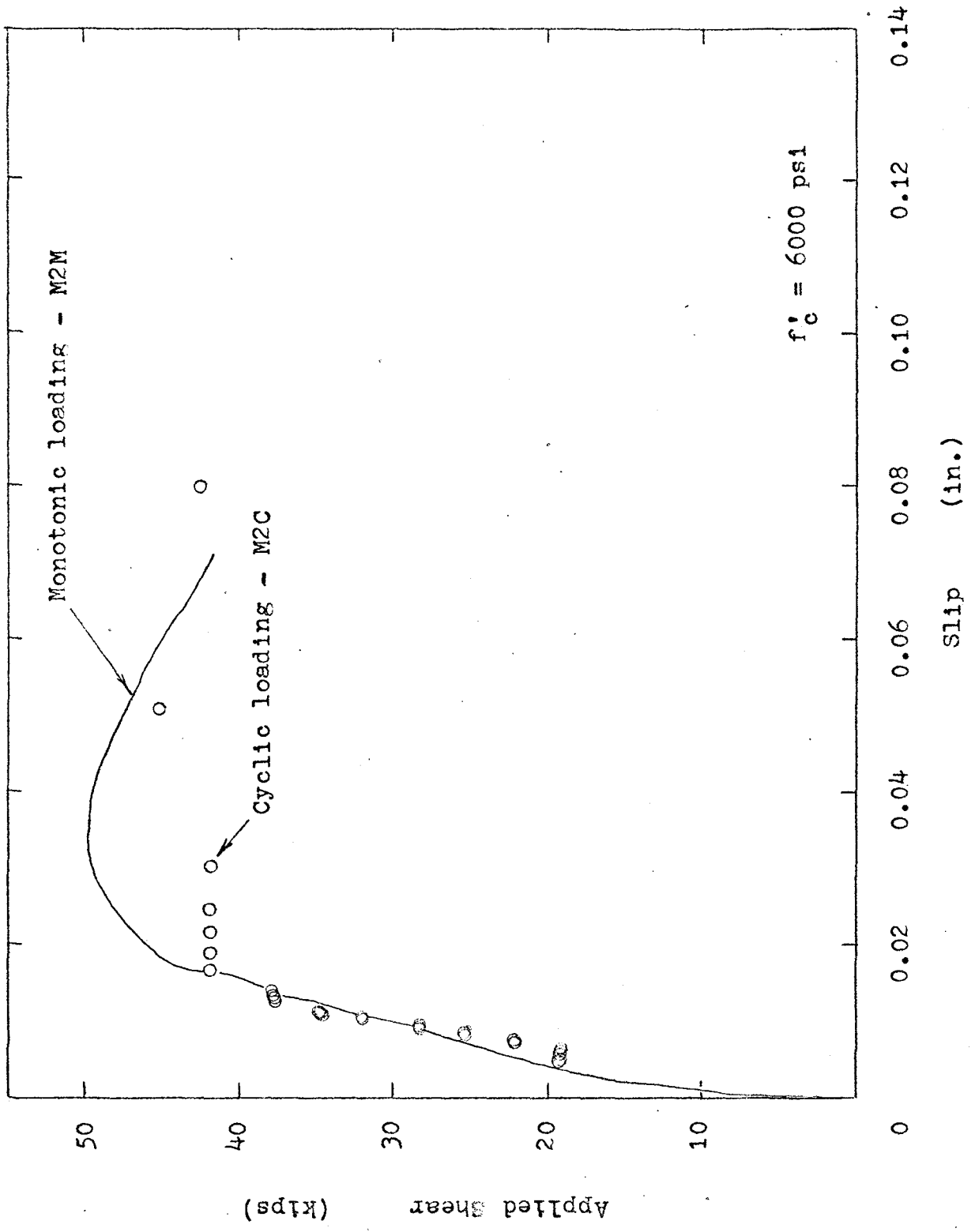


Fig. 4.3 - Comparison of shear - slip relations in cyclic and monotonic loading, for cracked, bonded, composite specimens.

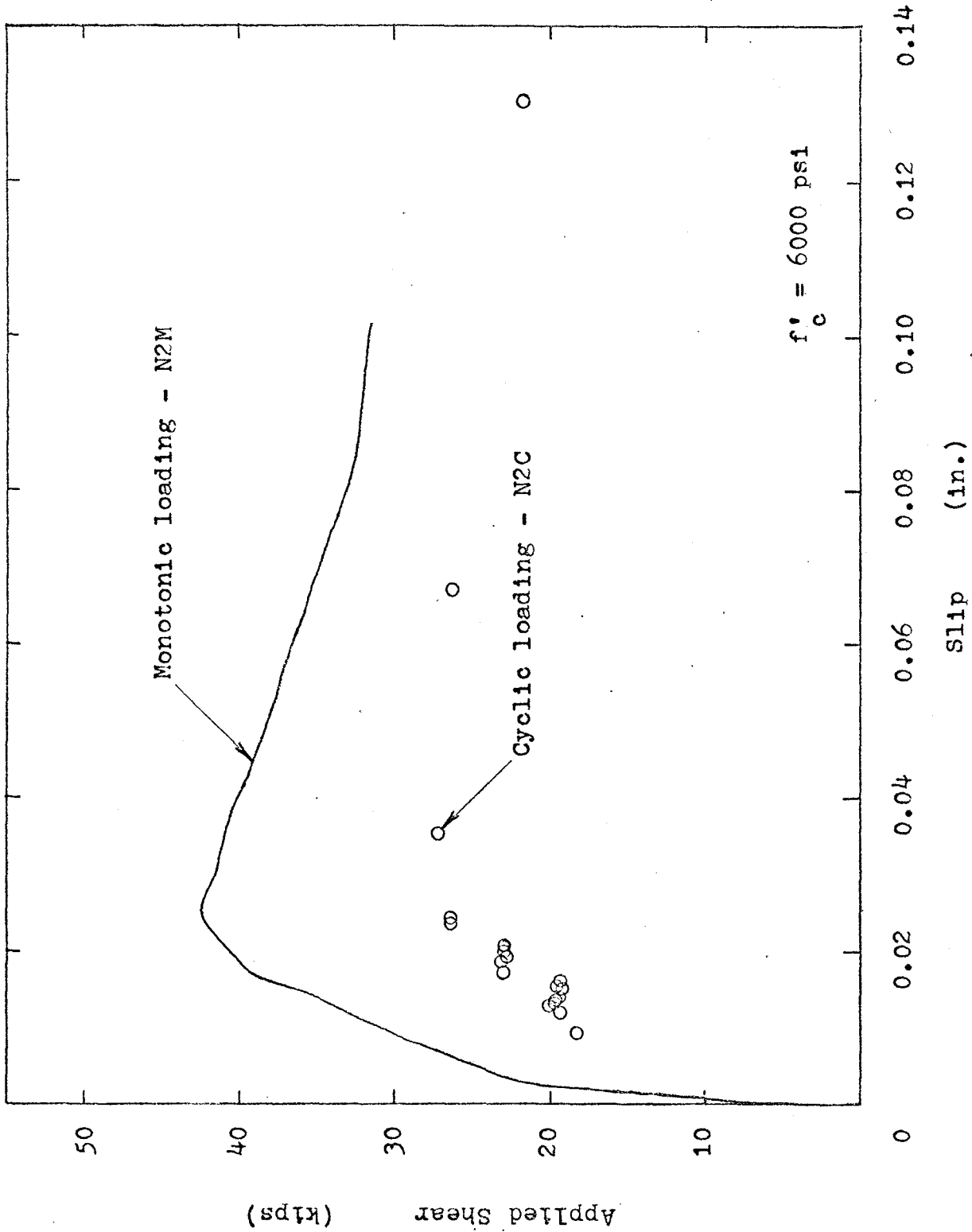


Fig. 4.4 - Comparison of shear - slip relations in cyclic and monotonic loading, for composite specimens with bond broken.

45

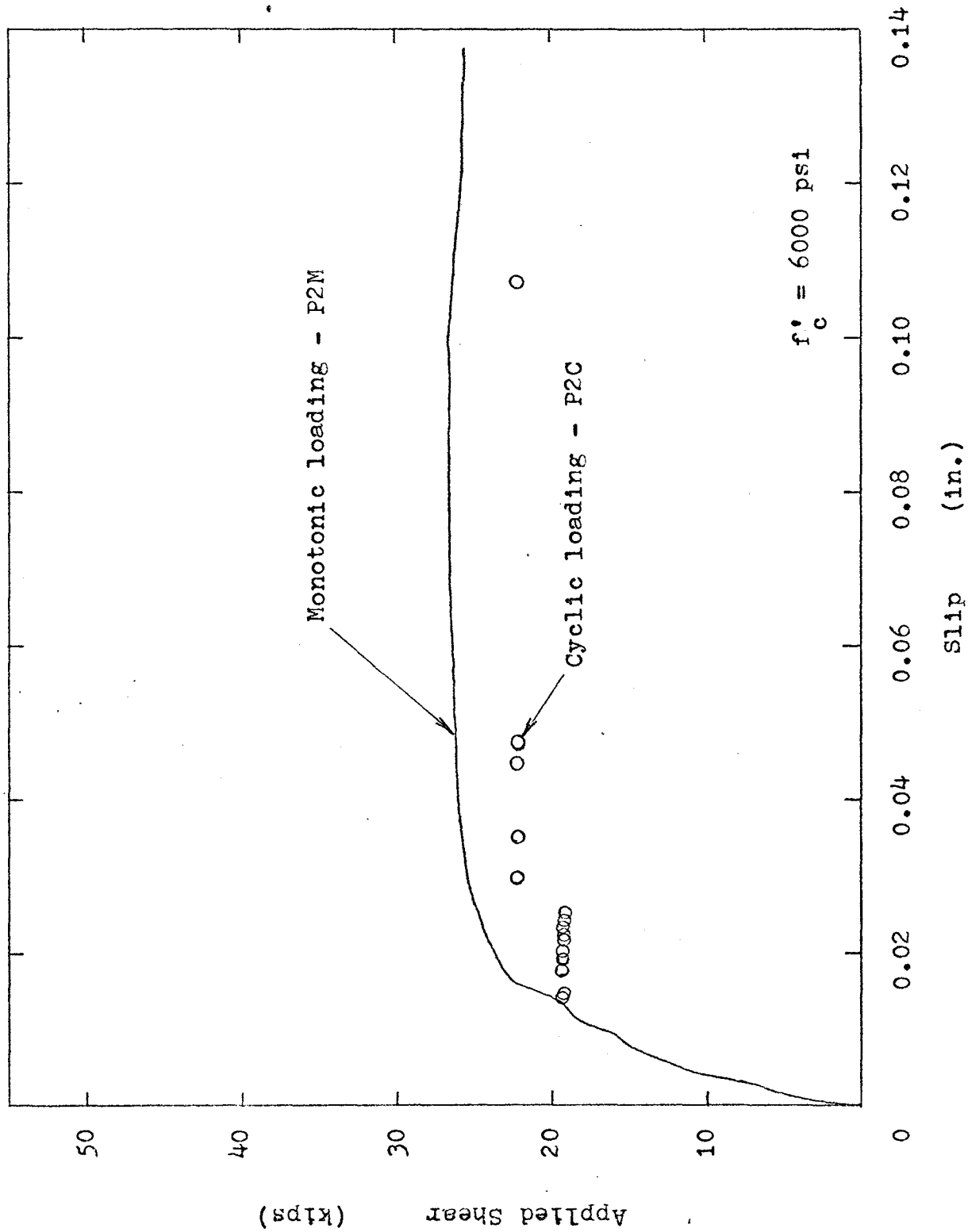


Fig. 4.5 - Comparison of shear - slip relations in cyclic and monotonic loading, for composite specimens with bond broken and also cracked before testing.

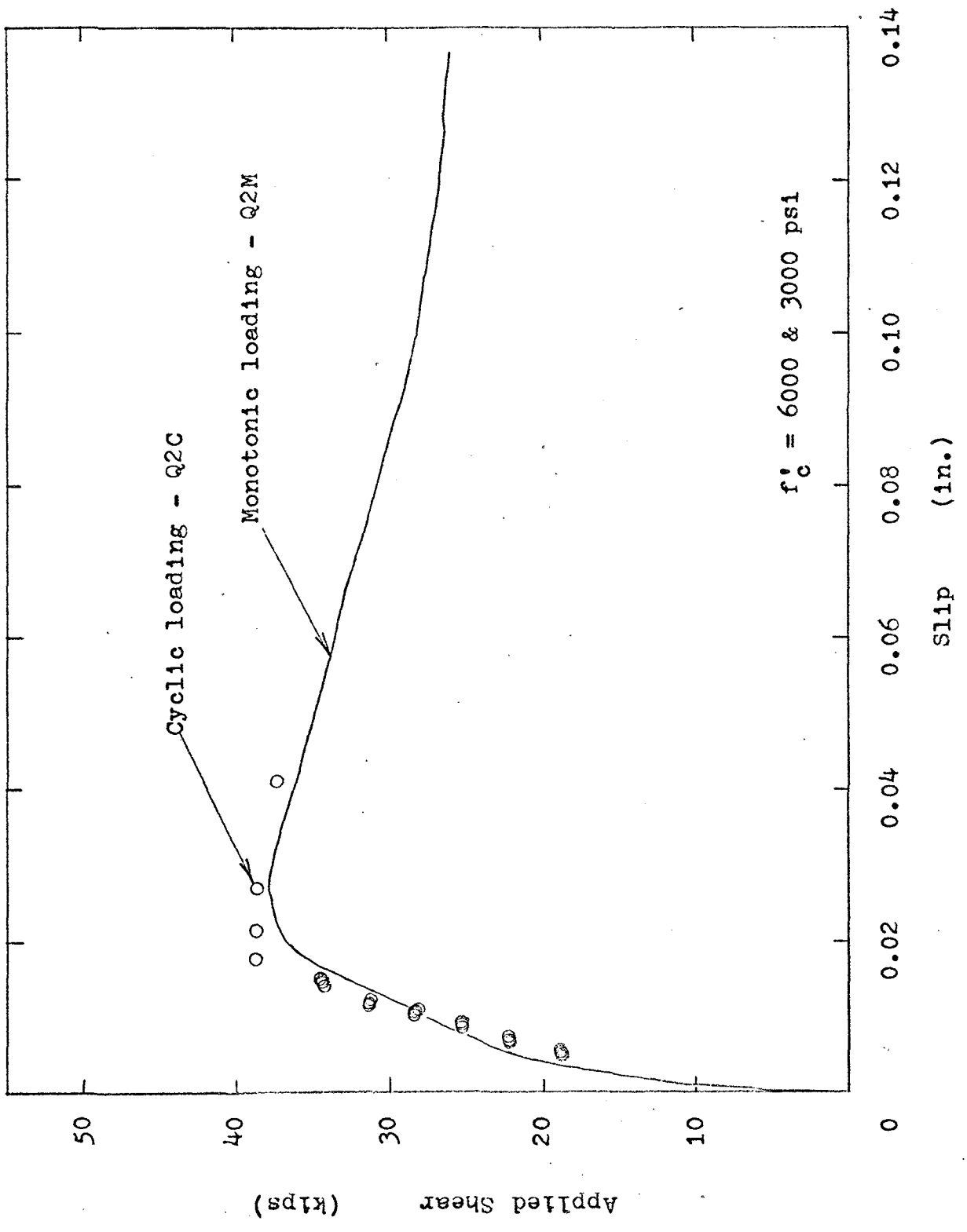


Fig. 4.6 - Comparison of shear - slip relations in cyclic and monotonic loading, for cracked, bonded, composite specimens made from concretes of different strength.

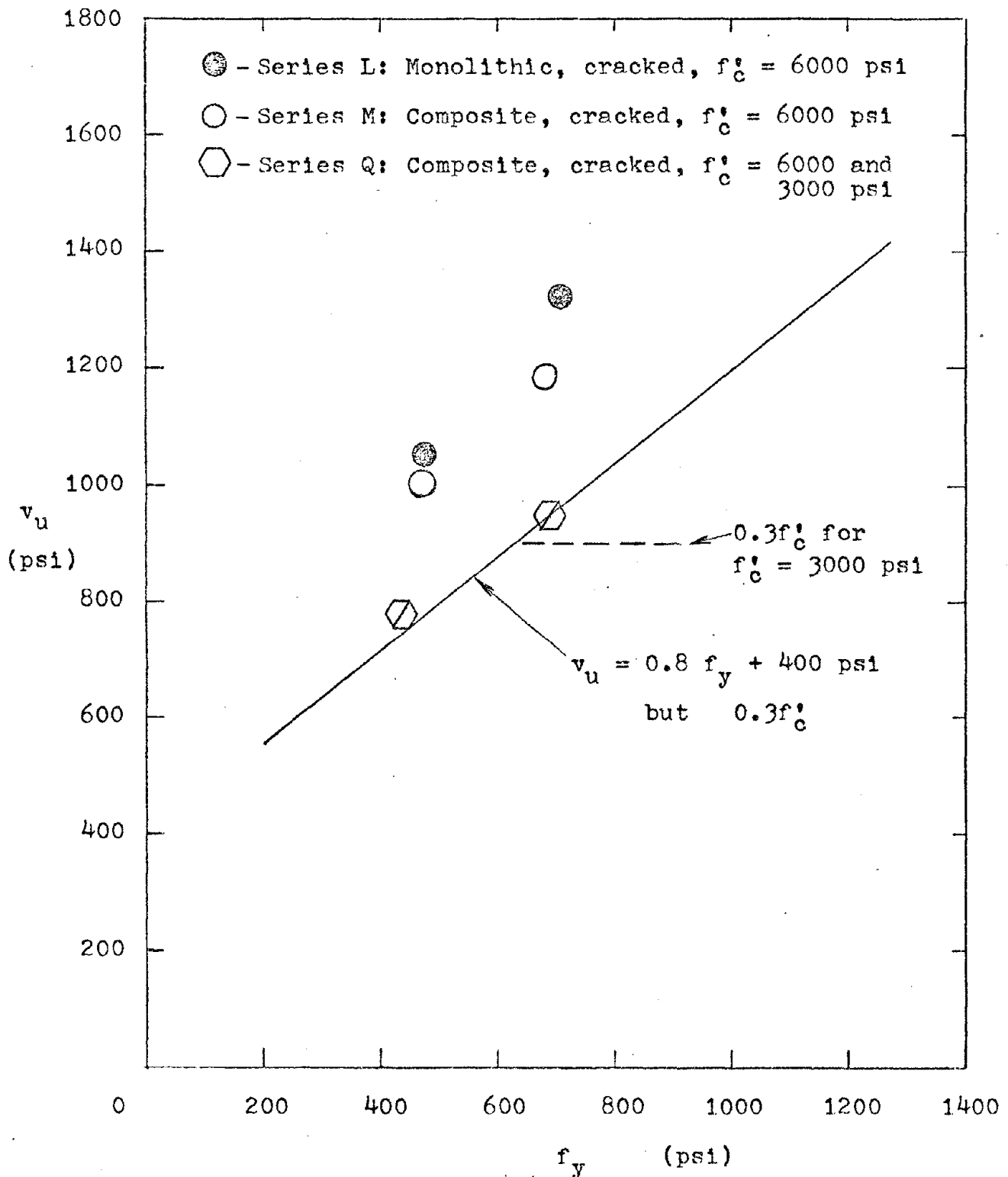


Fig. 4.7 - Shear transfer strength in monotonic loading tests of initially cracked, monolithic concrete and initially cracked, composite specimens with bond.

APPENDIX A

NOTATION

- A_{cr} = Area of shear plane, sq. in.
- A_{vf} = Area of reinforcement crossing the shear plane, sq. in.
- f'_c = Compressive strength of concrete measured on 6 x 12 in. cylinders, psi.
- f_y = Yield point stress of reinforcement, psi.
- V_u = Ultimate shear force, kips.
- v_u = Nominal ultimate shear stress, psi.
= $1000 V_u/A_{cr}$, psi.
- μ = Coefficient of friction used in shear-friction calculations.
- ρ = A_{vf}/A_{cr}
- ϕ = Capacity reduction factor, as per Sec. 9.2 of ACI 318-71.

APPENDIX B

TYPICAL SHEAR-SLIP AND SLIP-SEPARATION DATA
FOR CYCLIC LOADING TESTS

Fig.	Title
B1	Shear-slip curve, L2C, cycles 1 - 5
B2	Shear-slip curve, L2C, cycles 5 - 10
B3	Shear-slip curve, L2C, cycles 21 - 25
B4	Shear-slip curve, L2C, cycles 36 - 40
B5	Shear-slip curve, L2C, cycles 41 - 44
B6	Slip-separation curve, L2C, cycles 1 - 5
B7	Slip-separation curve, L2C, cycles 5 - 10
B8	Slip-separation curve, L2C, cycles 21 - 25
B9	Slip-separation curve, L2C, cycles 36 - 40
B10	Slip-separation curve, L2C, cycles 41 - 44
B11	Shear-slip curve, M2C, cycles 1 - 5
B12	Shear-slip curve, M2C, cycles 6 - 10
B13	Shear-slip curve, M2C, cycles 21 - 25
B14	Shear-slip curve, M2C, cycles 41 - 46
B15	Slip-separation curve, M2C, cycles 1 - 5
B16	Slip-separation curve, M2C, cycles 6 - 10
B17	Slip-separation curve, M2C, cycles 21 - 25
B18	Slip-separation curve, M2C, cycles 41 - 46
B19	Shear-slip curve, N2C, cycles 1 - 5
B20	Shear-slip curve, N2C, cycles 6 - 10
B21	Shear-slip curve, N2C, cycles 11 - 15
B22	Shear-slip curve, N2C, cycles 16 - 20

Fig.	Title
B23	Slip-separation curve, N2C, cycles 1 - 5
B24	Slip-separation curve, N2C, cycles 6 - 10
B25	Slip-separation curve, N2C, cycles 11 - 15
B26	Slip-separation curve, N2C, cycles 16 - 20
B27	Shear-slip curve, P2C, cycles 1 - 5
B28	Shear-slip curve, P2C, cycles 6 - 10
B29	Shear-slip curve, P2C, cycles 11 - 15
B30	Slip-separation curve, P2C, cycles 1 - 5
B31	Slip-separation curve, P2C, cycles 6 - 10
B32	Slip-separation curve, P2C, cycles 11 - 15
B33	Shear-slip curve, Q2C, cycles 1 - 5
B34	Shear-slip curve, Q2C, cycles 6 - 10
B35	Shear-slip curve, Q2C, cycles 21 - 25
B36	Shear-slip curve, Q2C, cycles 31 - 35
B37	Shear-slip curve, Q2C, cycles 36 - 39
B38	Slip-separation curve, Q2C, cycles 1 - 5
B39	Slip-separation curve, Q2C, cycles 6 - 10
B40	Slip-separation curve, Q2C, cycles 21 - 25
B41	Slip-separation curve, Q2C, cycles 31 - 35
B42	Slip-separation curve, Q2C, cycles 36 - 39

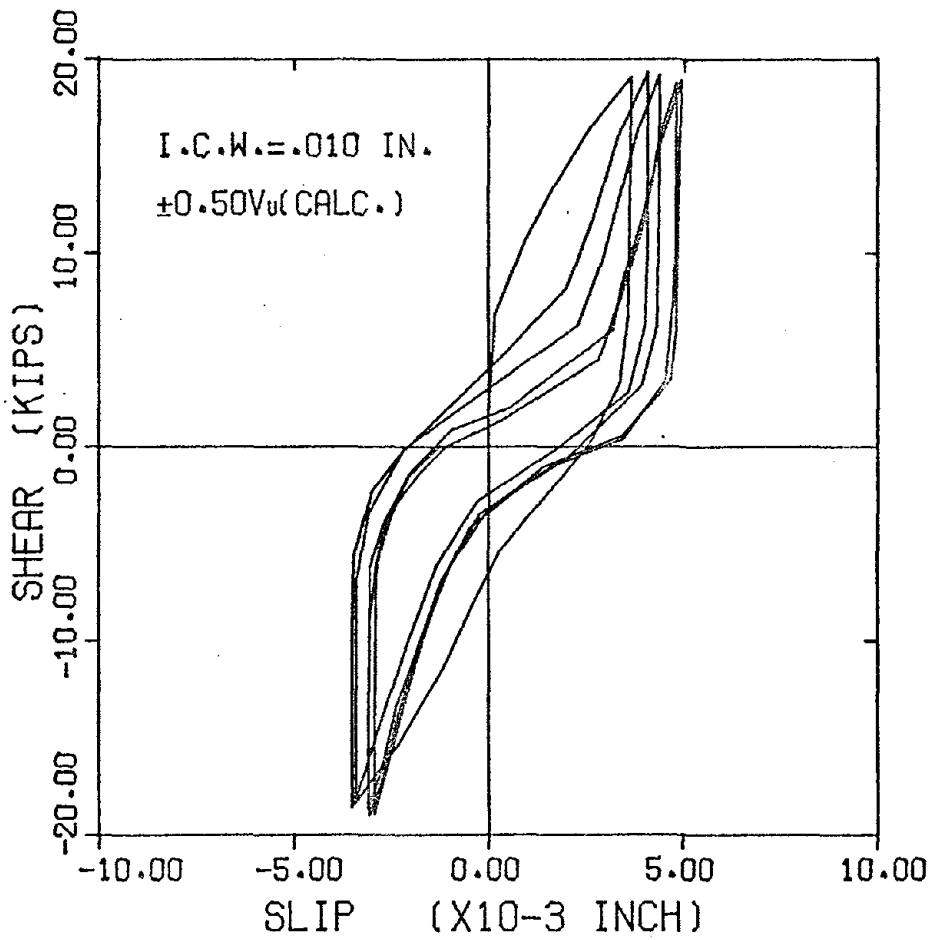


FIG. B1 - SHEAR-SLIP CURVE. L2C. CYCLES 1 TO 5

52

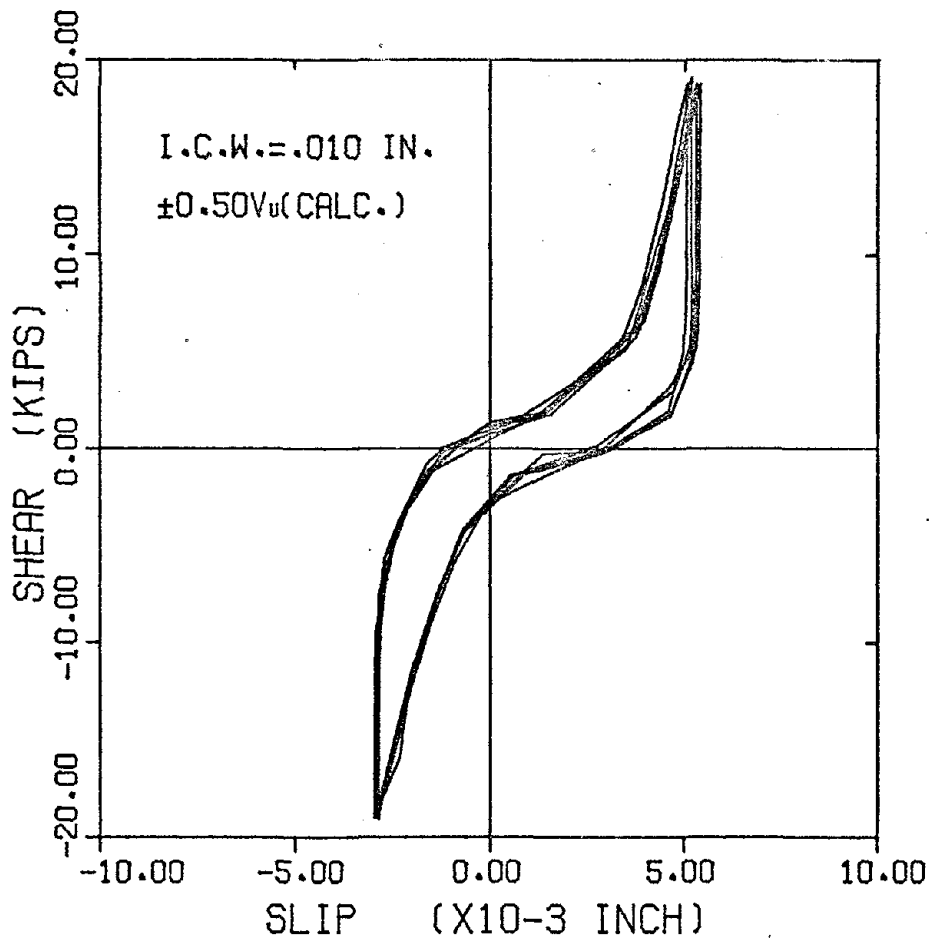


FIG. B2 - SHEAR-SLIP CURVE. L2C. CYCLES 6 TO 10

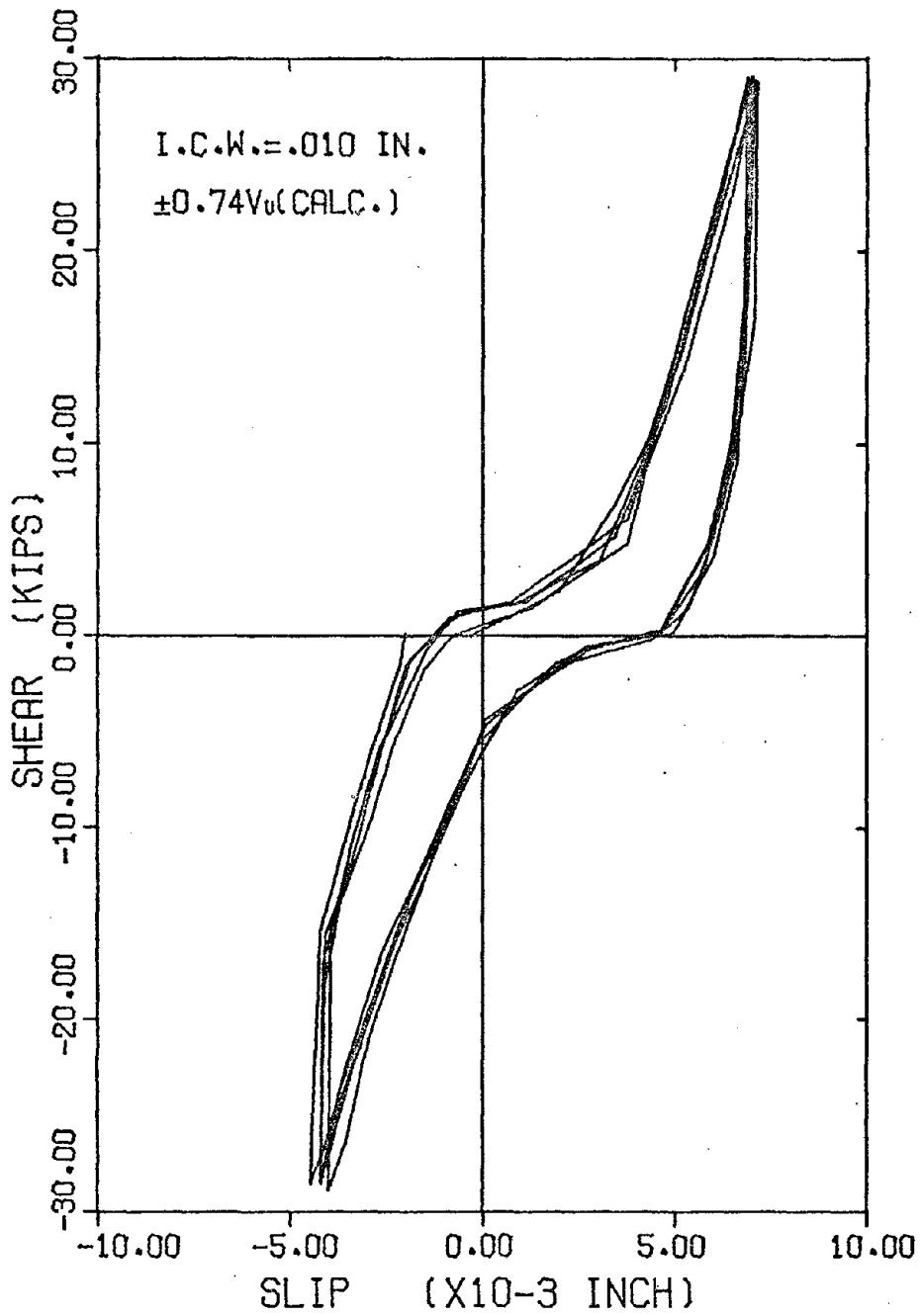


FIG. B3- SHEAR-SLIP CURVE. L2C. CYCLES 21 TO 25

54

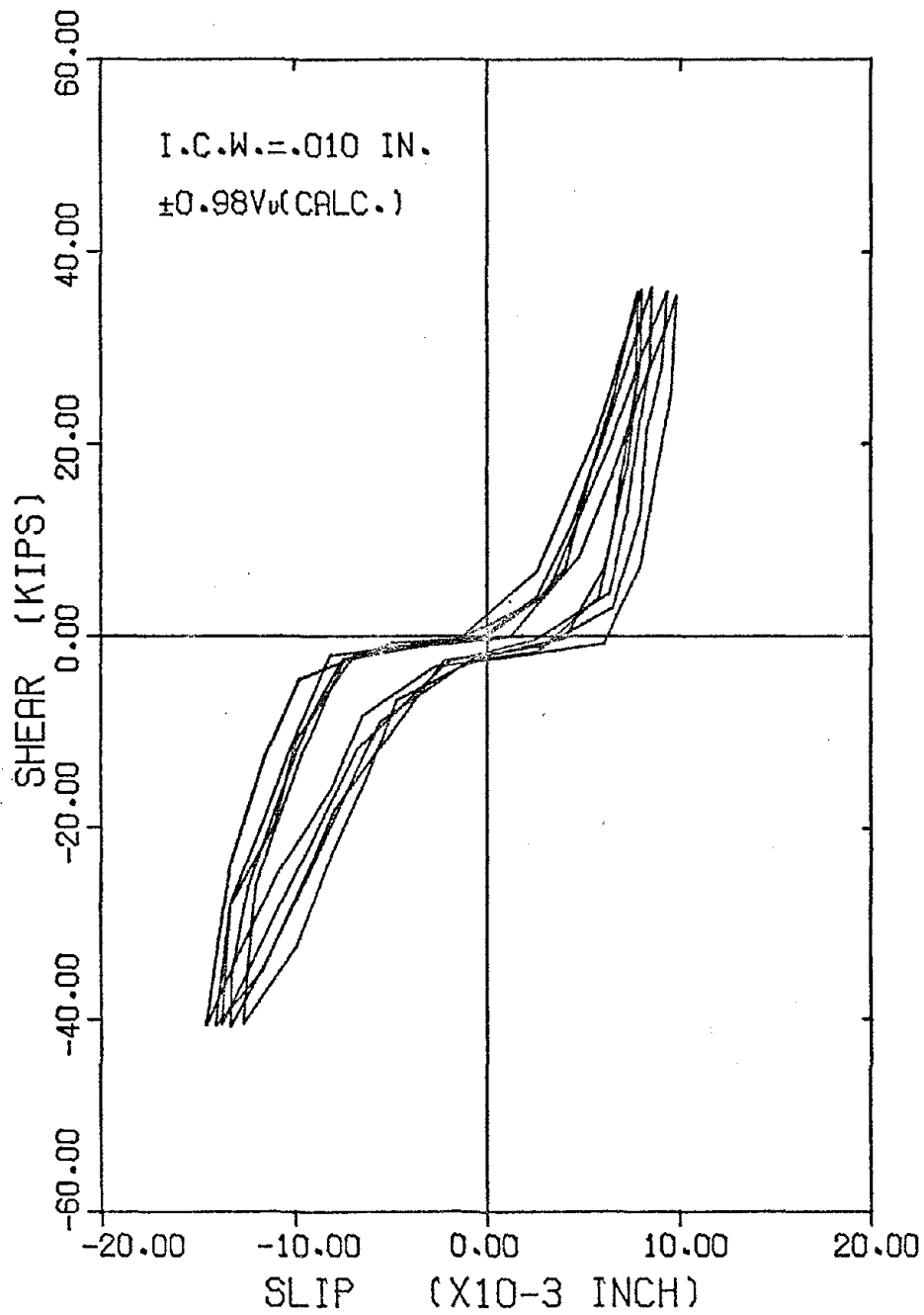


FIG. B4 - SHEAR-SLIP CURVE. L2C. CYCLES 36 TO 40

55

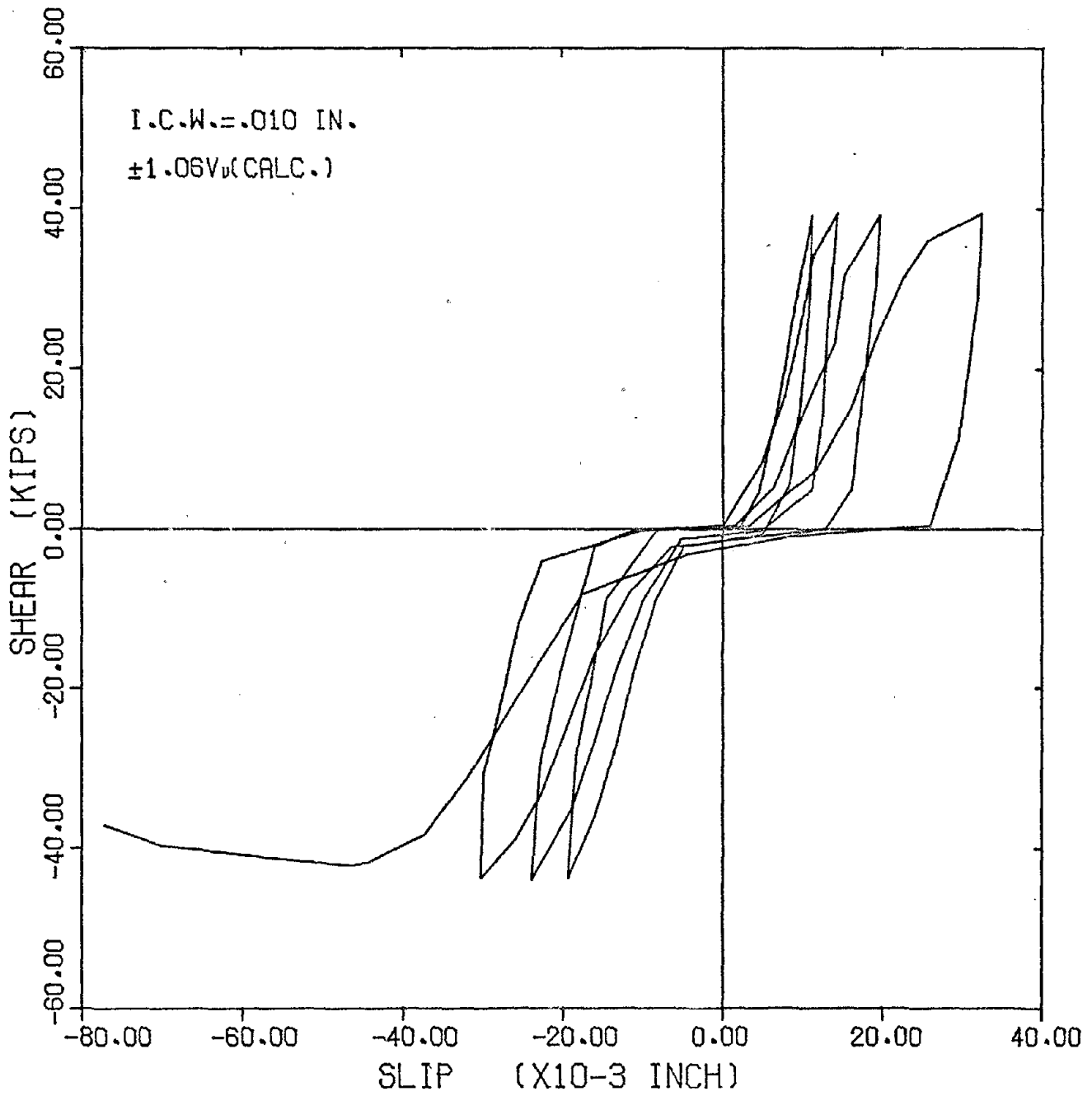


FIG.B5 - SHEAR-SLIP CURVE. L2C. CYCLES 41 TO 44

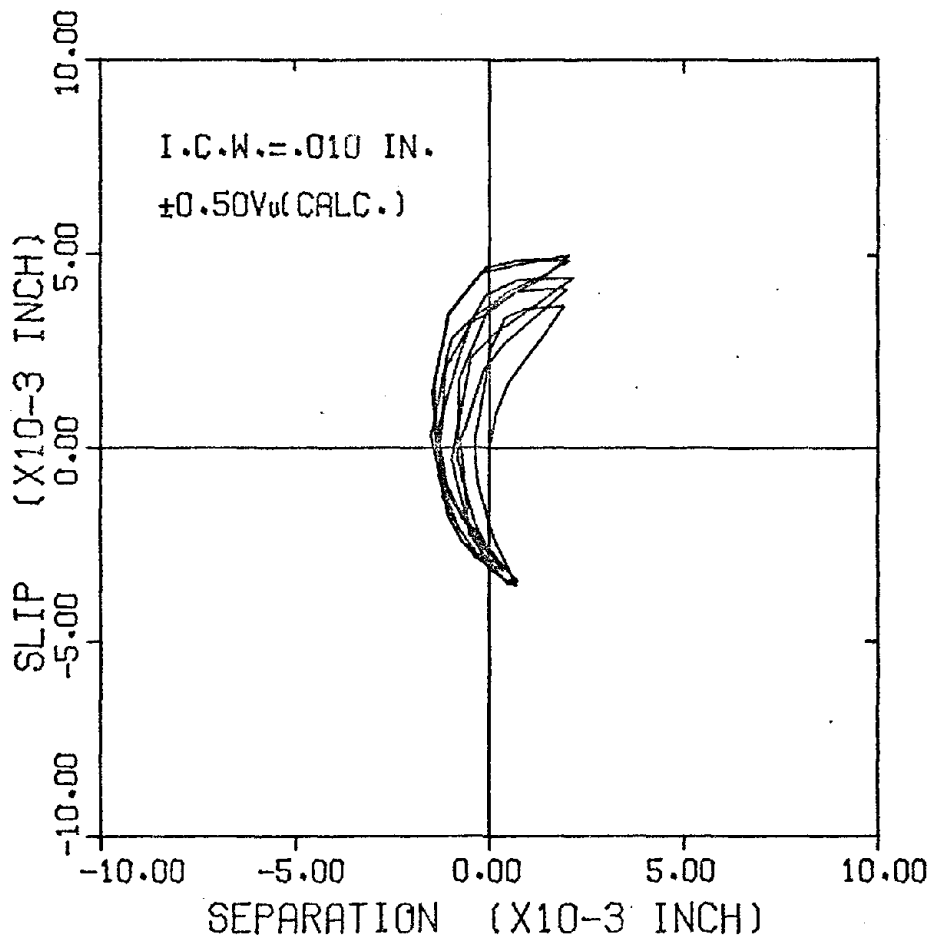


FIG. B6 - SLIP-SEPARATION CURVE. L2C. CYCLES 1 TO 5

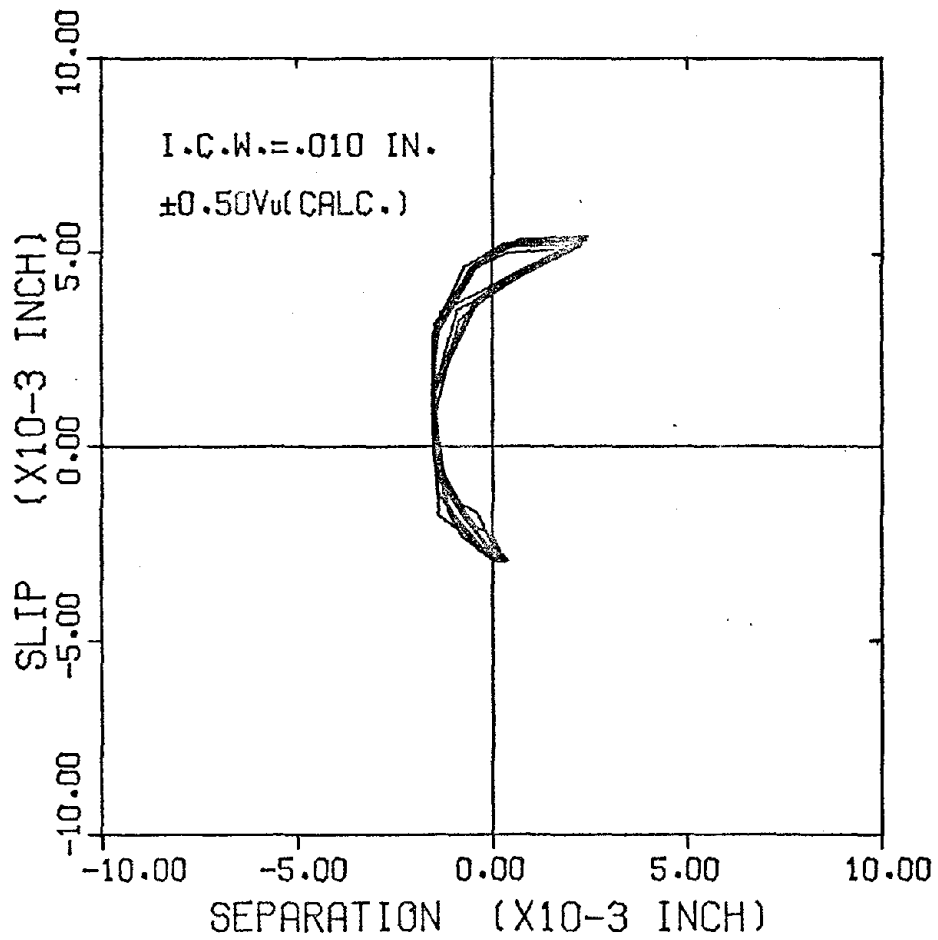


FIG. B7 - SLIP-SEPARATION CURVE, L2C, CYCLES 6 TO 10

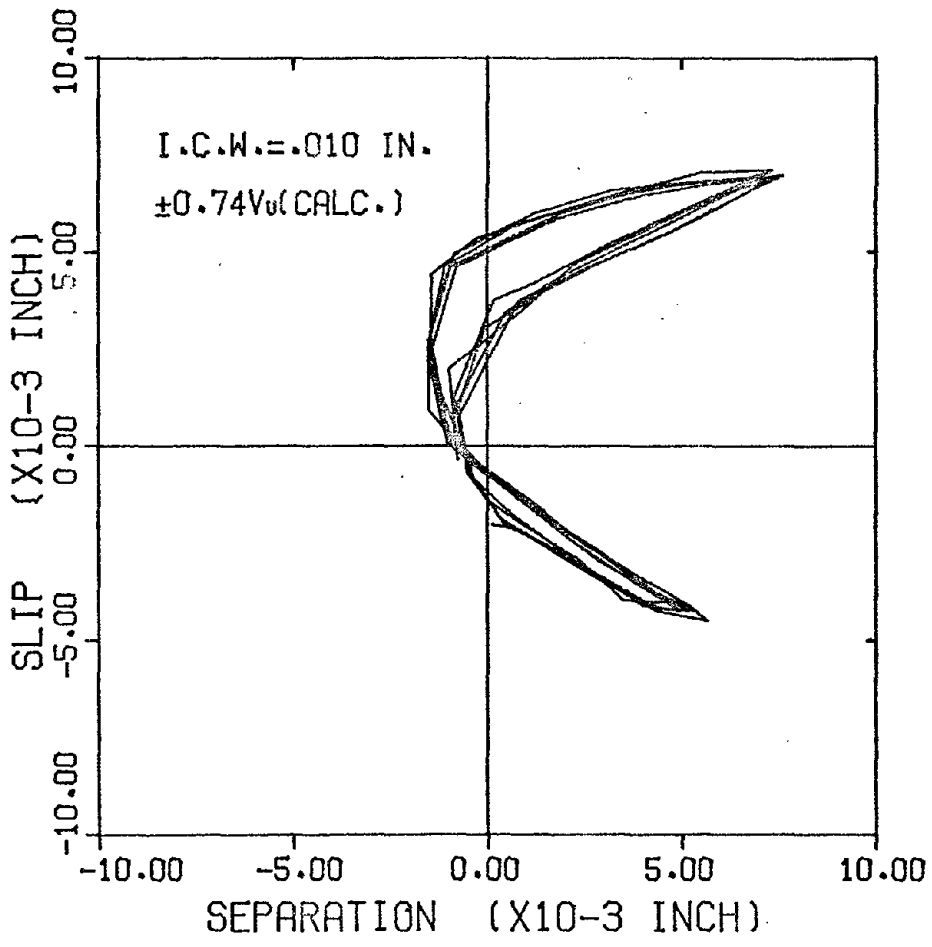


FIG. B8 - SLIP-SEPARATION CURVE. L2C. CYCLES 21 TO 25

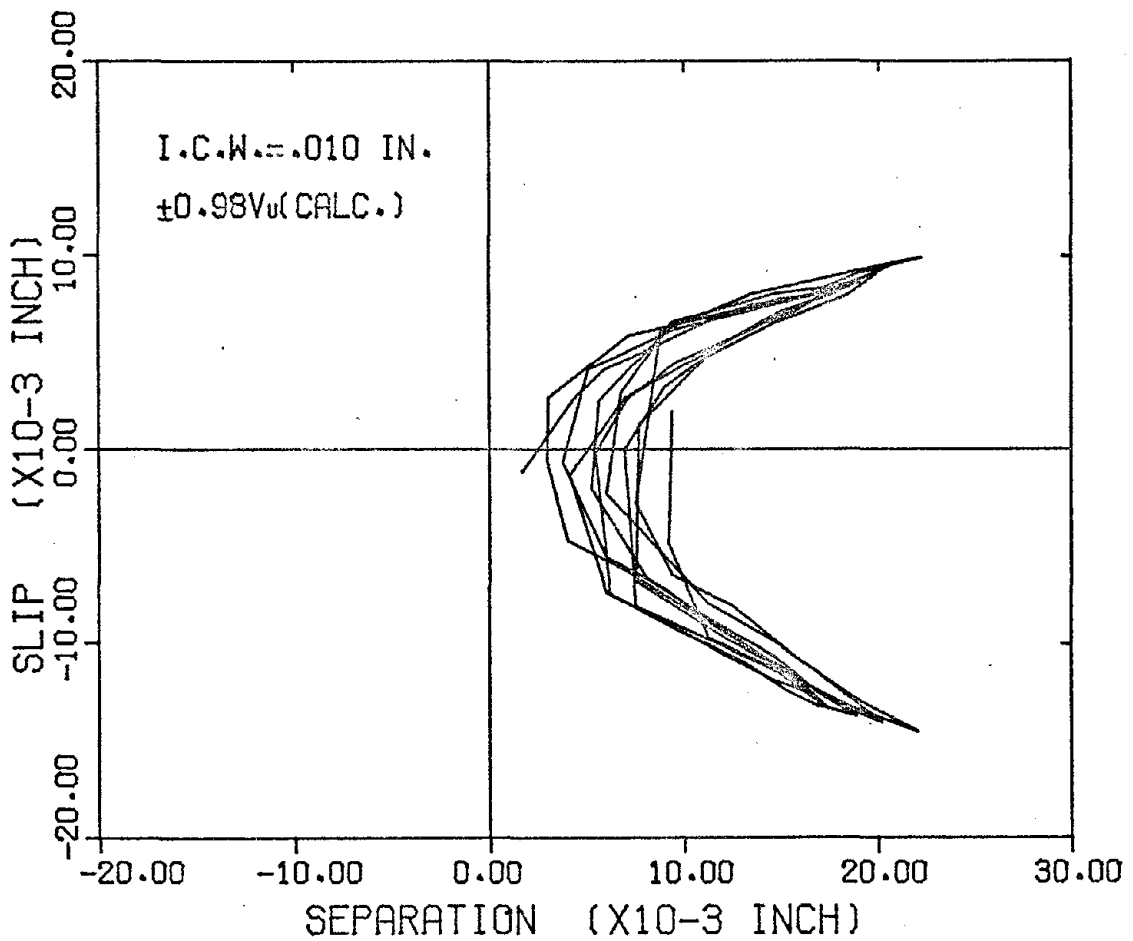


FIG.B9 - SLIP-SEPARATION CURVE. L2C. CYCLES 36 TO 40

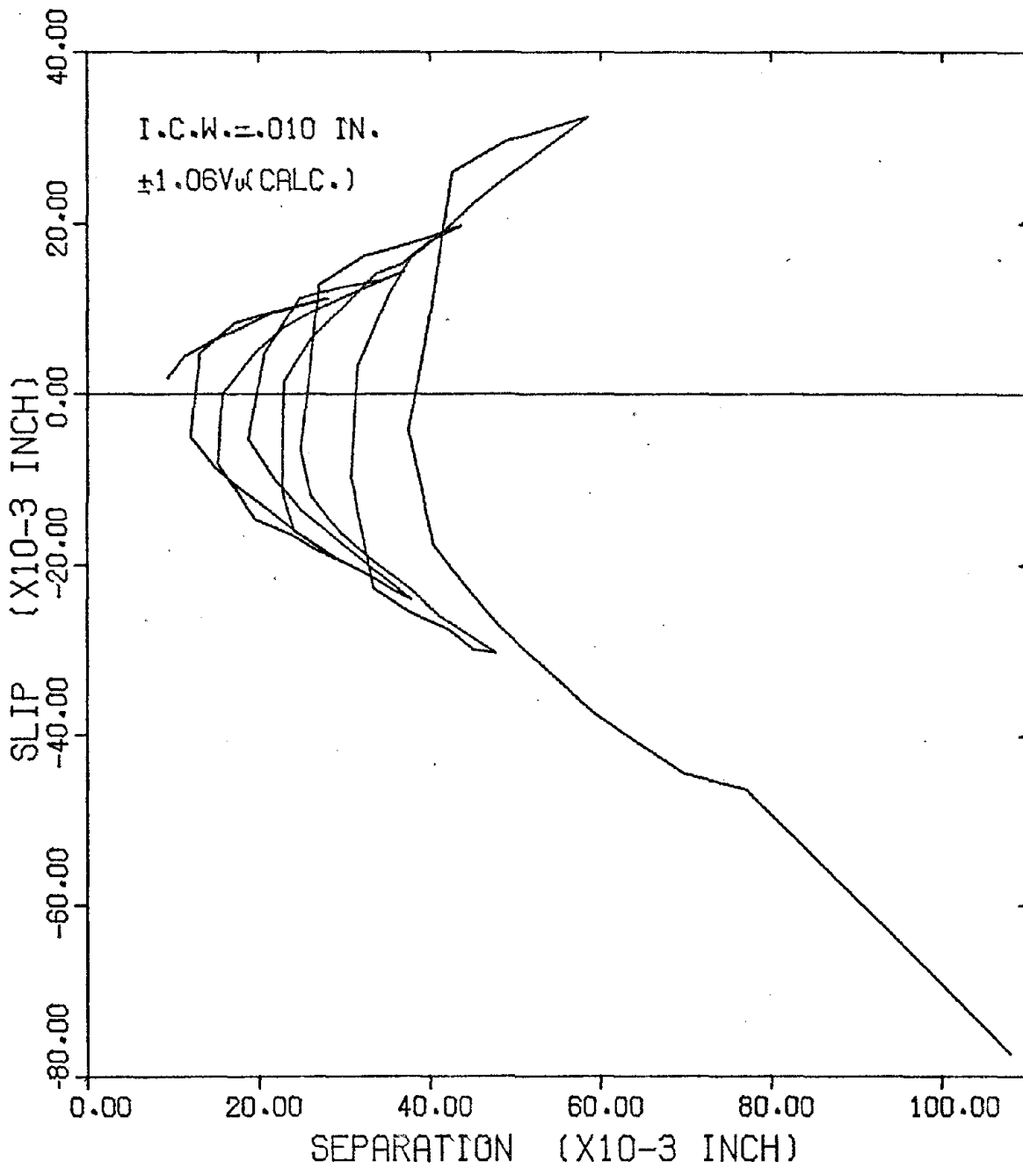


FIG. B10- SLIP-SEPARATION CURVE. L2C. CYCLES 41 TO 44

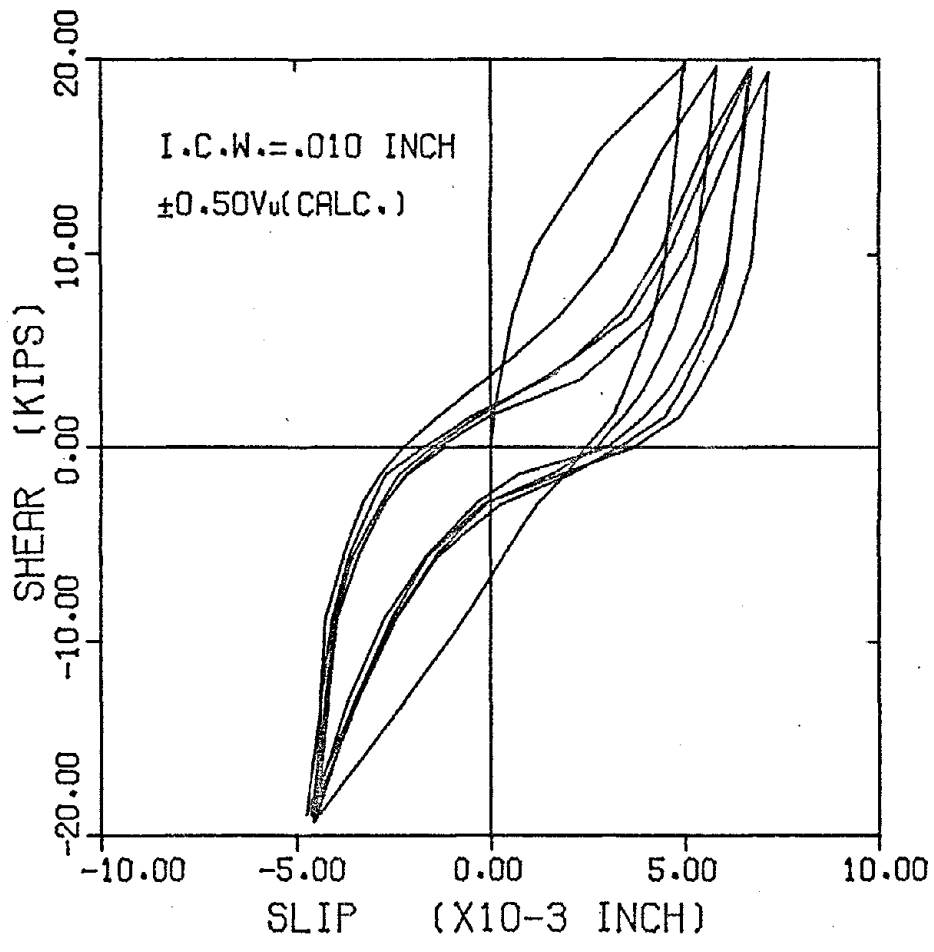


FIG. B11- SHEAR-SLIP CURVE, M2C, CYCLES 1 TO 5

62

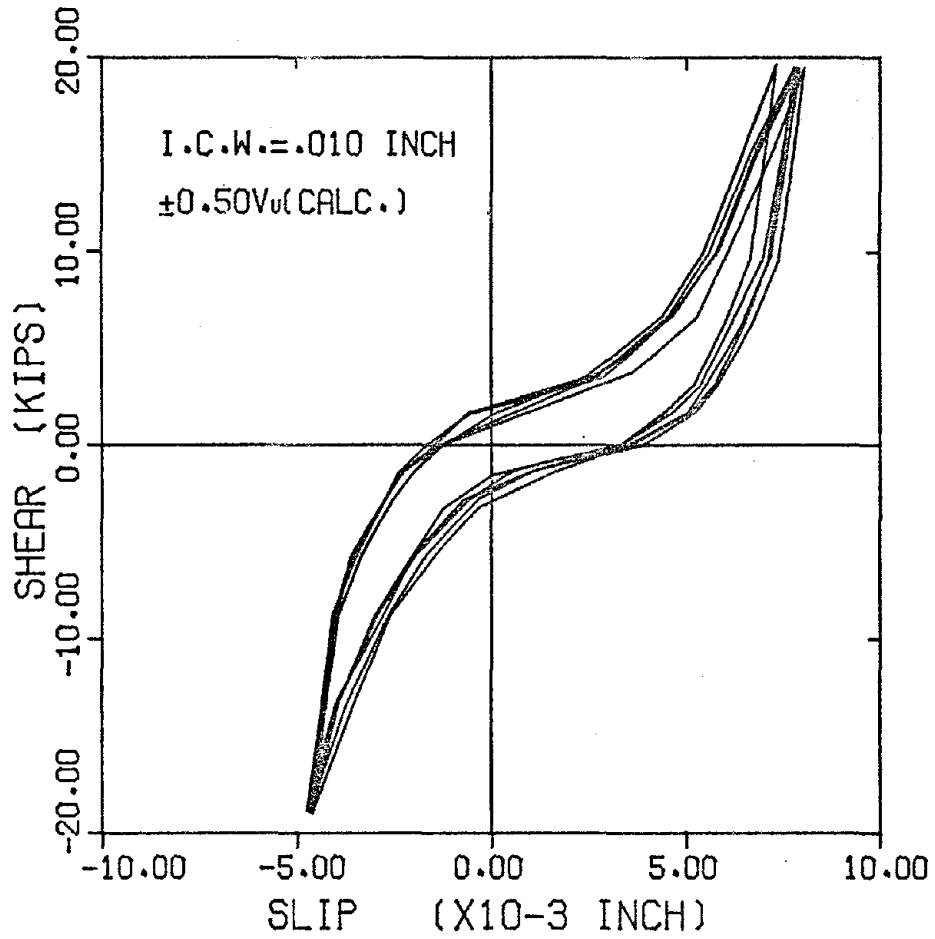


FIG. B12- SHEAR-SLIP CURVE. M2C. CYCLES 6 TO 10

63

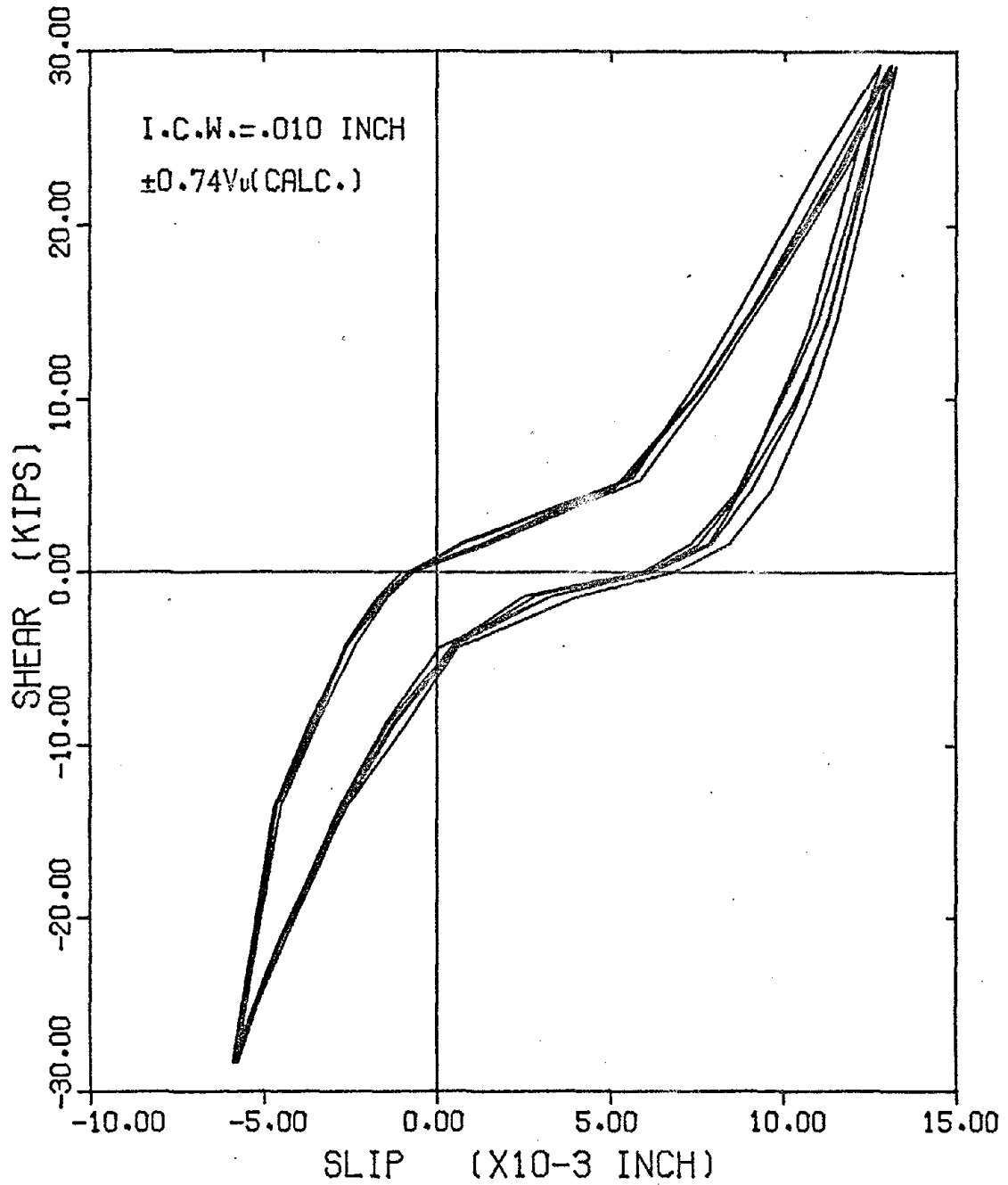


FIG. B13- SHEAR-SLIP CURVE. M2C. CYCLES 21 TO 25

64

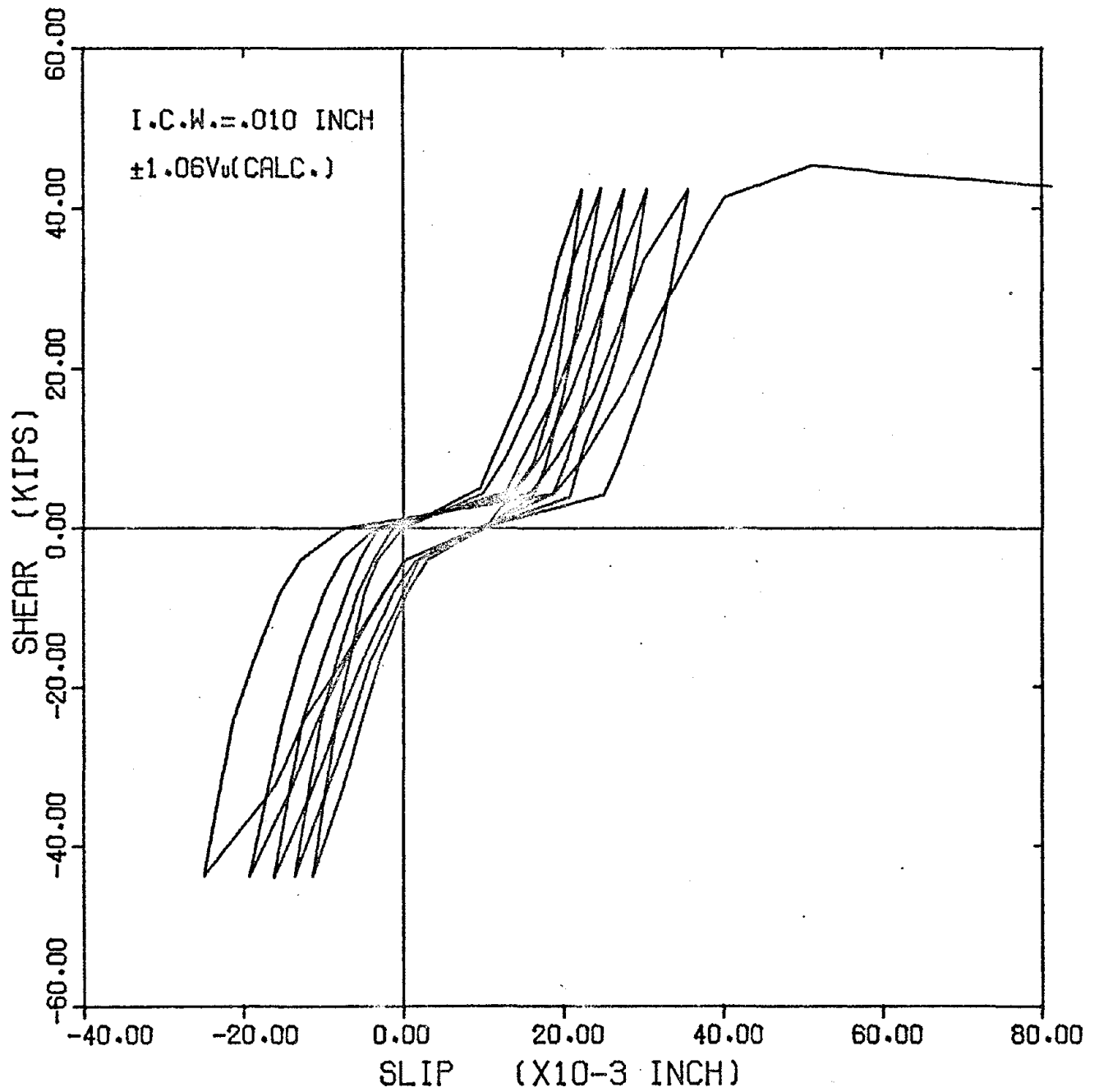


FIG. B14- SHEAR-SLIP CURVE. M2C. CYCLES 41 TO 46

65

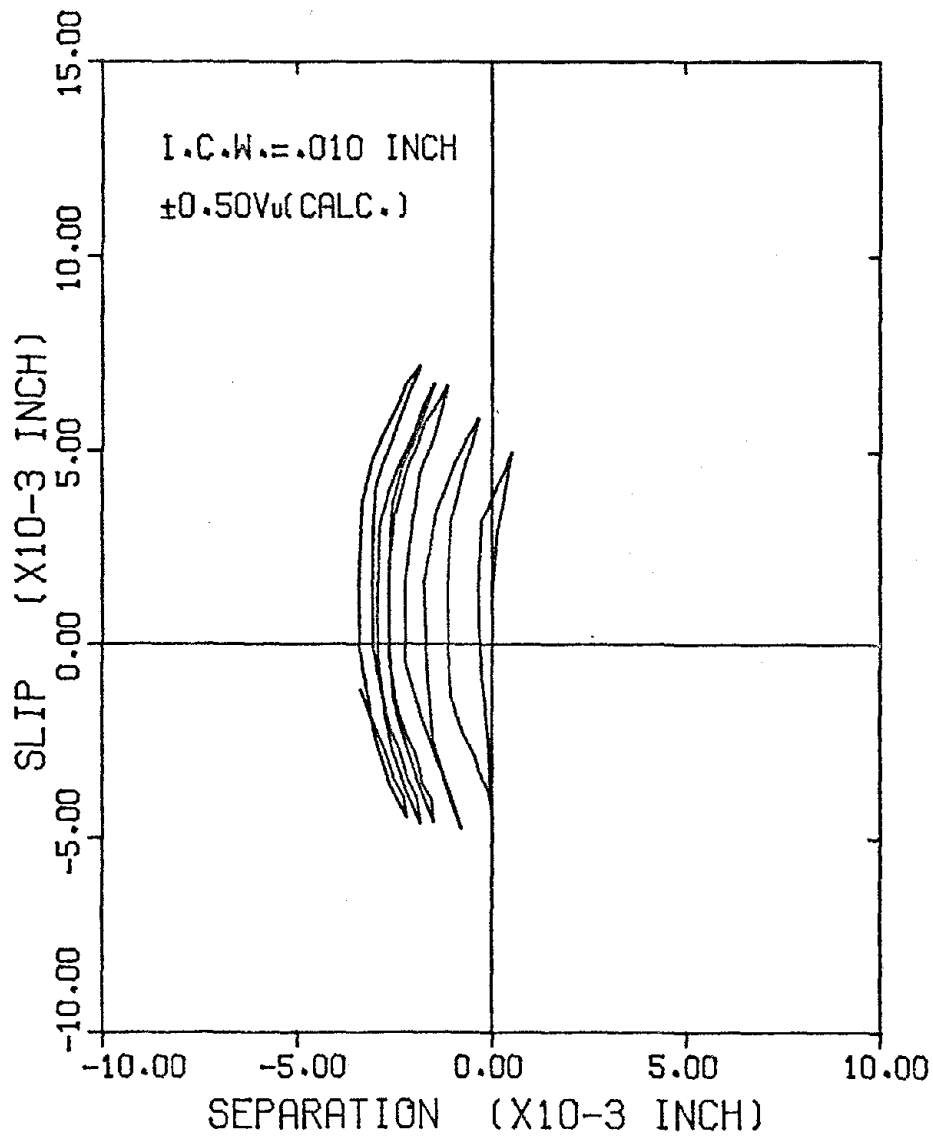


FIG. B15- SLIP-SEPARATION CURVE. M2C. CYCLES 1 TO 5

lde

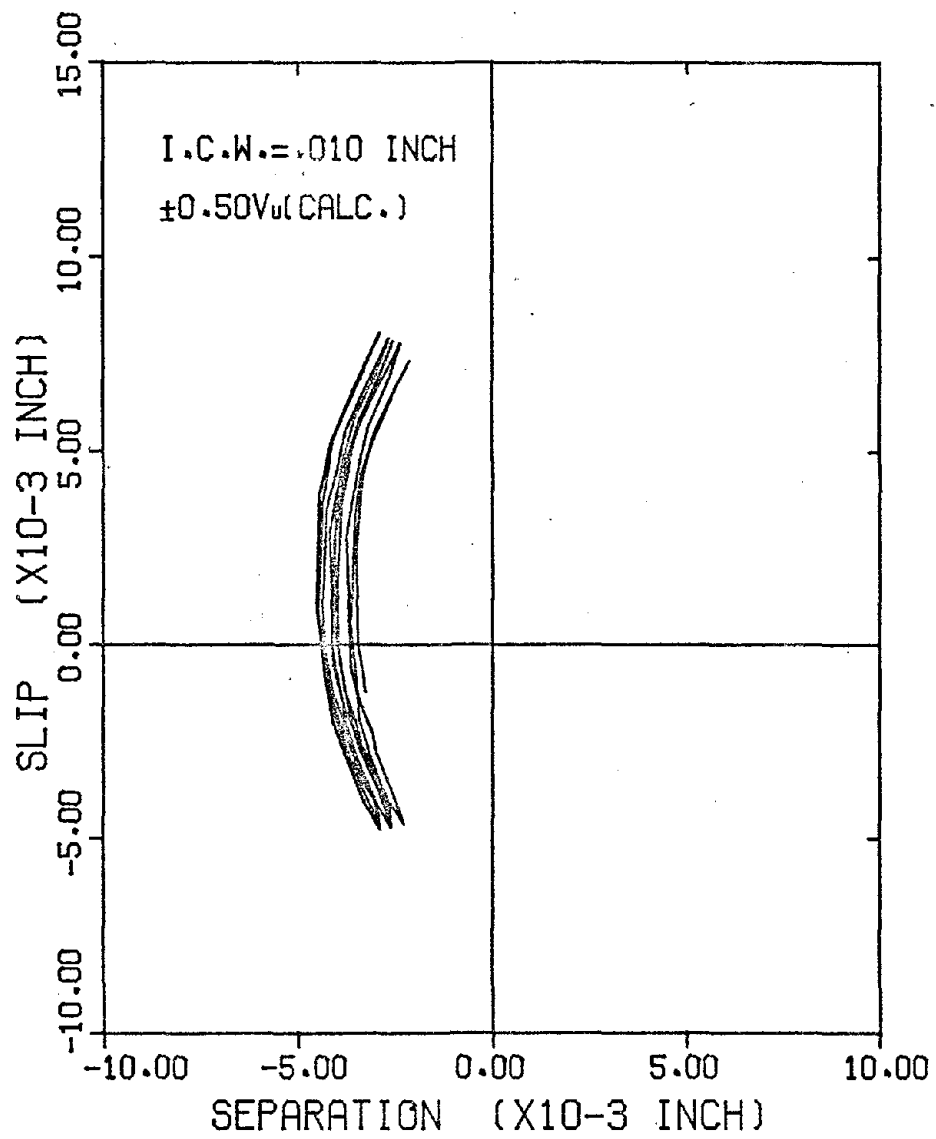


FIG. B10- SLIP-SEPARATION CURVE. M2C. CYCLES 6 TO 10

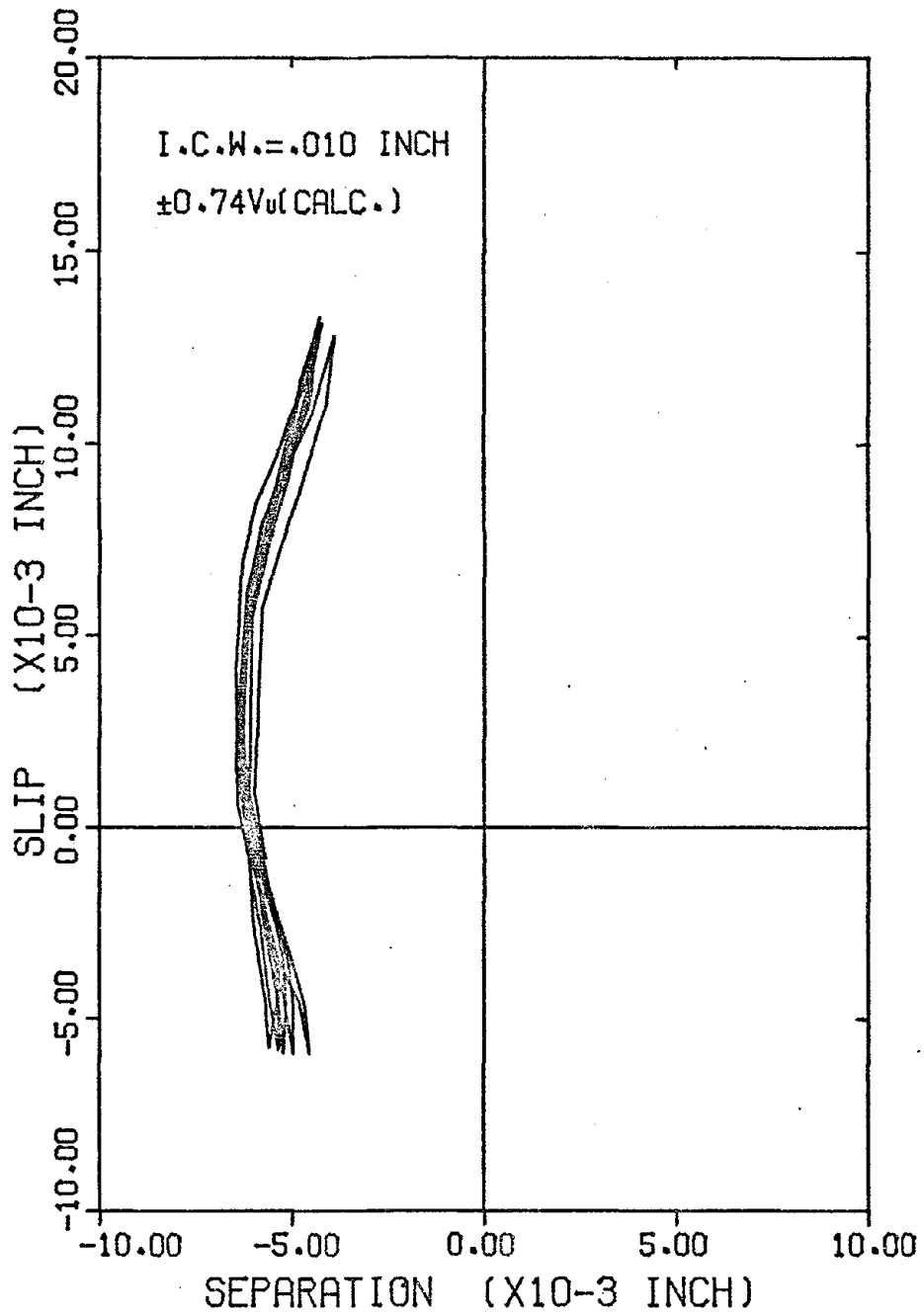


FIG. B17- SLIP-SEPARATION CURVE. M2C. CYCLES 21 TO 25

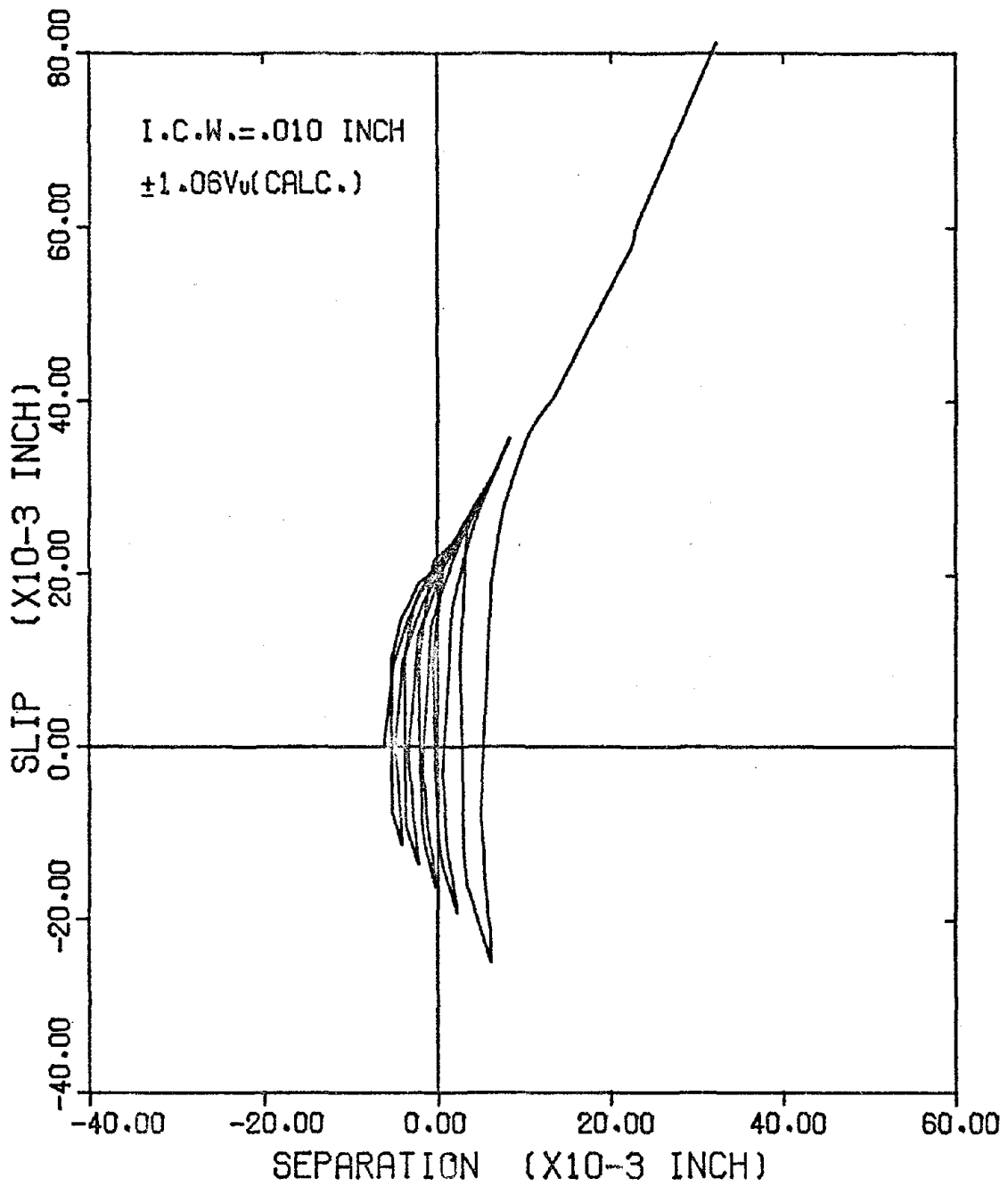


FIG. B18- SLIP-SEPARATION CURVE, M2C, CYCLES 41 TO 46

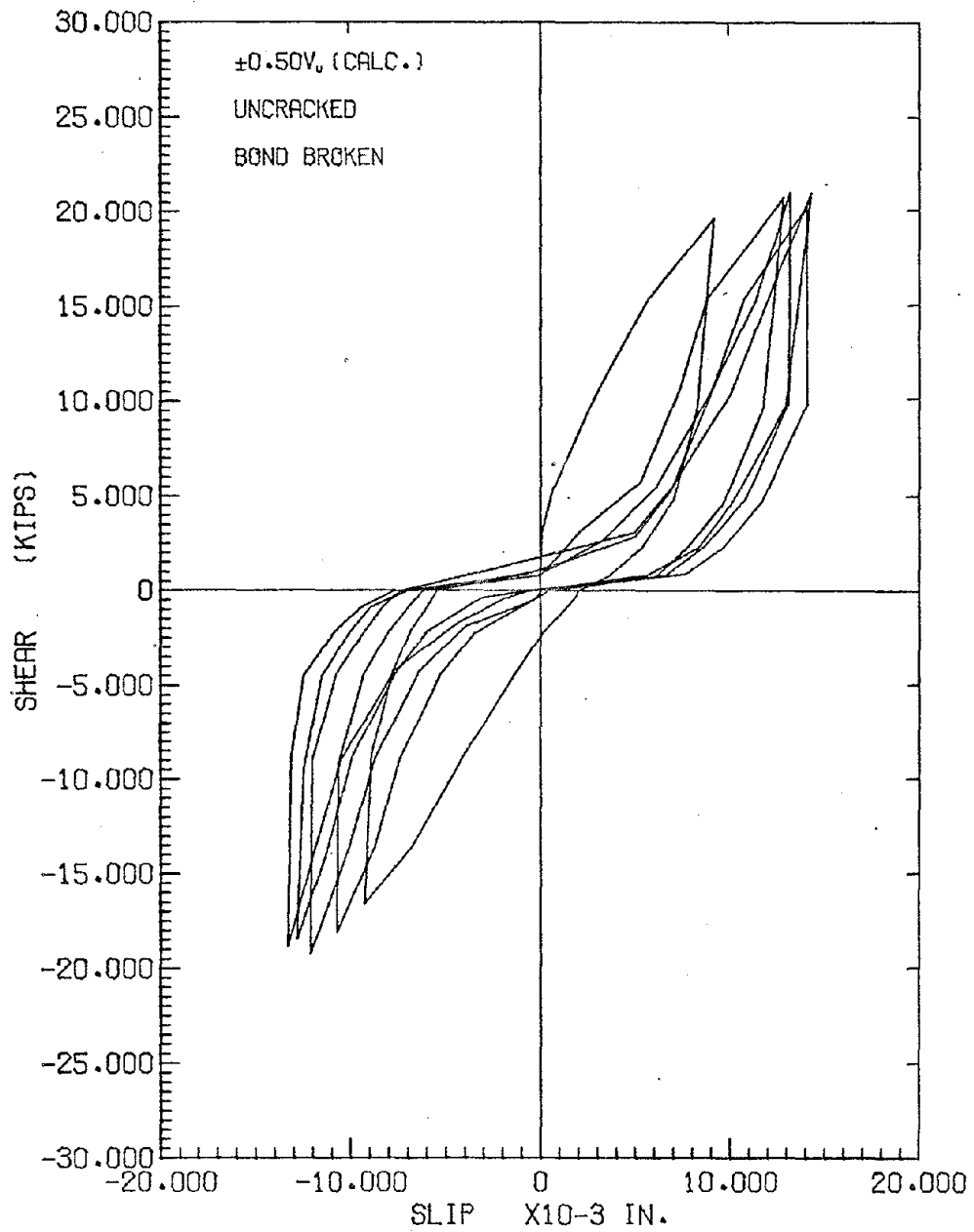


FIG.B19 - SHEAR-SLIP CURVE, N2C, CYCLES 1-5

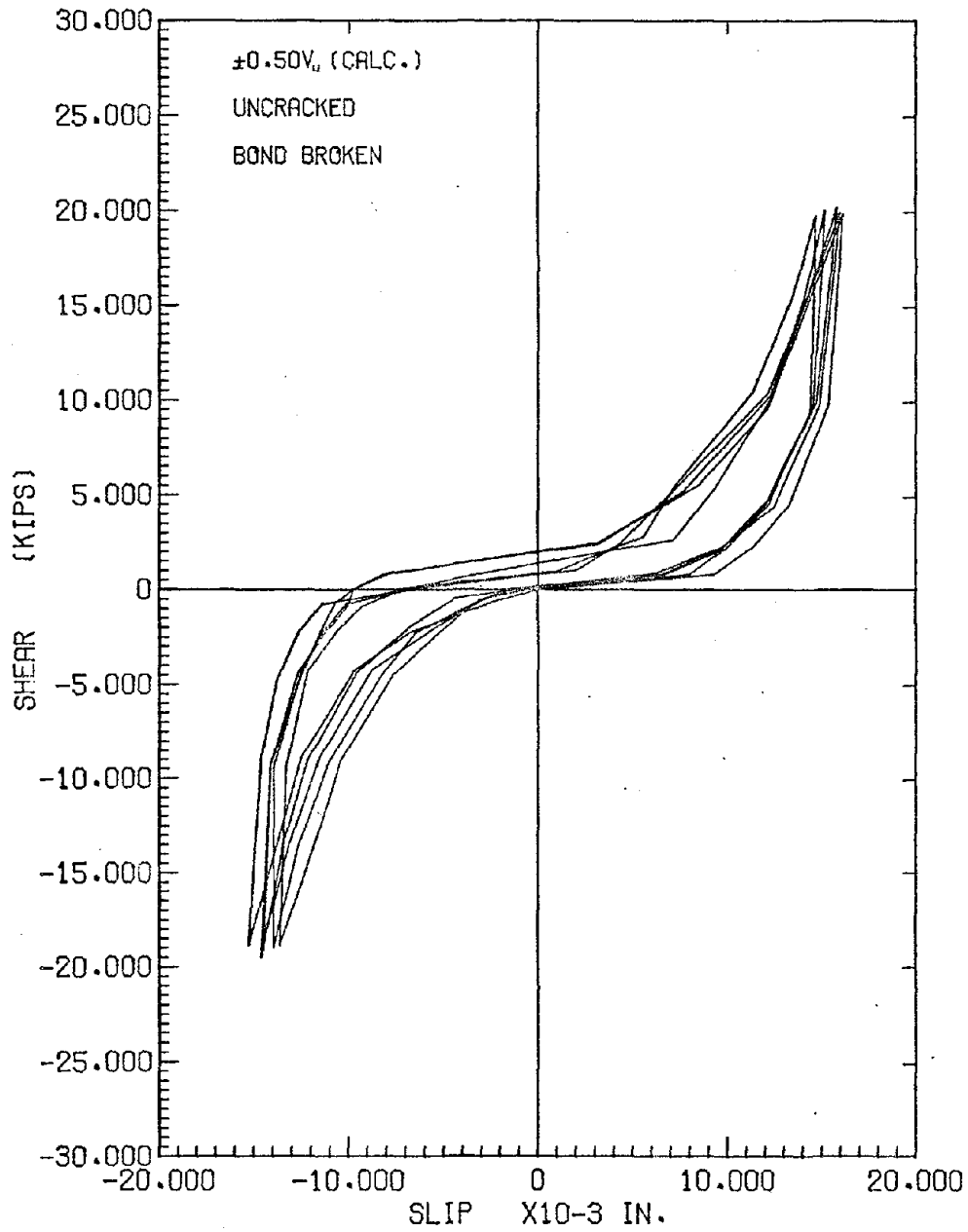


FIG. B20-SHEAR-SLIP CURVE, N2C, CYCLES 6-10

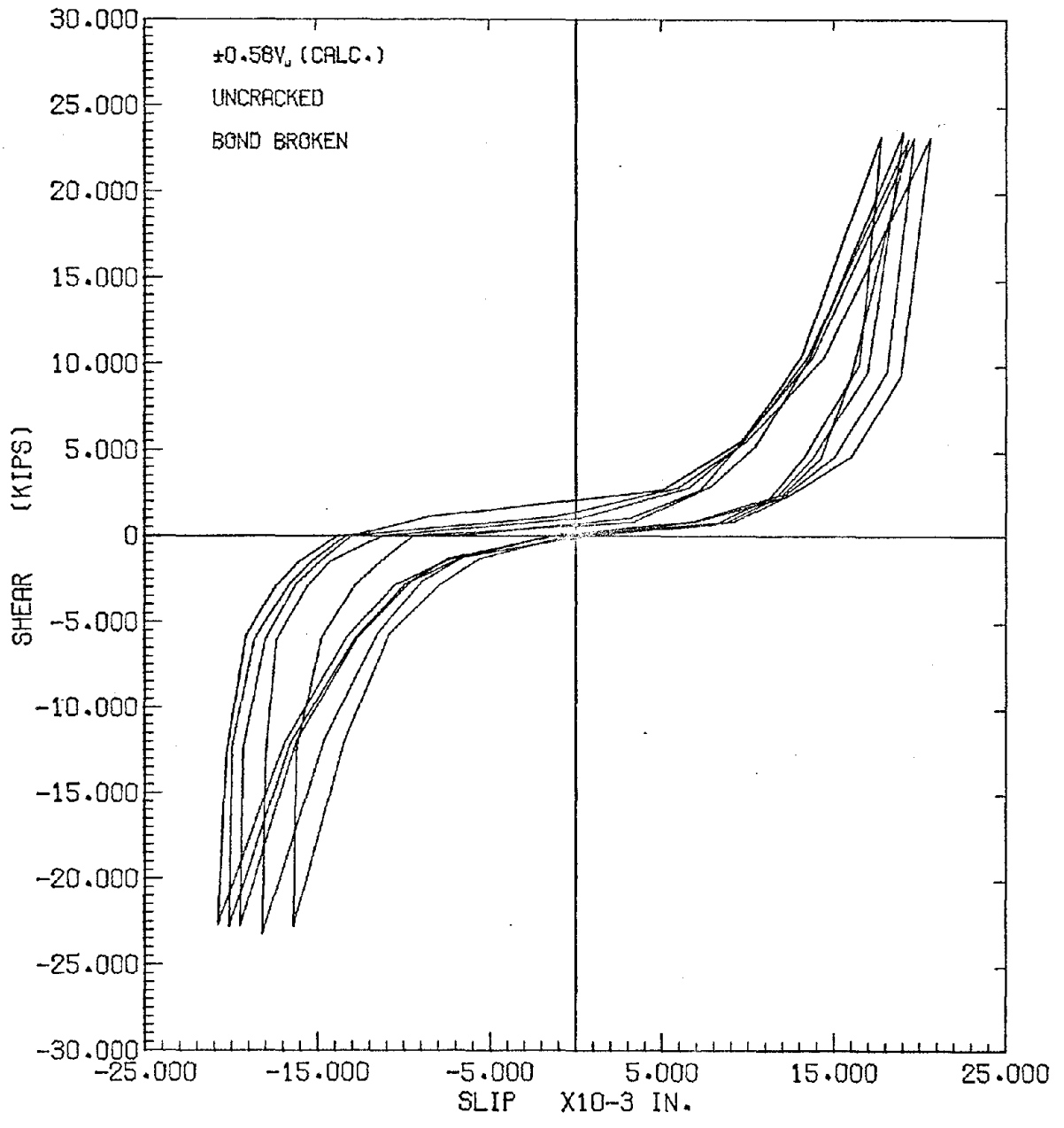


FIG. B21- SHEAR-SLIP CURVE, N2C, CYCLES 11-15

72

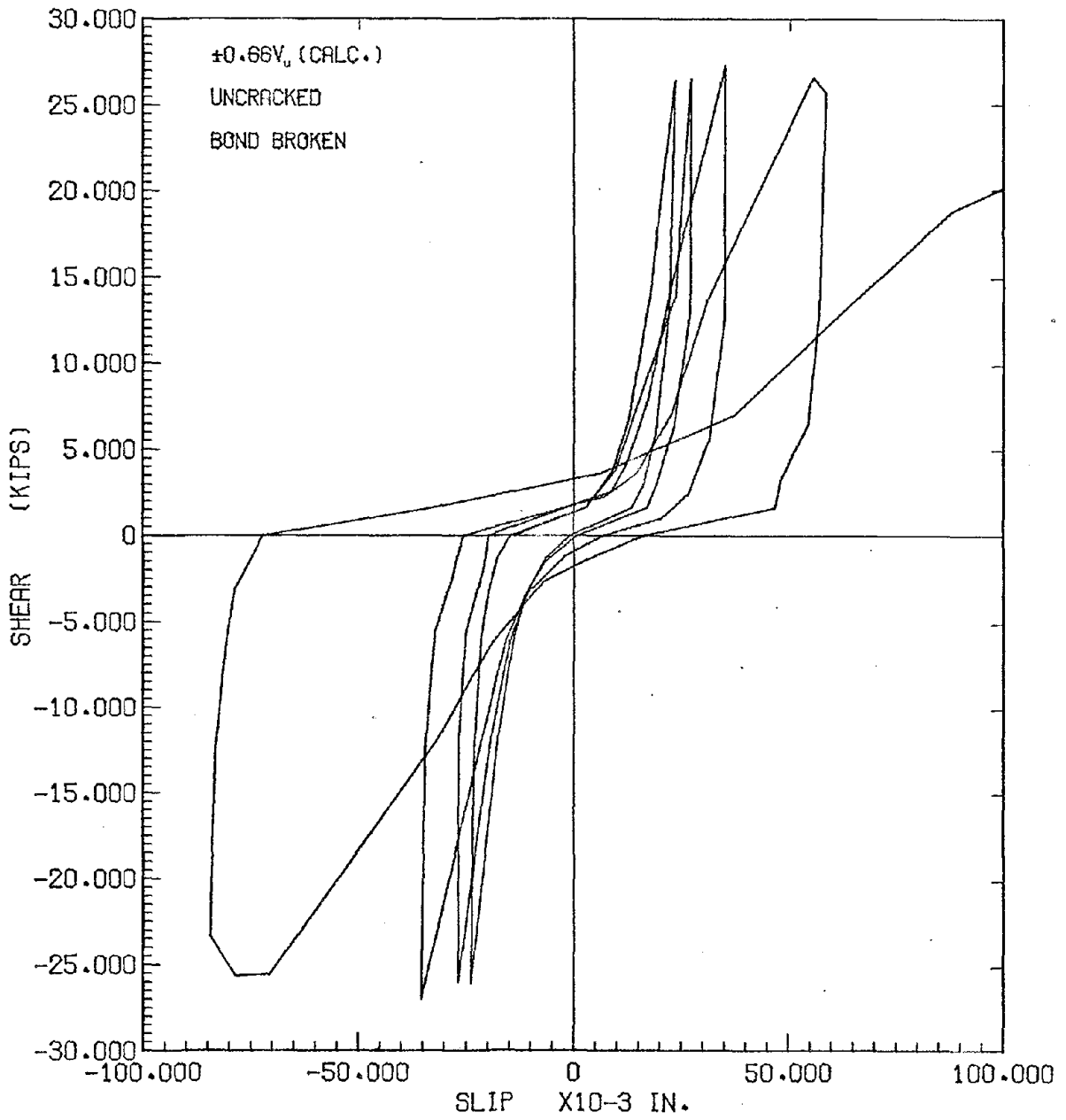


FIG. B22- SHEAR-SLIP CURVE, N2C, CYCLES 16-20

±0.50V_a (CALC.)

UNCRACKED

BOND BROKEN

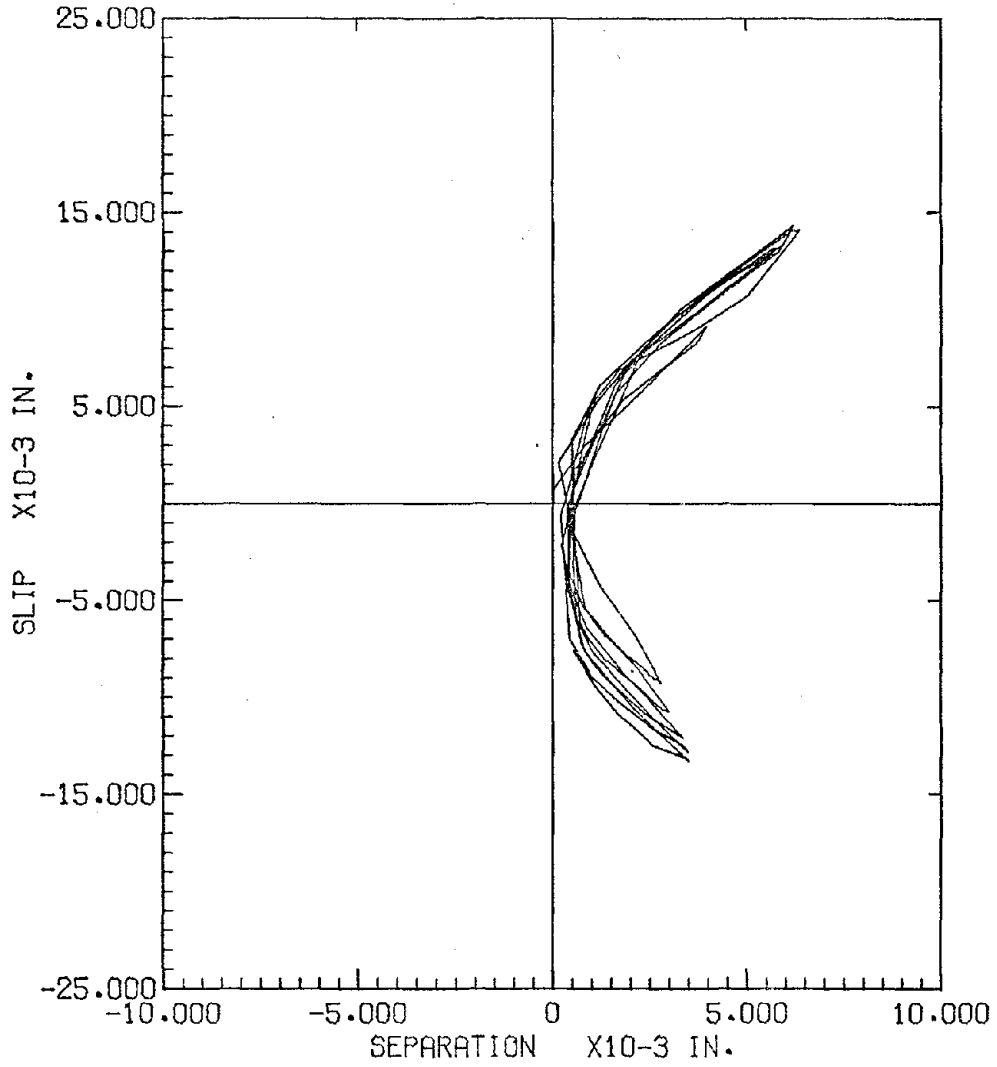


FIG. 223- SLIP-SEPARATION CURVE, N2C, CYCLES 1-5

74

±0.50V. (CALC.)

UNCRACKED

BOND BROKEN

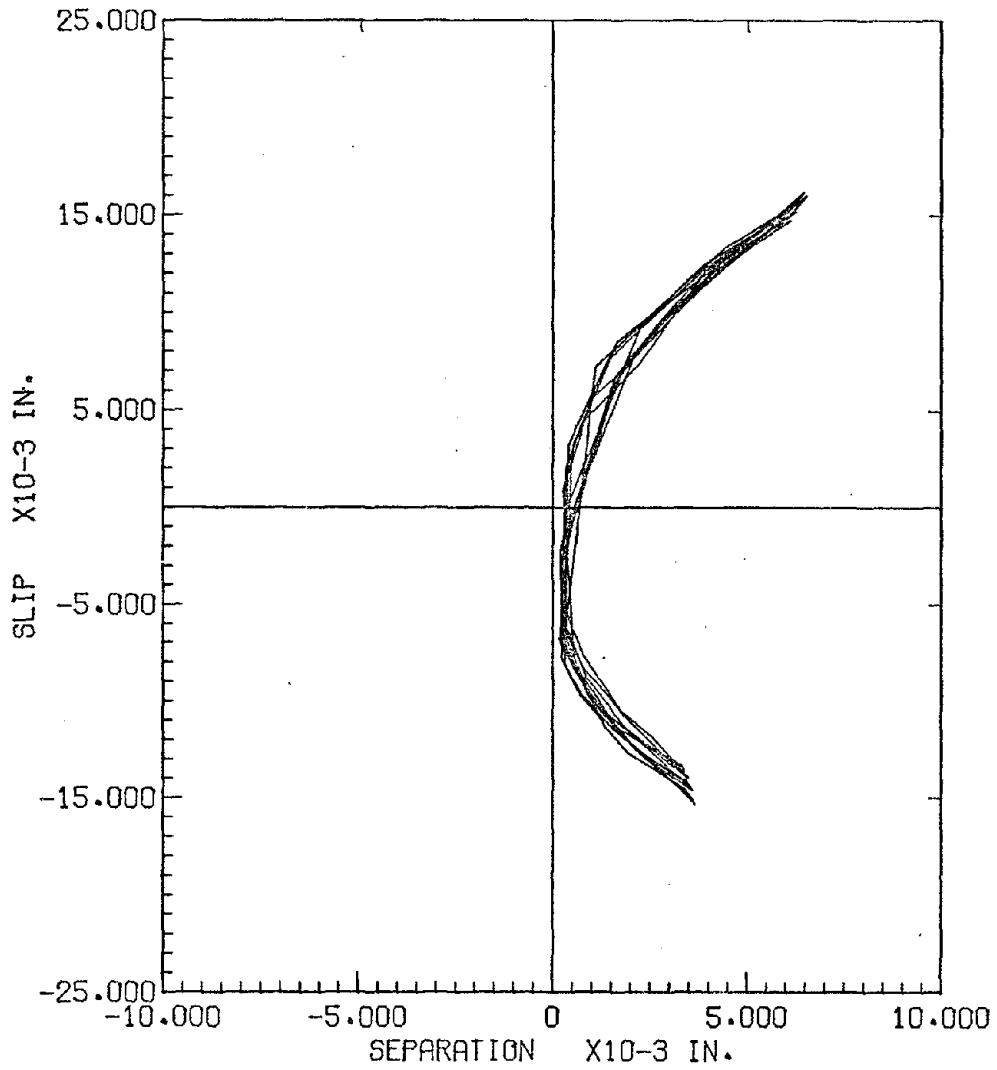


FIG.B24- SLIP-SEPARATION CURVE, N2C, CYCLES 6-10

$\pm 0.58V_c$ (CALC.)

UNCRACKED

BOND BROKEN

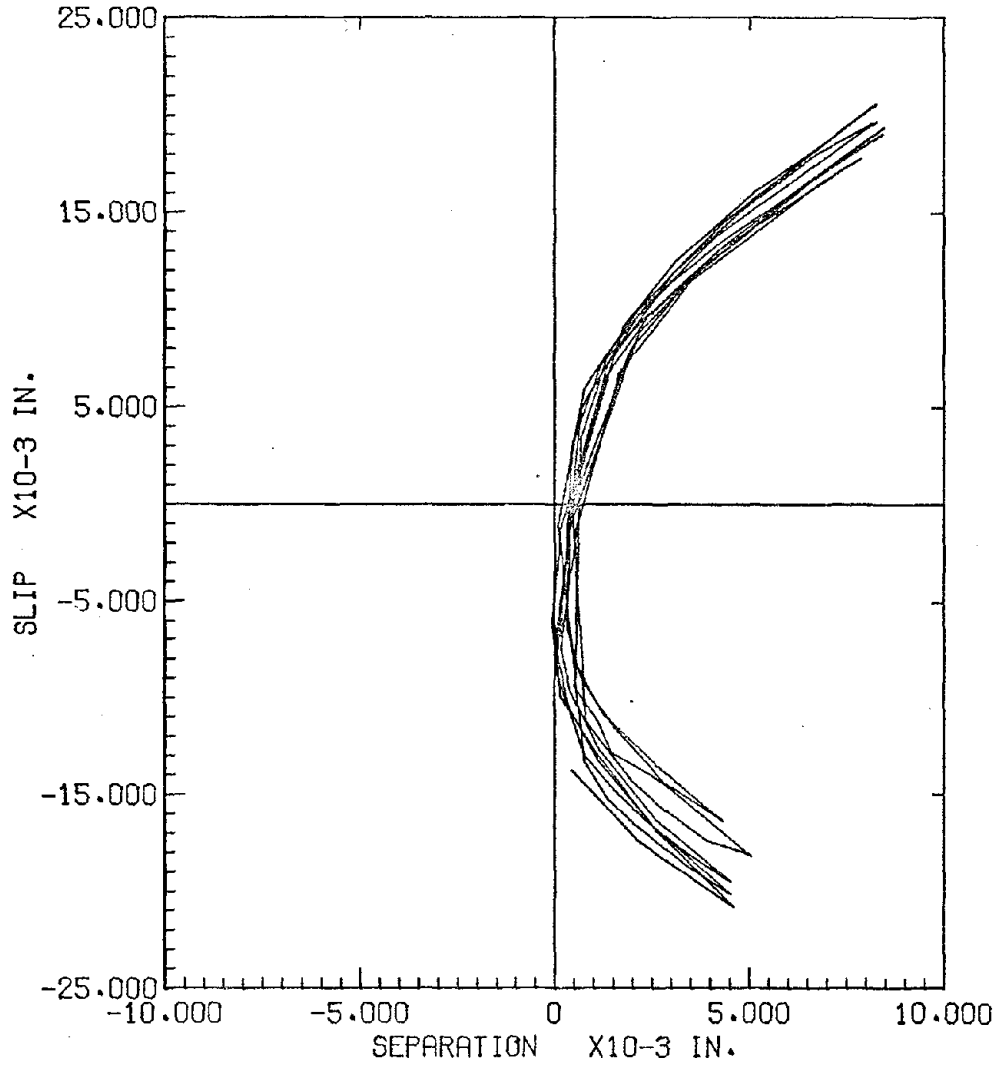


FIG.B25- SLIP-SEPARATION CURVE, N2C, CYCLES 11-15

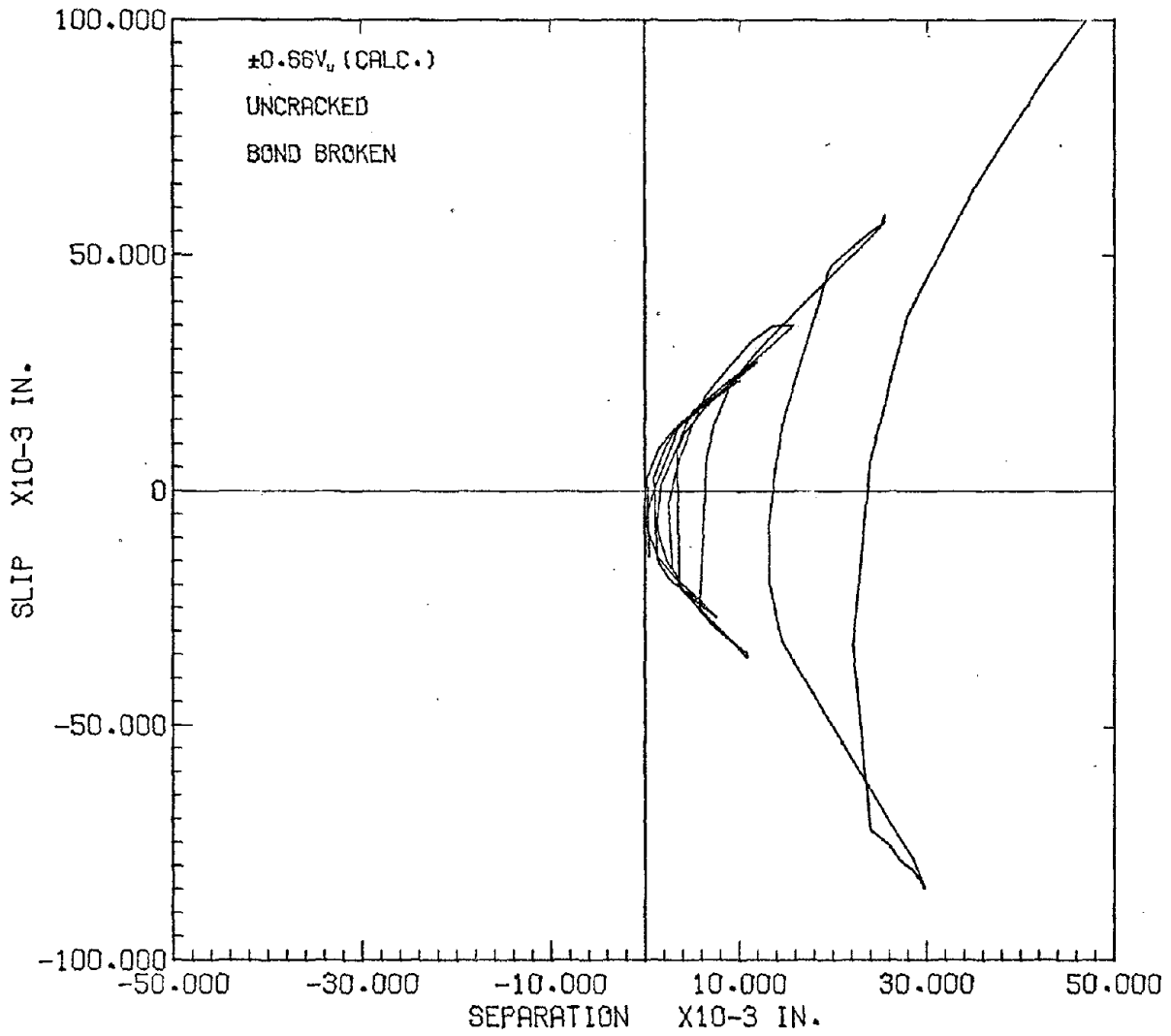
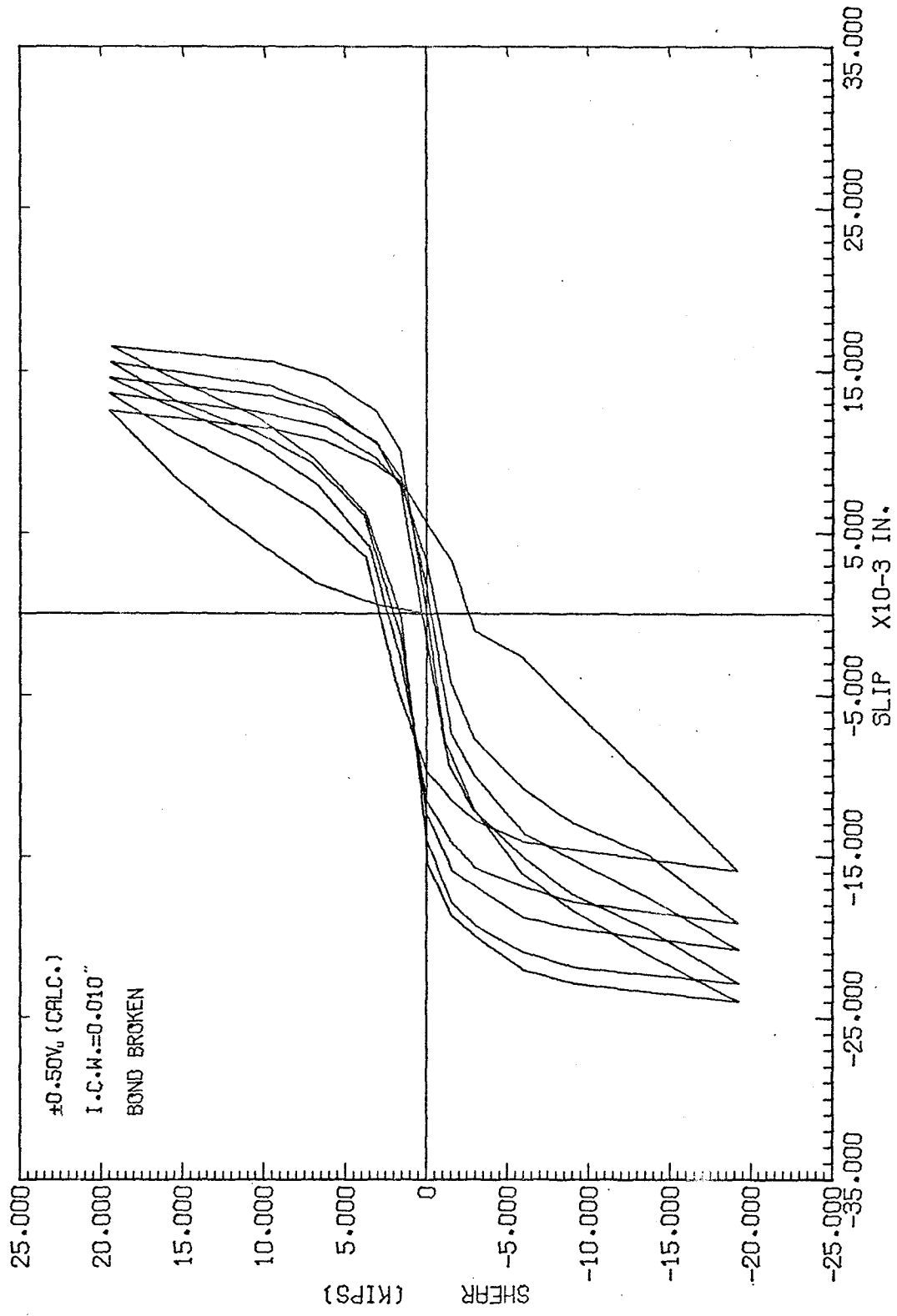


FIG. B26 - SLIP-SEPARATION CURVE, N2C, CYCLES 16-20



78

FIG. B27 - SHEAR-SLIP CURVE, P2C, CYCLES 1-5

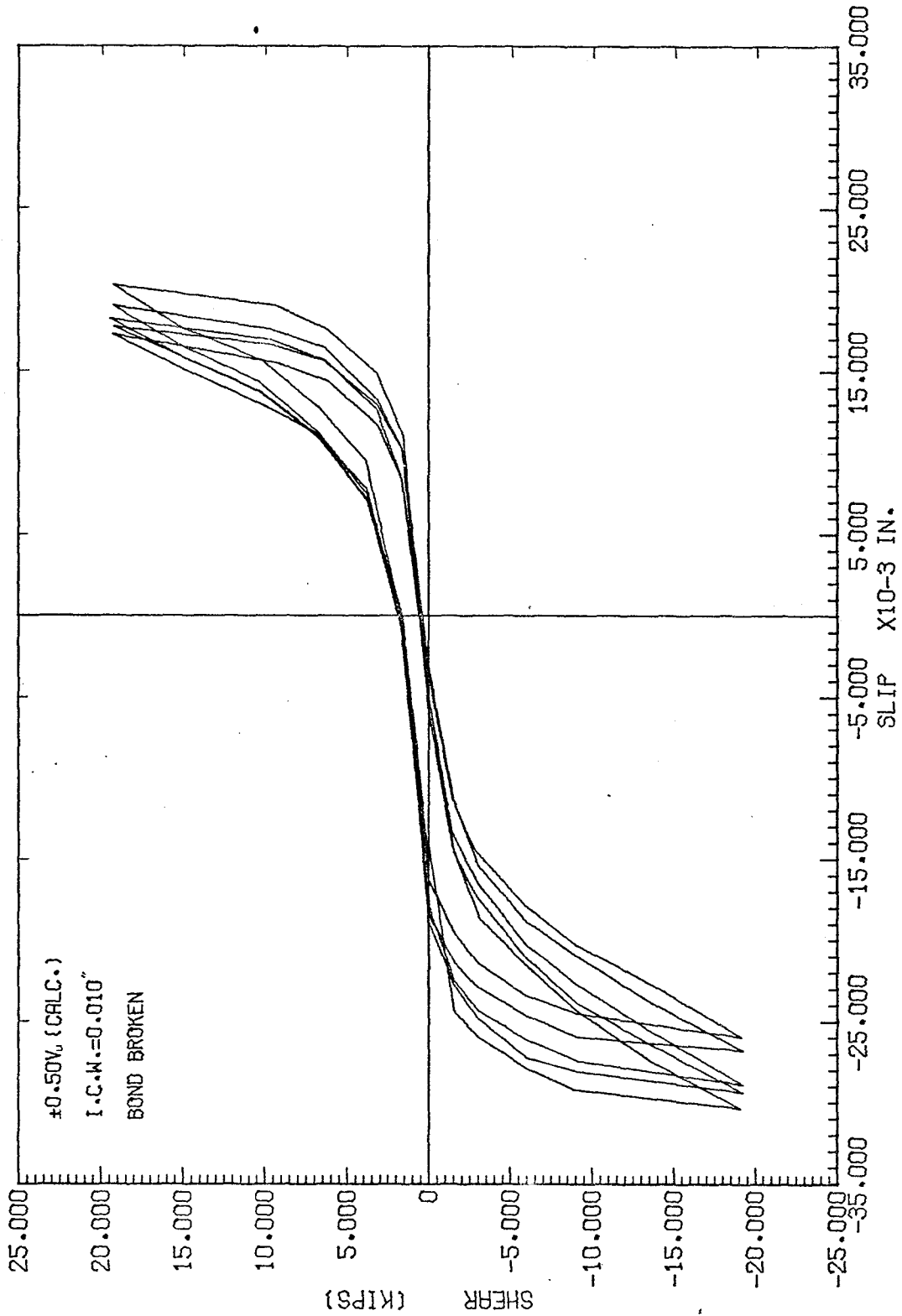


FIG. B28 - SHEAR-SLIP CURVE, P2C, CYCLES 6-10

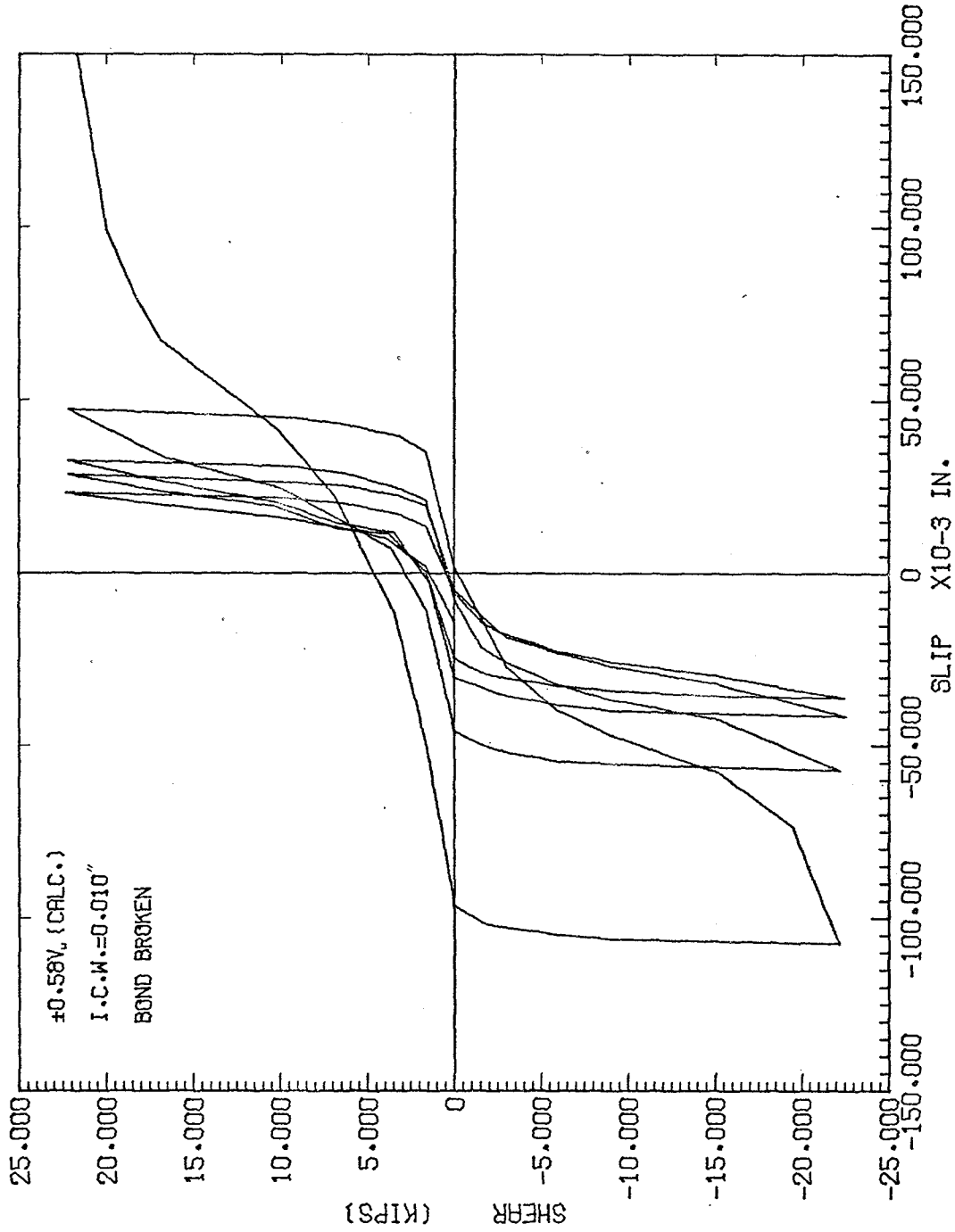


FIG. B29 - SHEAR-SLIP CURVE, P2C, CYCLES 11-15

08

±0.50V, (CALC.)

I.C.W.=0.010"

BOND BROKEN

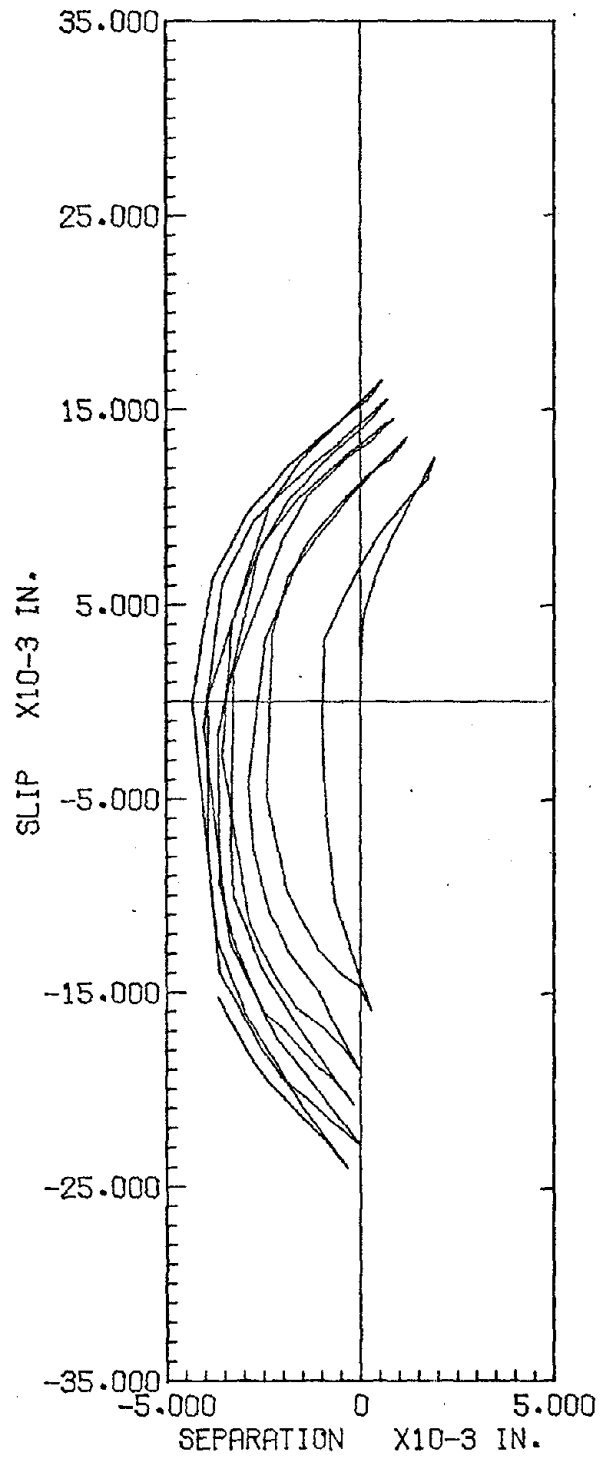


FIG. B30-SLIP-SEPARATION CURVE, P2C, CYCLES 1-5

±0.50V, (CALC.)

I.C.W.=0.010"

BOND BROKEN

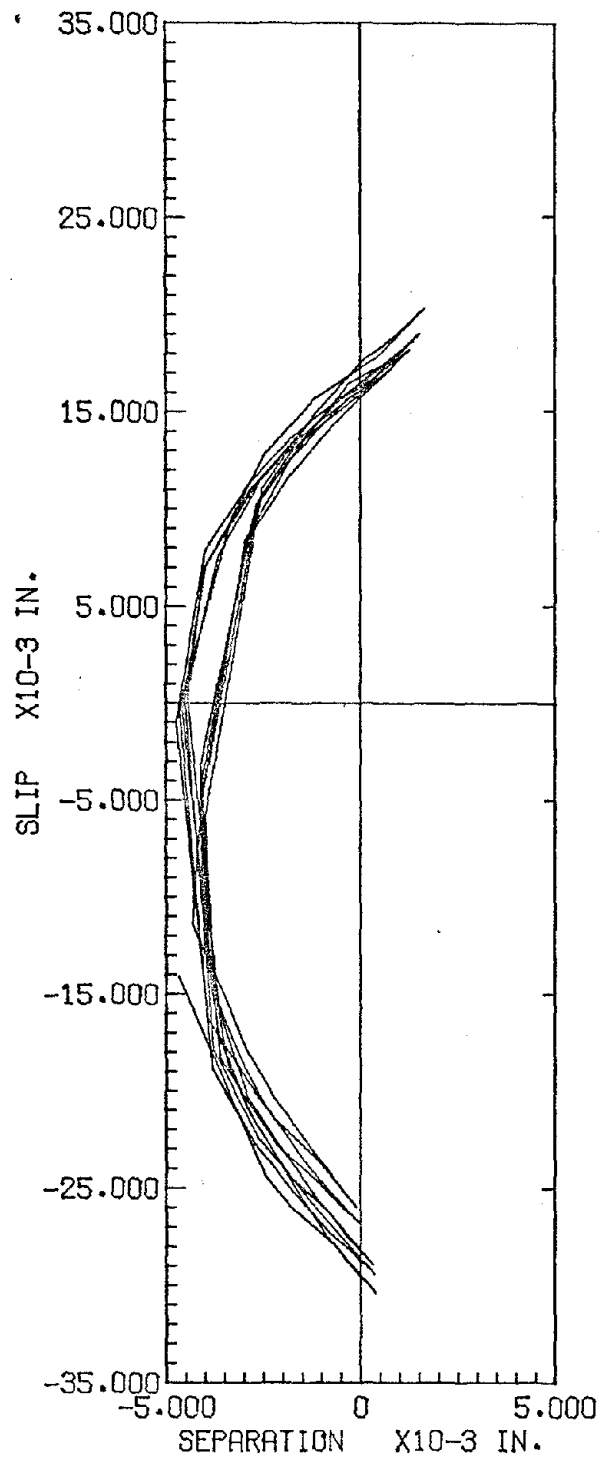


FIG. B31- SLIP-SEPARATION CURVE, P2C, CYCLES 6-10

82

$\pm 0.58V_u$ (CALC.)

I.C.W.=0.010"

BOND BROKEN

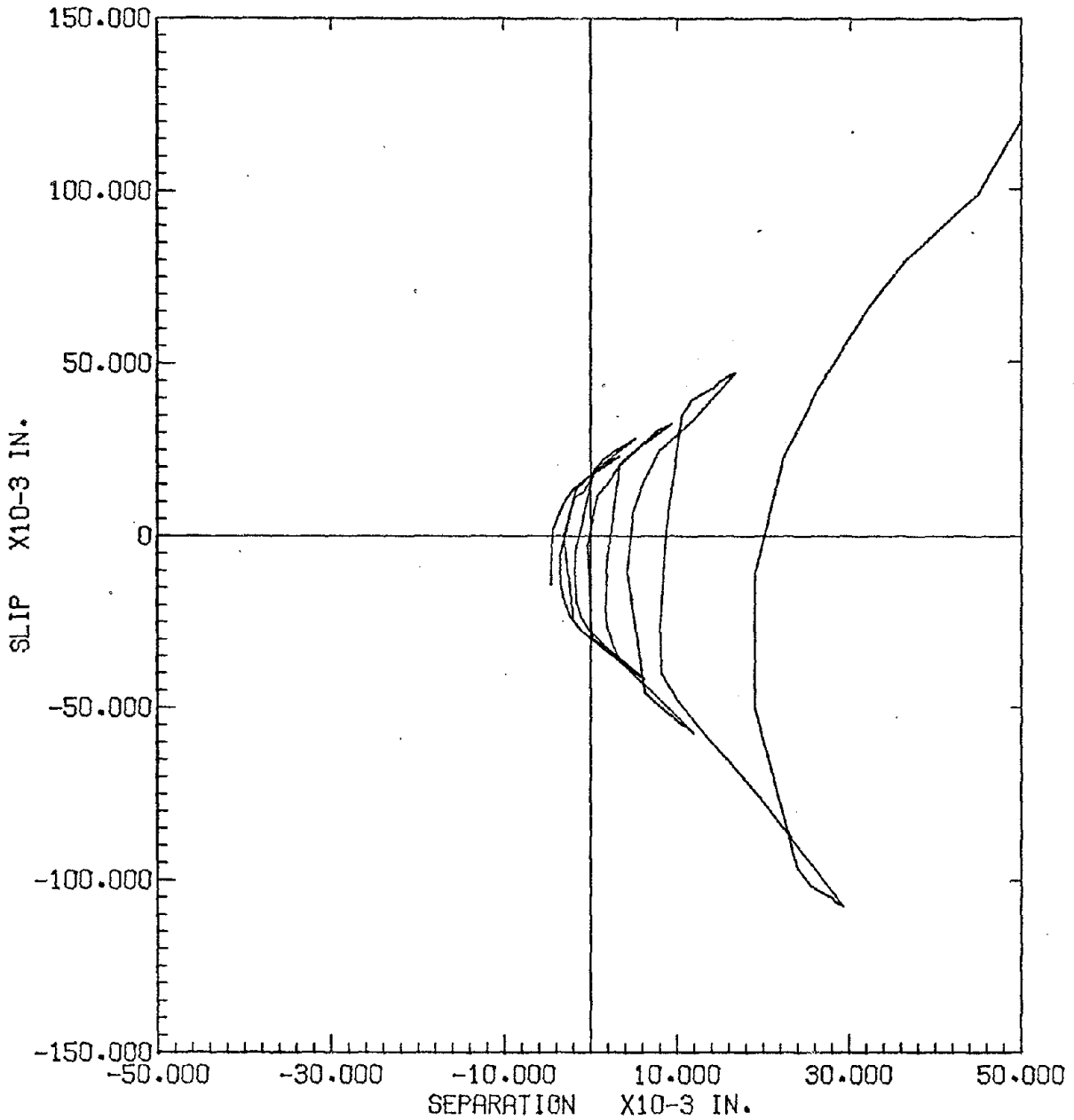


FIG. B32 - SLIP-SEPARATION CURVE, P2C, CYCLES 11-15

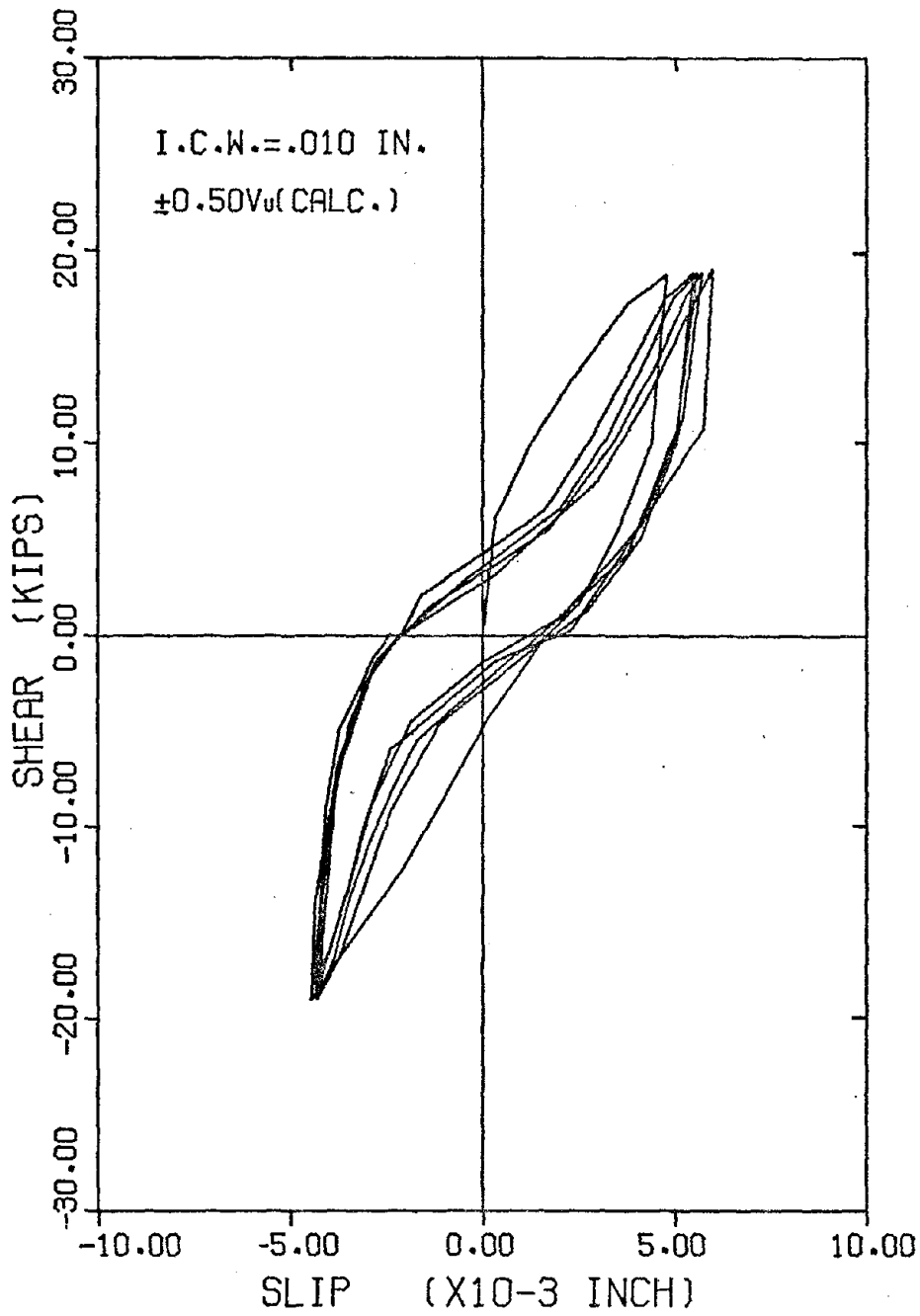


FIG. B33- SHEAR-SLIP CURVE. Q2C. CYCLES 1 TO 5

84

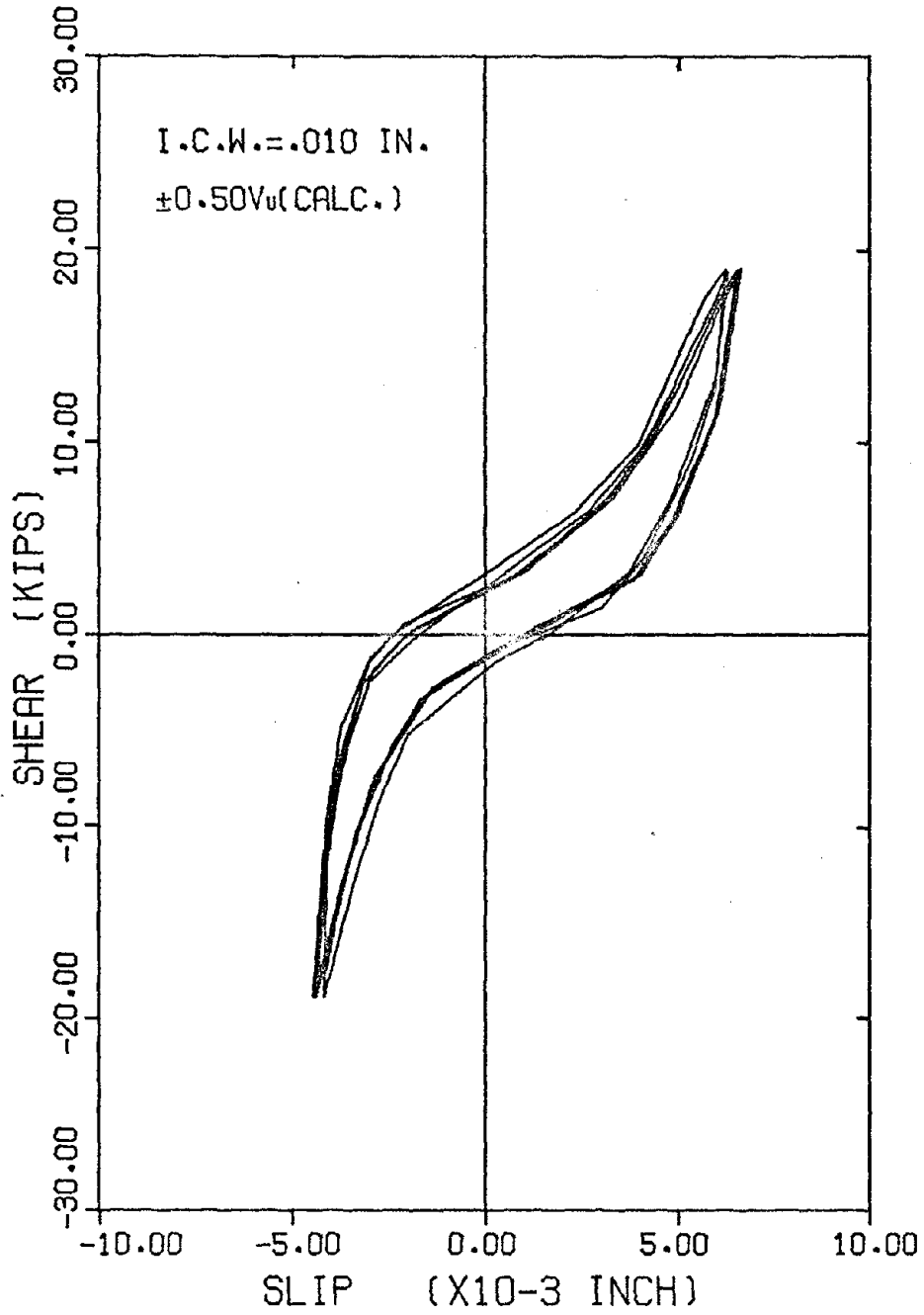


FIG. B34- SHEAR-SLIP CURVE. Q2C. CYCLES 6 TO 10

85

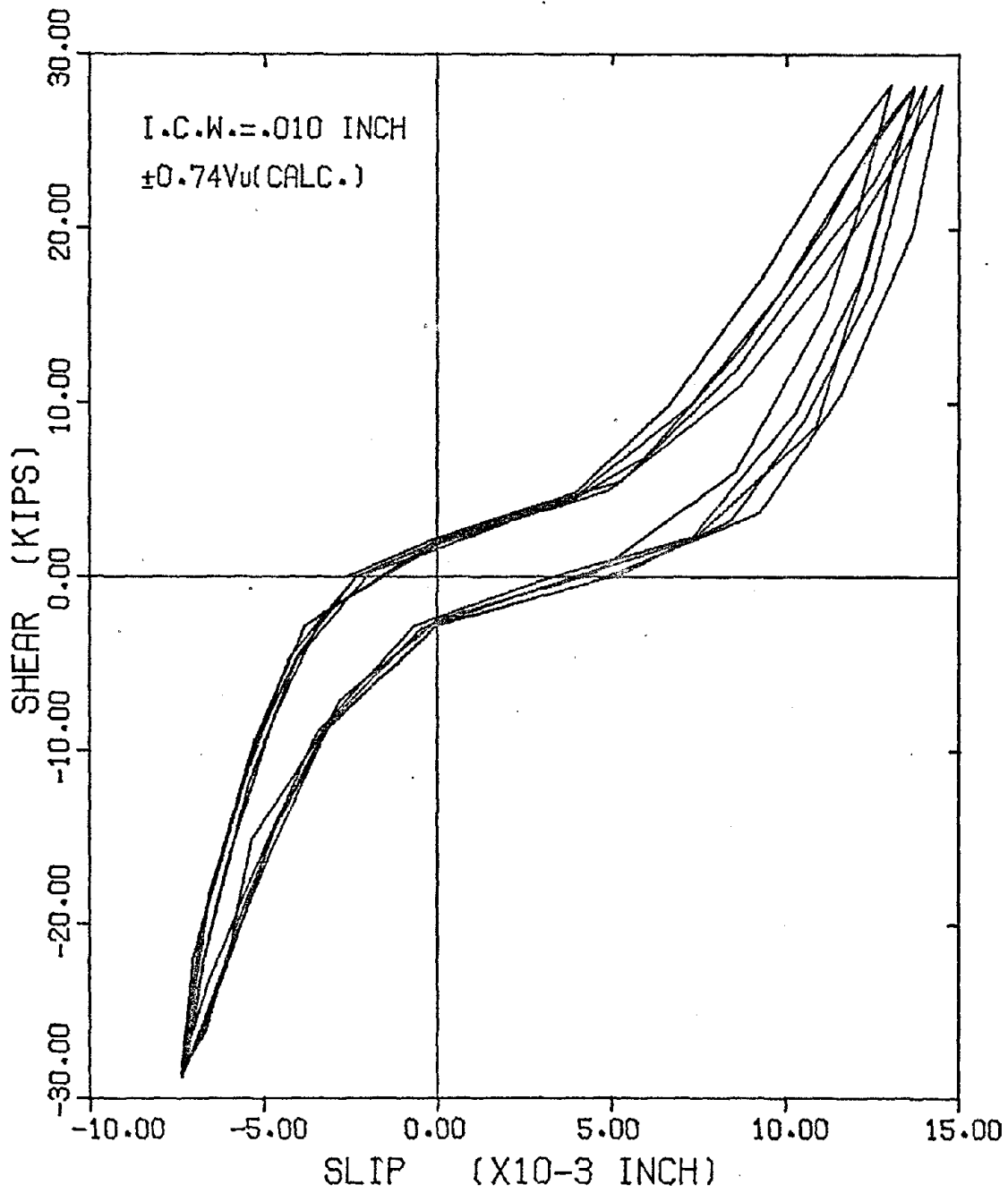


FIG.B35- SHEAR-SLIP CURVE. Q2C. CYCLES 21 TO 25

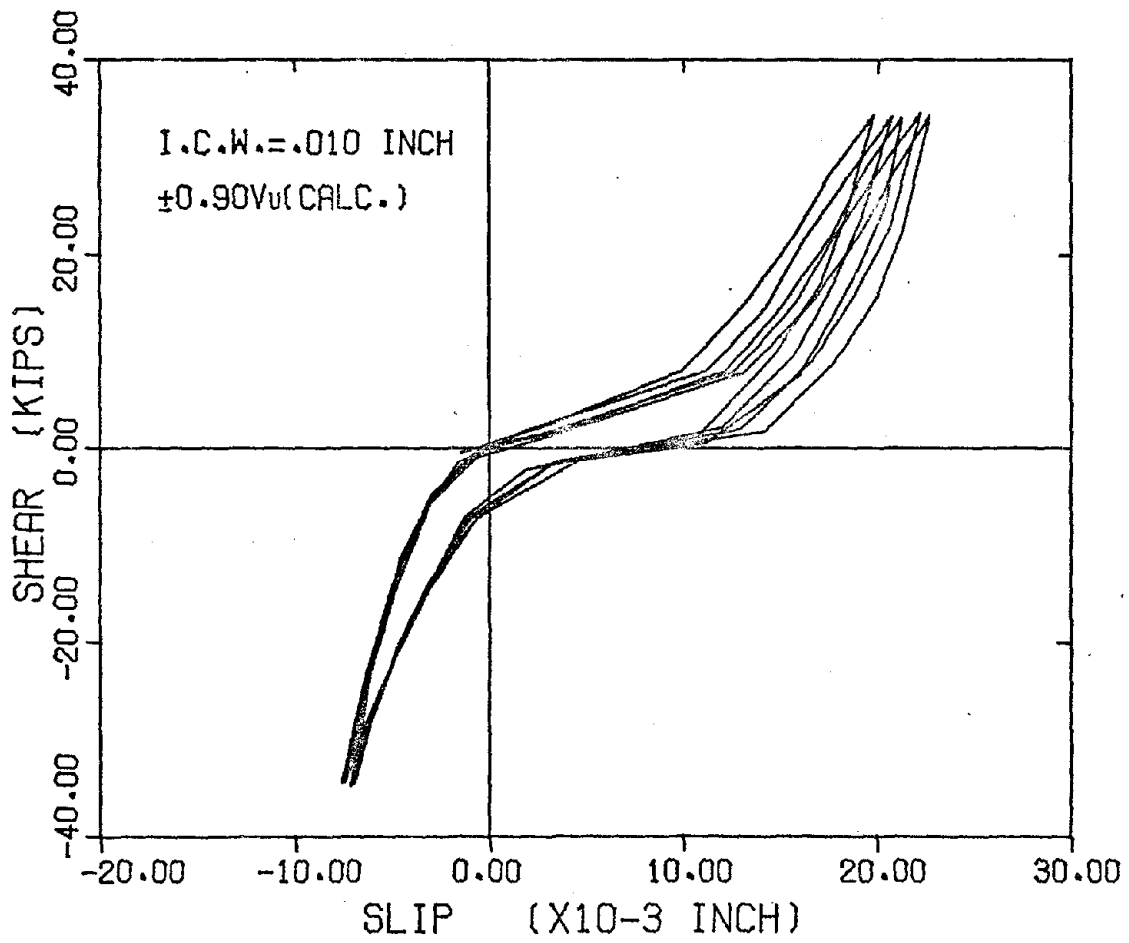


FIG.B36- SHEAR-SLIP CURVE. Q2C. CYCLES 31 TO 35

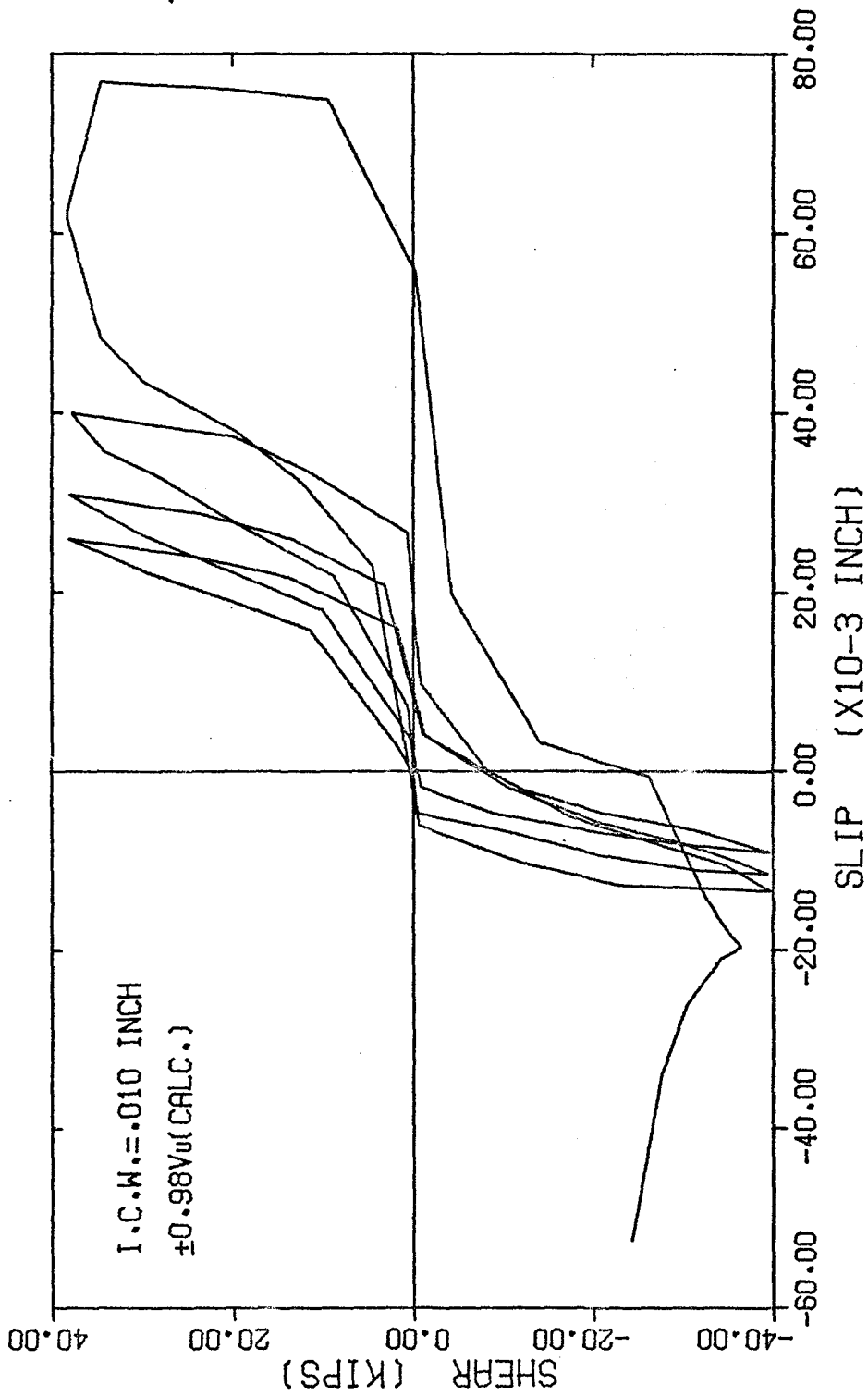


FIG. B37- SHEAR-SLIP CURVE. Q2C. CYCLES 36 TO 39

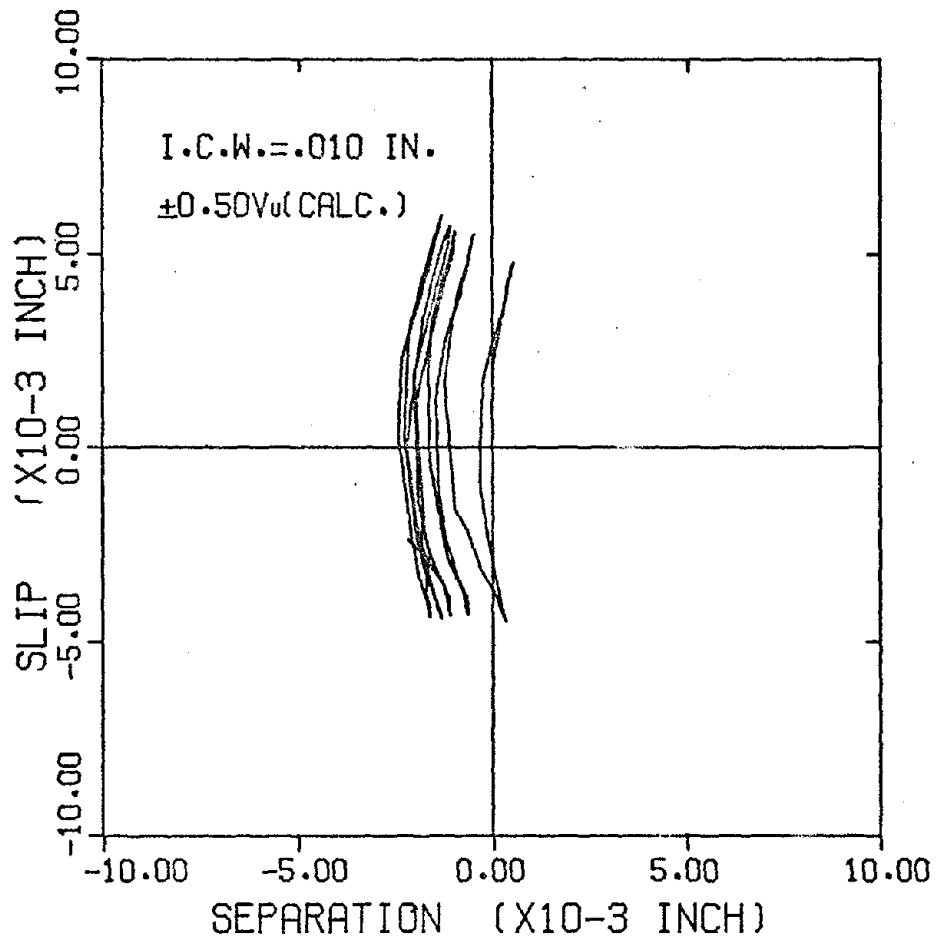


FIG. B38- SLIP-SEPARATION CURVE. Q2C. CYCLES 1 TO 5

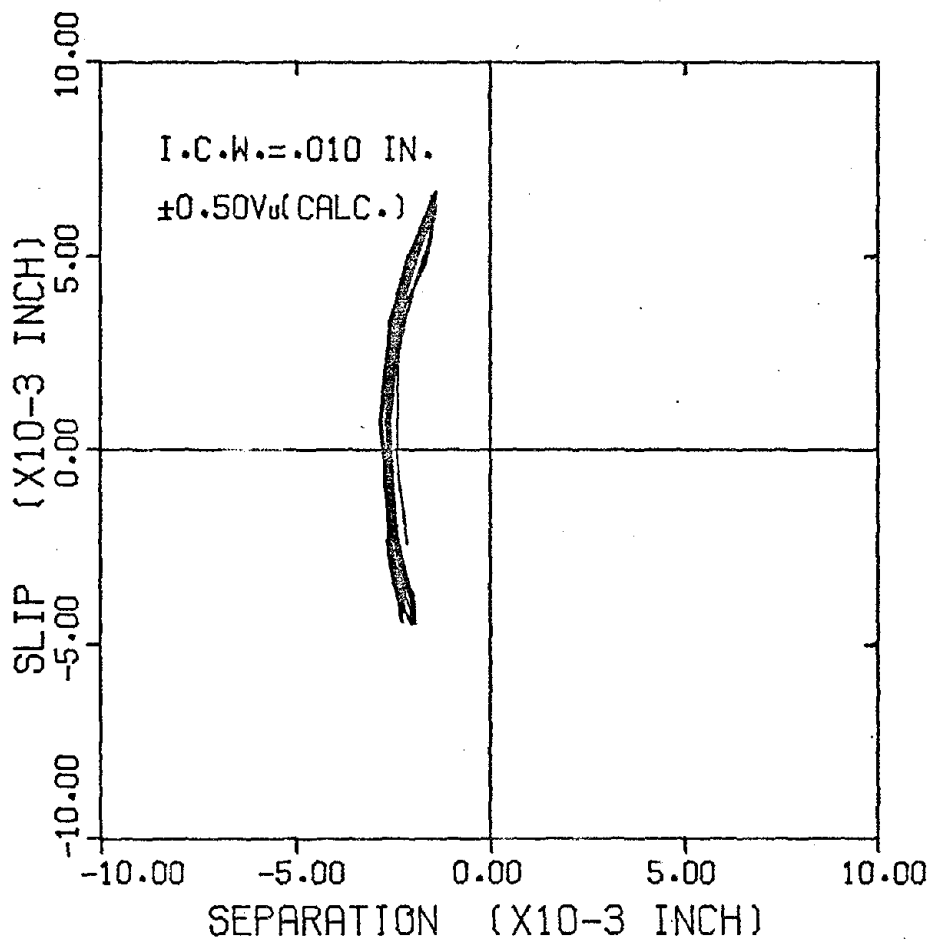


FIG.B39- SLIP-SEPARATION CURVE. Q2C. CYCLES 6 TO 10

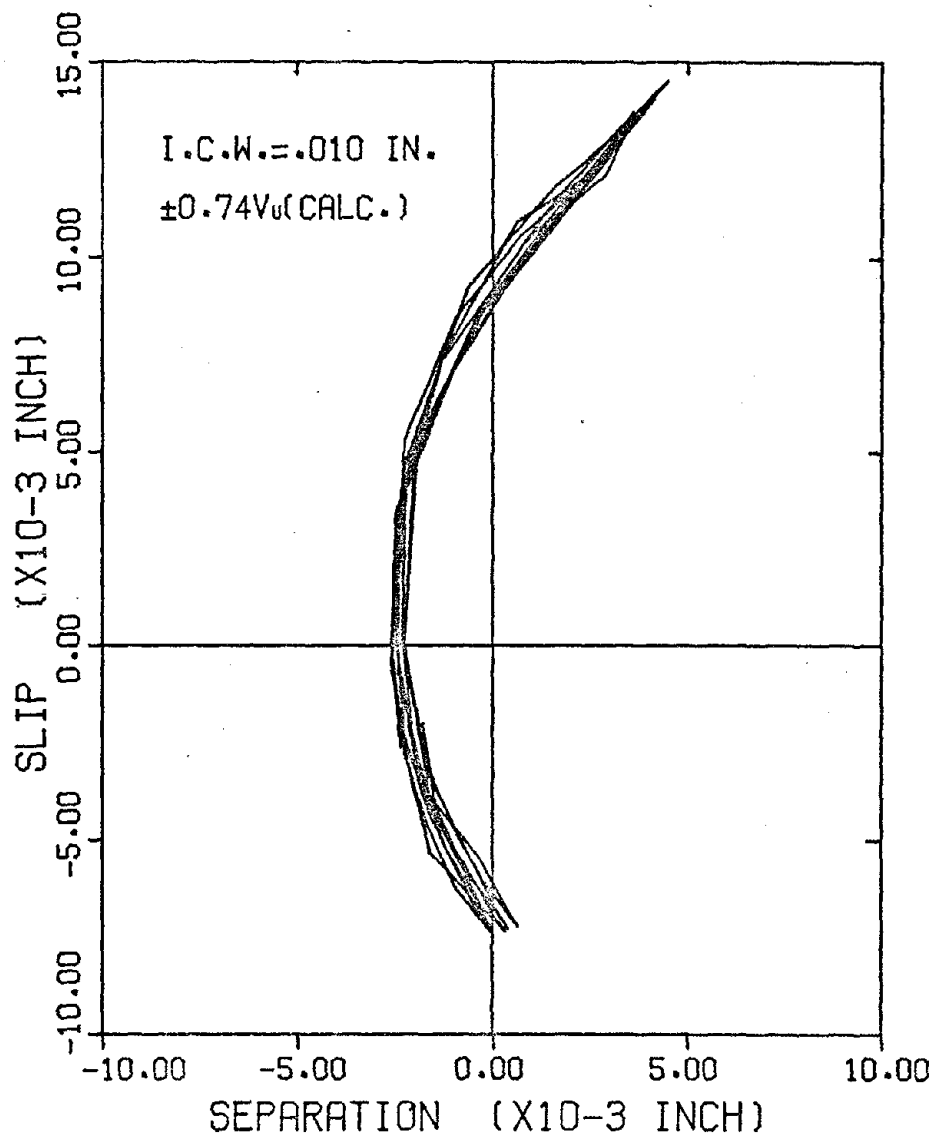


FIG. B40- SLIP-SEPARATION CURVE. Q2C. CYCLES 21 TO 25

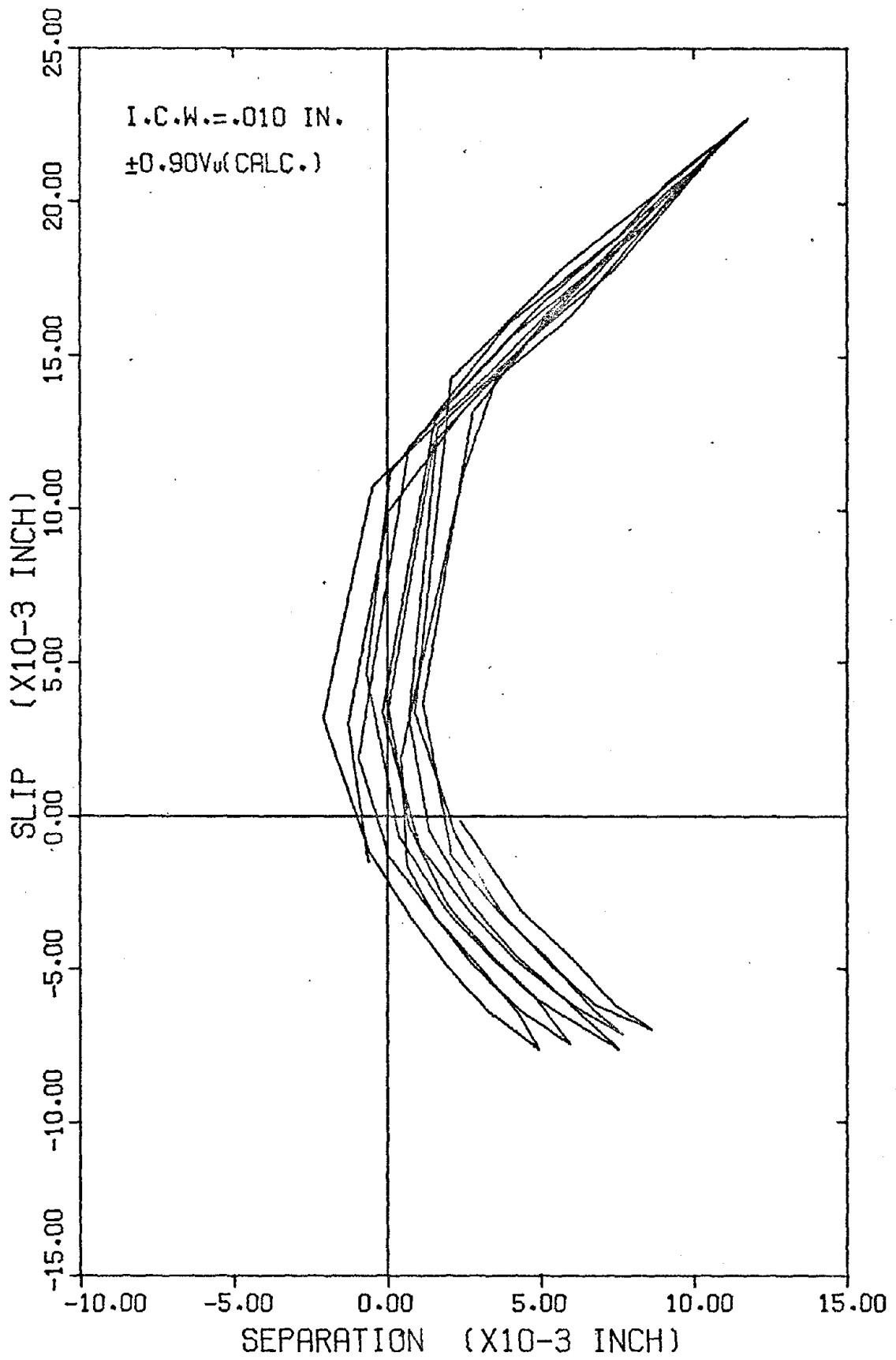


FIG.B41- SLIP-SEPARATION CURVE. Q2C. CYCLES 31 TO 35

